R006-01
Zoom meeting B ：11/1 AM1 (9:00-10:30)
9:15〜9:30

SC の PI 電流の詳細な解析結果について

#藤田 茂 [1)]
(1 データサイエンスセンター/統数研

Detailed analysis of the current system in the PI phase of the Sudden Commencement

#Shigeru Fujita[1)]
(1ROIS-DS/IMS

We already reported that there are two current systems in the Preliminary Impulse (PI) phase of the Sudden Commencement (SC). One of these current systems consists of two upward/downward field-aligned currents (FAC) and the field-perpendicular current (FPC) connecting the two FACs in the magnetopause region. The longitudinal propagation of this current is slow. FACs of this current system appear in the higher latitude in the ionosphere (type H current system). The other current system has ionospheric FAC and the magnetosheath current as well as the cross-magnetopause current. This system shifts in the longitudinal direction faster than the type H current system. FACs of this current system appear in the lower latitude in the ionosphere (type L current system). The characteristic ground magnetic variation of the PI, that is to say, longer duration of the PI geomagnetic variation and time delay of the peak of the PI geomagnetic variation in the higher latitudes, can be explained by the simultaneous occurrence of the two PI current systems. Furthermore, we also reported that 1) the cross-magnetopause current of the type L current system is driven by the acceleration of the magnetosheath plasmas associated with a sudden increase of the solar wind dynamic pressure and 2) convergence/divergence of the FPC invokes the FPC-FAC conversion of the type H current system in the magnetopause region.

In the talk, we stress the following three points that have not been treated previously.

1) The simultaneous occurrence of the two current systems does not completely explain the time delay of the peak of the PI current system because the time delay is detected in the latitude region of the type L current system. Detailed analysis of the type L current system reveals that the cross-magnetopause current of the type L current system in the higher-latitude side bents toward the noon direction in the outer magnetopause region. Thus, the peak FAC in the ionosphere appears in a longitude deviated from the longitude corresponding to the front of the solar wind impulse in the magnetosheath toward noon. On the other hand, the type L current system goes almost straight to the ionosphere.

2) We need to investigate the detailed process of the FPC-FAC conversion along the current lines of both current systems. The conversion is derived by the spatially non-uniform distribution of magnetic field intensity and plasma density (the Alfven speed) and magnetic field curvature. In addition, the displacement current of the Alfven wave also contributes to the FPC-FAC conversion in the lower magnetosphere near the ionosphere. The transition of high-beta plasma in the outer magnetosphere to the low-beta one in the inner magnetosphere does not play a role in the FPC-FAC conversion for the PI current system.

3) It is important to manifest how the latitude of the PI current in the ionosphere is determined because no papers are discussing how the latitude of the PI current is determined. Fujita et al. (2003) briefly mentioned that the PI appears in the latitude of the plasmapause because the FPC-FAC conversion of the PI current system occurs in the region of the steep spatial gradient of the Alfven speed. So, the PI current should have existed in the plasmapause latitude. But the simulation does not prove this estimation. The simulation reveals that the highest latitude of the PI current is located in the magnetopause latitude (the type H current). is located near the magnetopause latitude. In addition, as for the type L current system, the cross-magnetopause current (FPC) is gradually converted to the FAC due to the non-uniform distribution of the Alfven speed in the outer magnetosphere. The latitude of the PI current in the ionosphere is higher than the latitude of the plasmapause.

Fujita, S., T. Tanaka, T. Kikuchi, K. Fujimoto, K. Hosokawa, and M. Itonaga (2003), A numerical simulation of the geomagnetic sudden commencement: 1. Generation of the field-aligned current associated with the preliminary impulse, J. Geophys. Res., 108(A12), 1416, doi:10.1029/2002JA009407.

R006-02
Zoom meeting B ：11/1 AM1 (9:00-10:30)
9:30〜9:45

Region 1 沿磁力線電流の生成領域

#海老原 祐輔 [1)], 田中 高史 [2)]
[(1] 京大生存圏,[(2]REPPU code Institute

Generation regions of Region 1 field-aligned currents

#Yusuke Ebihara[1)],Takashi Tanaka[2)]
[(1]RISH, Kyoto Univ.,[(2]REPPU code Institute

We investigated the generation regions of the Region 1 field-aligned currents (FACs) by using the global magnetohydrodynamics (MHD) simulation. Unlike conventional means, we considered Alfven and convective transit time by tracing a packet backward in time from the ionosphere to the solar wind. Two potential regions are identified for the generation of the Region 1 FACs. One is located near the (low-latitude) magnetopause (G1), and the other is in the (high-latitude) bow shock (G2). In these regions, plasma performs negative work against the magnetic tension force and the divergence of FACs is non-zero. Interestingly, these regions are far from the original magnetic field line because of relatively slow Alfven speed in the outer magnetosphere and beyond. G2 can be on the magnetic field lines detached from the Earth. As the packet proceeds in the magnetosheath, the field line extending from the packet experienced reconnection with Earth's field line. Immediately after the reconnection, the packet enters the region (G1) where plasma performs negative work against the magnetic tension force. That is, plasma originating in the solar wind pulls lobe magnetic field lines. Large part of the FACs are canceled just inside G1, where the plasma performs positive work against the tension force. That is, the magnetic field lines pull lobe plasma. The remnant of the FACs propagates to the ionosphere. Since the contribution from G2 is negligible, it is concluded that the flank magnetopause (G1) is the major region for the generation of the Region 1 FACs. We discuss the relation between the generation of FACs, configuration of the magnetic field, and energy conversion.

R006-03
Zoom meeting B ：11/1 AM1 (9:00-10:30)
9:45〜10:00

Implementation of Alfvenic Coupling in Global MHD Magnetosphere Simulation

#Aoi Nakamizo[1)],Akimasa Yoshikawa[2)],Hiroyuki Nakata[3)],Keiichiro Fukazawa[4)],Takashi Tanaka[5)]
([1]NICT,[2]ICSWSE/Kyushu Univ.,[3]Grad. School of Eng., Chiba Univ.,[4]ACCMS, Kyoto Univ.,[5]REPPU code Institute

Presently, most global MHD magnetosphere models equip ionospheric solvers at their inner boundaries and then simulate the magnetospheric and ionosphere (M-I) processes. Here the ionospheric solver is the so-called ”thin shell model” which solves the Ohm’s law under the thin shell approximated ionosphere with FACs in the polar region and the height-integrated ionospheric conductivity. With this solver, the global MHD models solve the inner boundary condition of electromagnetic field in the following manner. (1) The FAC distribution obtained from the rotation of the magnetic field at the inner boundary (usually placed at the altitude of 2-3 Re) is mapped to the ionospheric altitude. (2) The mapped FAC is inputted to the solvers equipped at the ionospheric altitude, then the ionospheric potential is calculated. (3) The potential is mapped back to the inner boundary and the bulk velocity is updated there.

On the other hand, Yoshikawa et al. [2010] proposed a new M-I coupling algorithm which guarantees the continuities of physical quantities between the magnetosphere and ionosphere and therefore the momentum and energy conservations by considering the incident and reflection process of shear Alfven waves. We call the new algorithm ’Alfvenic coupling.’ We discuss in detail the characteristics of the traditional algorithm and the concept of Alfvenic coupling algorithm. We report on the progress of the implementation of Alfvenic coupling in a global MHD code and show the preliminary results.

R006-04
Zoom meeting B ：11/1 AM1 (9:00-10:30)
10:00〜10:15

沿磁力線電流と電離圏電流の 3 次元結合

#矢野 有人 [1)], 海老原 祐輔 [2)]
[(1] 京都大学生存圏研究所,[(2] 京都大学生存圏研究所

3-dimensional coupling between field-aligned currents and ionospheric currents

#Yuto Yano[1)],Yusuke Ebihara[2)]
[(1]RISH, Kyoto Univ.,[(2]RISH, Kyoto Univ.

By developing a simplified 3-dimensional Hall-MHD simulation, we investigated the coupling between field-aligned currents (FACs) and the ionosphere with horizontally-homogeneous (Case 1) and horizontally-inhomogeneous (Case 2) electron number density. Since the ion-neutral collision frequency depends on the altitude, two layers appear, one dominated by the Pedersen current (Pedersen layer) and the other dominated by the Hall current (Hall layer). We imposed electric fields to the topside boundary to excite the Alfven waves and FACs. When the electron density is horizontally homogeneous (Case 1), most of the FACs are connected with the Pedersen current. A few of them are connected with the Hall current. When the electron density is artificially enhanced in a longitudinally elongated region (Case 2), the convergent (divergent) Hall current appears near the leading (trailing) edge of the high-density band, resulting in divergent (convergent) polarization electric field. The rotationally-flowing plasma associated with the polarization is confirmed to perform negative work against the Lorentz force associated with the Hall current. As a consequence of the negative work, magnetic energy and localized FACs are generated in the Hall layer. The localized FACs are found to bridge between the Hall and Pedersen layers. Some current lines originating in the topside boundary of the simulation box are connected to the Hall current by way of the localized FACs. The current lines can pass underneath those flowing in the Pedersen layer. Such ”intersection” is not allowed in the traditional thin-layer assumption. These results suggest that the current lines are fully 3-dimensional, primarily due to the localized FACs that bridge the Pedersen and the Hall layers. The localized FACs are thought to play an important role in the magnetosphere-ionosphere coupling, in particular, the formation of a traveling surge of aurora during substorms.

簡略化した 3 次元ホール MHD シミュレーションを用い、沿磁力線電流（FAC）と電離圏電流の結合について調べた。電子密度については水平方向に均一な場合（Case 1）と均一でない場合（Case 2）を考えた。高さに依存したイオンと中性大気の衝突周波数を与え、ペダーセン電流が支配的な層（ペダーセン層/高高度）とホール電流が支配的な層（ホール層/低高度）を表現することができる。アルベン波と FAC を励起するため上端に電場を与えた。電子密度が水平方向に均一な場合（Case 1）、ほとんどの FAC がペダーセン電流とつながった。僅かではあるがホール電流と接続するものもある。帯状の狭い領域で電子密度を高めたところ（Case 2）、高密度帯の前縁（後縁）付近でホール電流が収束（発散）し、発散型（収束型）の分極電場が現れた。この発散型（収束型）の分極電場に伴って回転方向に動くプラズマは、ホール電流によるローレンツ力に対して負の仕事をしていることを確認した。この負の仕事は磁場エネルギーへの変換がおきていることを意味し、ホール層付近の限られた高度範囲で見られる局所的な FAC の発生に関与していると考えられる。この局所的な FAC はホール層とピダーセン層を接続している。FAC から繋がる電流線の一部局所的な FAC を軽油してホール電流と繋がっている。この電流線は高高度を流れるペダーセン電流線の下を通ることができる。このような「交差」は、従来の薄層近似で表現することができない。これらの結果は、沿磁力線電流と電離圏を接続する電流線は完全に 3 次元的であることを示唆している。この 3 次元性は主にペダーセン層とホール層をつなぐ局所的な FAC によるもので、この局所的な FAC は磁気圏・電離圏結合過程、特にサブストーム時に見られるオーロラサージの形成に重要な役割を果たしていると考えられる。

R006-05
Zoom meeting B ：11/1 AM2 (10:45-12:30)
10:45〜11:00

Diagnosis of solar-wind effects on the AE indices based on an echo state network model

#Shin ya Nakano[1)],Ryuho Kataoka[2)]
([1]The Institute of Statistical Mathematics,[2]NIPR

The AE indices consist of the AU and AL indices. The former represents the strength of the eastward auroral electrojet and the latter represents the strength of the westward auroral electrojet. Although the AE indices are widely used for monitoring geomagnetic activity, it is not easy to model the behavior of the AE indices because of the complicated physical processes of the auroral electrojets.

In this study, we employ an echo state network for modeling the relationship of the AE indices to solar wind parameters. The echo state network is a kind of recurrent neural networks where the connections and weights between hidden state variables are fixed, and it can be easily implemented for modelling dynamical systems and time series data. Our echo state network model successfully reproduces temporal variations of the AU and AL indices with comparable accuracy to other existing modelling studies.

Using this echo state network model, we can obtain synthetic AE indices under artificial input conditions. In order to assess the impact of the solar-wind speed and density on the AE indices, we derived synthetic AE indices under some artificial solar wind conditions: a high speed solar wind, a high density solar wind, and a low density solar wind. The results show the followings.

1. The solar wind speed has significant effects on the AE indices. In particular, many events of the AL enhancements are related with high-speed solar wind streams.

2. The solar wind density also makes effects on both the AU and AL indices. However, the AL index is influenced by the solar wind density only under high-speed solar wind conditions, while the density effect on the AU index is observed even under low-speed solar wind conditions.

The latter result is consistent with a simulation result by Ebihara et al. (JGR, 2019). However, it is likely to be relatively rare that solar wind density actually contributes to the AL index because high solar wind density is mostly concurrent with a low-speed region in the front of a high-speed stream of the solar wind.

R006-06
Zoom meeting B ：11/1 AM2 (10:45-12:30)
11:00〜11:15

Relationship between the cusp ion precipitation from lobe reconnection and the magnetosheath flow

#Haruto Koike[1)],Satoshi Taguchi[1)]
[(1]Grad school of Science, Kyoto Univ.

Lobe reconnection occurs in the presence of tailward magnetosheath flow which is parallel to the high-latitude magnetopause. How the parallel flow is related to the reconnection process is still unclear. The purpose of this study is to understand this relationship through the statistical analysis of the lobe reconnection events identified in the low-altitude cusp. Lobe reconnection allows the magnetosheath ions to precipitate directly into the cusp. We examined precipitating particle data obtained in the low-altitude cusp by DMSP F16, F17, and F18. We introduced a method of automated event identification to the data obtained for 11 years, and took the cusp ion events in more than 1800 satellite orbits from the data obtained during stably northward IMF periods. The events were identified at latitudes higher than 78 MLAT, and the MLT distribution of the events clearly showed the well-known IMF By-dependence. The result of the statistical analysis has shown that the total number flux of the precipitating ions in the cusp tends to increase with the increase of the magnetosheath flow speed as well as the magnetosheath number density. The result has also revealed that the average energy of the precipitating ions in the cusp tends to be higher as the magnetosheath flow is faster. These strongly suggest that the parallel magnetosheath flow acts in the reconnection process in such a manner that the ion outflow jet from the reconnection can be enhanced. We discuss this relationship in terms of the enhancement of the Hall electric field in the ion diffusion region of the reconnection.

R006-07
Zoom meeting B ：11/1 AM2 (10:45-12:30)
11:15〜11:30

Mini-broadband electron precipitation in the cusp for northward IMF

#Satoshi Taguchi[1)],Kohei Takasu[1)],Yushin Oda[1)],Haruto Koike[1)],Keisuke Hosokawa[2)]
([1]Grad school of Science, Kyoto Univ.,([2]UEC

We investigated what type of structure of the electron precipitation occurs typically in the cusp for northward IMF by using auroral image data obtained by an all-sky imager on the ground and precipitating particle/magnetic field data obtained by DMSP F16 spacecraft. From five winter seasons we took the DMSP conjugate observations of the cusp with the all-sky imager. The result from the conjugate observations showed that mini-broadband electron precipitations, which are coincident with upward field-aligned currents, occur in the cusp for northward IMF. Those mini-broadband electron precipitations tend to occur in more places within the longitudinal extent of the cusp with an increase in the flux of the less-structured background electron precipitation. The result of the analysis also showed that the background electron precipitation tends to increase its flux as the magnitude of the IMF increases, suggesting that the entry of the background electron is controlled by lobe reconnection. Multiple structures of mini-broadband electron precipitation, embedded in the less-structured background electron precipitation, are typical for the winter-hemisphere cusp for northward IMF. We discuss the generation of the mini-broadband electron precipitation in terms of the flux of the background electron precipitation.

R006-08
Zoom meeting B ：11/1 AM2 (10:45-12:30)
11:30〜11:45

「すざく」と XMM-Newton 衛星による地球周辺電荷交換 X 線の多点同時観測

#伊師 大貴 [1)], 石川 久美 [1)], 江副 祐一郎 [1)], 三好 由純 [2)], 寺田 直樹 [3)]
([1] 東京都立大,[2] 名古屋大 ISEE,[3] 東北大・理・地物

Simultaneous Suzaku and XMM-Newton observations of solar-wind charge-exchange X-ray emission from the Earth's magnetosphere

#Daiki Ishi[1)],Kumi Ishikawa[1)],Yuichiro Ezoe[1)],Yoshizumi Miyoshi[2)],Naoki Terada[3)]
([1]Tokyo Metropolitan Univ.,[2]ISEE, Nagoya Univ.,[3]Dept. Geophys., Grad. Sch. Sci., Tohoku Univ.

Geocoronal solar wind charge exchange (SWCX) occurs when highly charged solar wind ions like O^{7+} and N^{5+} strip electrons from exospheric hydrogen atoms. This provides not only time-variable background signals for all the X-ray astronomical observations but also useful information such as the exospheric neutral density and the Earth's bow shock and magnetopause postions (e.g., Ezoe 2018 The astronomical herald). However, its prediction and dependence on several observational conditions such as line of sight directions and/or solar wind parameters are not clear.

We previously analyzed all the archival Suzaku data and detected about 90 events among 3055 data sets covering from 2005 August to 2015 May (Ishikawa 2013 Ph. D. thesis, Ishi et al. 2017 Proc. XRU). To investigate an overall picture of geocoronal SWCX, we additionally analyzed about 100 data obtained from XMM-Newton. These data sets are overlapped with our Suzaku detections. As a result, we found about 20 events simultaneously affected by geocornal SWCX. A correlation of geocoronal SWCX emissivities between the Suzaku and XMM-Newton observations seems to depend on their line of sight directions. Each emissivity deduced from a spherical exospheric density profile and empirical bow shock and magnetopause positions tends to be underestimated by a factor of 5-10. In this talk, we report on these results and discuss future prospects such as XRISM and GEO-X.

近年、「すざく」や XMM-Newton 衛星などの高感度 X 線観測により、地球周辺の電荷交換反応 (Charge eXchange; CX) が確立してきた (Snowden et al. 2004 ApJ, Fujimoto et al. 2007 PASJ, Ezoe et al. 2010 PASJ)。太陽風に含まれる重イオン (主に O^{7+}, N^{5+} など) が 10 地球半径以上に広がる希薄な超高層大気から電子を奪い、その電子がイオン中で脱励起する際に軟 X 線を放出する。地球周辺 CX は太陽風の変動に伴って数時間スケールで強度変動しているため (Snowden et al. 1994 ApJ)、全ての地球周回衛星による天体観測の前景雑音として重要である。一方で、太陽風観測衛星のプラズマフラックスを用いれば、発光強度から希薄で観測が困難な中性大気の密度分布を推定でき、さらには発光場所から磁気圏の衝撃波や境界面を可視化できると期待されている (江副 2018 天文月報)。特に太陽風プラズマまたは中性大気の密度が高くなるシースやカスプ付近が明るくなると予想されているが、その正確な時空間構造は未だ不明である。

我々は地球周辺 CX に対して感度が高い「すざく」衛星の全公開データの系統解析を進めてきた (Ezeo et al. 2011 PASJ, Ishikawa et al. 2013, Ishi et al. 2019 PASJ)。天体以外の領域の軟 X 線の有意な時間変動および太陽風変動との有意な時間相関を評価することで、全 3055 データ (2005 年 8 月-2015 年 5 月) から約 90 例の発光イベントを検出している (石川 2013 博士論文, Ishi et al. 2017 Proc. XRU)。カスプを含む様々な方向からの地球周辺 CX を捉えることに成功したが、一つの衛星データだけでは、観測可能な領域が限られているため、その全体像を把握するのは容易ではない。

そこで我々は新たに XMM-Newton 衛星データの系統解析に着手した。「すざく」衛星は近地球軌道、XMM-Newton 衛星は長楕円軌道を周回しているため、両衛星の位置または観測時の視線方向の違いを利用すれば、3 次元的な発光分布を推定できる。「すざく」衛星で検出した約 90 例と観測時期が重なる XMM-Newton 衛星の約 100 データを解析した結果、両衛星で同時に発光が受かっているイベントを約 20 例見つけた。太陽風プロトンフラックスで規格化した発光強度を同時発光イベント毎に比較すると、昼側の磁気圏境界面を指向している衛星データの方が発光効率が高い傾向が見られた。これはシースやカスプ付近が明るくなるという従来の描像を示唆する。一方で、経験的な磁気圏モデルや既存の外圏密度モデルを用いて発光効率を計算したところ、観測に比べてモデル発光効率が 5-10 倍過小評価していることが分かった。本講演では、「すざく」と XMM-Newton 衛星を用いた系統解析の結果を報告するとともに、XRISM や GEO-X 衛星などによる将来観測の展望も議論する。

R006-09
Zoom meeting B ：11/1 AM2 (10:45-12:30)
11:45〜12:00

地球磁気圏 X 線撮像計画 GEO-X の現状

#江副 祐一郎 [1)], 船瀬 龍 [2,3)], 三好 由純 [4)], 石川 久美 [1)], 笠原 慧 [3)], 山崎 敦 [2)], 長谷川 洋 [2)], 三谷 烈史 [2)], 松本 洋介 [5)], 藤本 正樹 [2)], 上野 宗孝 [2)], 川勝 康弘 [2)], 岩田 隆浩 [2)], 沼澤 正樹 [6)], 細川 敬祐 [7)]
[1 東京都立大,[2JAXA 宇宙研,[3 東京大,[4 名古屋大,[5 千葉大,[6 理研,[7 電通大

Status of GEO-X (GEOspace X-ray imager) mission

#Yuichiro Ezoe[1)],Ryu Funase[2,3)],Yoshizumi Miyoshi[4)],Kumi Ishikawa[1)],Satoshi Kasahara[3)],Atsushi Yamazaki[2)],Hiroshi Hasegawa[2)],Takefumi Mitani[2)],Yosuke Matsumoto[5)],Masaki Fujimoto[2)],Munetaka Ueno[2)],Yasuhiro Kawakatsu[2)],Takahiro Iwata[2)],Masaki Numazawa[6)],Keisuke Hosokawa[7)]
[1Tokyo Metropolitan University,[2ISAS/JAXA,[3University of Tokyo,[4Nagoya University,[5Chiba University,[6RIKEN,[7UEC

GEO-X (GEO-space X-ray imager) aims to realize the visualization of the Earth’s magnetosphere by X-rays and to reveal dynamical couplings between solar wind and Earth’s magnetosphere. Most knowledge about the nature of the solar- magnetosphere interaction has been revealed through a number of in-situ observations by spacecrafts.

In recent years, soft X-ray emission associated with the magnetosphere. The emission originates from a charge exchange (CX) reaction between solar wind ions and geocorona (neutral gas of the exosphere). Using the Japanese ”Suzaku” satellite launched in 2005, we have studied the CX emission and have proposed the idea to realize the global imaging of the dayside magnetosphere with he CX emission. However, this idea can not be demonstrated by conventional X-ray astronomy satellites due to narrow field observation from low altitude.

We thus develop a new satellite GEO-X having a large delta v system to increase an apogee altitude to the vicinity of Moon. It will carry a novel compact and high sensitivity X-ray imaging spectrometer using cutting edge instrument technologies. In this paper, we outline the GEO-X mission and present development status.

GEO-X (GEOspace X-ray imager) は世界初の X 線による地球磁気圏の可視化を実現し、ダイナミックに変動する地球磁気圏の姿を明らかにすることを目的とした衛星計画である。太陽風と地球磁場の相互作用によって形作られる地球磁気圏は「その場」のプラズマ計測によって理解が進んできた。しかし、広大な磁気圏を点で繋ぐため、大局構造の把握やその過渡的な応答といった重要課題は点観測を補間して議論する必要がある。

一方で近年、 X 線天文衛星「すざく」などの観測において、地球磁気圏起因と考えられるX線放射が発見されてきた。太陽風に含まれる酸素や炭素などのイオンが地球の高層大気である外圏の主に水素原子から電子を奪う電荷交換反応に伴う X 線である。我々は 2005 年に打ち上げられた「すざく」衛星のデータ解析を進める中で、X線で昼側磁気圏境界面を可視化できることに気が付いた。しかし X 線天文衛星による観測は遠方天体を主な観測対象とするため、放射源である磁気圏内からの狭い視野の観測であり、未実証である。

そこで我々は地球磁気圏 X 線撮像を実現する衛星計画 GEO-X を推進している。相乗り打ち上げから磁気圏外すなわち月付近の高度まで出るための大推力の推進系付きの超小型衛星に、広がった軟X線放射を捉えるための超軽量撮像分光装置を搭載する。本講演では計画の現状と将来展望について述べる。

R006-10
Zoom meeting B ：11/1 PM1 (13:45-15:30)
13:45〜14:00

Field-aligned low-energy O+ (FALEO) ion flux enhancements in the inner magnetosphere: A possible source of warm plasma cloak

#Masahito Nose[1)],Ayako Matsuoka[2)],Yoshizumi Miyoshi[3)],Kazushi Asamura[4)],Tomoaki Hori[3)],Mariko Teramoto[5)],Iku Shinohara[6)],Masafumi Hirahara[1)],Craig A. Kletzing[7)],Charles W. Smith[8)],Robert J. Macdowall[9)],Harlan Spence[10)],Geoff Reeves[11)]
([1]ISEE, Nagoya Univ.,[2]Kyoto University,[3]ISEE, Nagoya Univ.,[4]ISAS/JAXA,[5]Kyutech,[6]ISAS/JAXA,[7]Department of Physics and Astronomy, UoI,[8]Department of Physics, UNH,[9]NASA/GSFC,[10]Univ. New Hampshire,[11]LANL

Recent satellite observations in the inner magnetosphere have shown that unidirectional/bidirectional energy-dispersed O+ flux appears a few minutes after substorms in the inner magnetosphere and lasts for >10 min with a decrease in its energy from ˜5 keV to 10-100 eV [Chaston et al., 2015; Kistler et al., 2016; Nose et al., 2016, 2018, 2021; Gkioulidou et al., 2019; Hull et al., 2019]. From the Van Allen Probes observations, Nose et al. [2016] revealed that the unidirectional energy-dispersed O+ flux is observed in 80% of the total events and that its direction is parallel (antiparallel) to the magnetic field when the satellites are located below (above) the geomagnetic equator. This strongly implies that these O+ ions are extracted from the ionosphere at the onset of substorms and flow along the magnetic field toward the geomagnetic equator. The similar features of the O+ flux enhancements were also observed by the Arase satellite in the more inner magnetosphere and at the higher geomagnetic latitudes [Nose et al., 2018, 2021]. These field-aligned low-energy O+ (FALEO) ions experience pitch angle scattering near the geomagnetic equator and remain bouncing between both hemispheres. They drift eastward because of their low energy (<1 keV) and can contribute to the O+ content of the inner magnetospheric plasma such as the warm plasma cloak and the oxygen torus. A resultant increase in the O+ density may provide a precondition for the O+-rich ring current.

In the present study, we examine FALEO flux enhancements simultaneously observed by multiple satellites, Arase, Van Allen Probe A and B satellite, on September 22, 2018. The O+ fluxes are enhanced after the substorm onset at 05:24 UT, at which three satellites are located in the nightside inner magnetosphere (Arase at MLT=0.3 hr, L=6.2, GMLAT=— 9.6 deg; Probe A at MLT=0.7 hr, L=5.5, GMLAT=14.7 deg; Probe B at MLT=0.0 hr, L=5.3, GMLAT=10.6 deg). Arase observes FALEO only in the parallel direction to the magnetic field in the energy range from a few keV to 100 eV. Probes A and B, however, identify FALEO in both parallel and antiparallel directions at a few keV to 10 eV. The antiparallel fluxes appear earlier than the parallel fluxes. Multiband flux structure is clearly observed by Probe A. We perform a numerical calculation of O+ ion trajectories to reproduce the observed E-t spectrograms at three satellites. In the presentation, we will show the results of data analysis and numerical simulation in more detail, and discuss the contribution of FALEO to the O+ content of the inner magnetospheric background plasma.

R006-11
Zoom meeting B ：11/1 PM1 (13:45-15:30)
14:00〜14:15

Contribution of magnetospheric pressure inhomogeneities to SAPS Wave Structures: Arase and SuperDARN conjugated observations

#Takehiro Fukami[1)],Atsushi Kumamoto[2)],Yuto Katoh[1)],Nozomu Nishitani[3)],Tomoaki Hori[3)],Yasumasa Kasaba[4)],Fuminori Tsuchiya[2)],Mariko Teramoto[5)],Tomoki Kimura[6)],Yoshiya Kasahara[7)],Masafumi Shoji[3)],Satoko Nakamura[8)],Masahiro Kitahara[3)],Ayako Matsuoka[9)],Shun Imajo[10)],Satoshi Kasahara[11)],Shoichiro Yokota[12)],Kunihiro Keika[13)],Yoichi Kazama[14)],Shiang-Yu Wang[15)],ChaeWoo Jun[16)],Kazushi Asamura[17)],Yoshizumi Miyoshi[3)],Iku Shinohara[18)],Simon G. Shepherd[19)]
([1]Dept. Geophys., Grad. Sch. Sci., Tohoku Univ.,[2]Planet. Plasma Atmos. Res. Cent., Tohoku Univ.,[3]ISEE, Nagoya Univ.,[4]Tohoku Univ.,[5]Kyutech,[6]Tokyo University of Science,[7]Kanazawa Univ.,[8]ISEE,[9]Kyoto University,[10]ISEE, Nagoya Univ.,[11]The University of Tokyo,[12]Osaka Univ.,[13]University of Tokyo,[14]ASIAA,[15]Institute of Astronomy and Astrophysics, Academia Sinica, Taiwan,[16]ISEE, Nagoya Univ.,[17]ISAS/JAXA,[18]ISAS/JAXA,[19]Dartmouth College

Contribution of magnetospheric pressure inhomogeneities to SAPS Wave Structures (SAPSWS) is investigated on the basis of the case analyses of conjugated Arase satellite and SuperDARN observations.

Erickson et al. (2002) reported substructures with a scale size of tens of km within SAPS. Mishin and Burke (2005) called them ”SAPSWS”, and reported that high-temperature ions were transported into the inner magnetosphere and showed energy dispersion (ion nose structure) when the electromagnetic field fluctuations of SAPSWS were observed. Using the numerical simulation of hot plasma dynamics in the inner magnetosphere coupled with the ionosphere, Ebihara et al. (2009) showed that hot plasma with a complex pressure distribution could contribute to variations of SAPS.

Further detailed comparisons among electromagnetic field and hot ions in the magnetosphere and flow in the ionosphere are important for understanding the mechanism of SAPSWS. So, We analyzed data from conjugate Arase and SuperDARN Christmas Valley East (CVE) radar observations during 2:30 to 3:00 UT on 9 July 2017.

From the CVE radar observation, we obtained 2-dimensional flow distributions of SAPSWS with velocity fluctuations of 200 m/s near the ionospheric footprint of Arase, assuming that the flows are zonally-directed. These structures extended over at least 0.5 h MLT azimuthally, separated latitudinally at intervals of ˜230 km, and moved equatorward. Near the magnetic equator, Arase encountered electric field variations with an amplitude of 2.5 mV/m and a period of 5-6 minutes in the ion nose structure, during an outbound pass from L = 3.2 to 5.4 around 20 h MLT. The isotropic pressure of hot ions was derived from ion flux in an energy range of 10-180 keV. Variations of the eastward magnetic field and the ion pressure were roughly in phase and had a close period to that of the electric field variations. The phase relation and flow distribution in the ionosphere suggested that earthward hot ions with fine pressure inhomogeneities generate field-aligned currents in the inner magnetosphere and thereby cause SAPSWS.

We consider substorm-related plasma sheet flow channels [e.g. Lyons et al. (2012)] and interchange instability in the inner magnetosphere [Sazykin et al. (2002)] could generate such pressure inhomogeneities in the magnetosphere. In conjugate Arase and SuperDARN observation event, GOES-13 observed dipolarization and an increase of proton flux around 21 h MLT at 2:19 UT. Equatorial projection of ionospheric flow structures along the magnetic field given by the Tsyganenko 04s model (T04s model; Tsyganenko & Sitnov, 2005) moved earthward from L˜6 to ˜4 during 2:30 to 3:00 UT. The movement may reflect earthward transportation of hot plasma driving fine-scale ionospheric flow. These results imply that substorm injection possibly contributes to the formation of pressure inhomogeneities in the inner magnetosphere and SAPSWS.

R006-12
Zoom meeting B ：11/1 PM1 (13:45-15:30)
14:15〜14:30

SuperDARN レーダーとあらせ衛星によるプラズマ圏境界/SAPS 領域周辺の電場・粒子観測: イベント解析初期結果

#高田 知弥[1)], 西谷 望[2)], 堀 智昭[2)],Shepherd Simon G.[3)], 笠羽 康正[4)], 熊本 篤志[5)], 加藤 雄人[6)], 笠原 禎也[7)], 小路 真史[2)], 中村 紗都子[8)], 北原 理弘[2)], 土屋 史紀[5)], 風間 洋一[10)], 浅村 和史[9)], 三好 由純[2)], 横田 勝一郎[11)], 笠原 慧[7,12)], 桂華 邦裕[13)], 松岡 彩子[14)], 今城 峻[15)], 篠原 育[16)]
([1]ISEE,[2] 名大 ISEE,[3]Dartmouth College,[4] 東北大・理,[5] 東北大・理・惑星プラズマ大気,[6] 東北大・理・地球物理,[7] 金沢大,[8] 京大・理・地球惑星,[9] 宇宙研,[10]ASIAA,[11] 大阪大,[12] 東京大学,[13] 東大・理,[14] 京都大学,[15] 京大・地磁気センター,[16] 宇宙研／宇宙機構

Observation of the ionospheric outflow associated with SAPS by SuperDARN radar and Arase

#Tomoya Takada[1)],Nozomu Nishitani[2)],Tomoaki Hori[2)],Simon G. Shepherd[3)],Yasumasa Kasaba[4)],Atsushi Kumamoto[5)],Yuto Katoh[6)],Yoshiya Kasahara[7)],Masafumi Shoji[2)],Satoko Nakamura[8)],Masahiro Kitahara[2)],Fuminori Tsuchiya[5)],Yoichi Kazama[10)], Kazushi Asamura[9)],Yoshizumi Miyoshi[2)],Shoichiro Yokota[11)],Satoshi Kasahara[7,12)],Kunihiro Keika[13)],Ayako Matsuoka[14)],Shun Imajo[15)],Iku Shinohara[16)]
([1]ISEE,[2]ISEE, Nagoya Univ.,[3]Dartmouth College,[4]Tohoku Univ.,[5]Planet. Plasma Atmos. Res. Cent., Tohoku Univ.,[6]Dept. Geophys., Grad. Sch. Sci., Tohoku Univ.,[7]Kanazawa Univ.,[8]Dept. of Geophys., Kyoto Univ.,[9]ISAS/JAXA,[10]ASIAA,[11]Osaka Univ.,[12]The University of Tokyo,[13]University of Tokyo,[14]Kyoto University,[15]WDC for Geomagnetism, Kyoto, Kyoto University,[16]ISAS/JAXA

The ionospheric upflow plays a significant role in the ionosphere-magnetosphere coupling as one of the generation mechanisms of escaping ionospheric particles to the magnetosphere. It is known that the upflow occurs in the subauroral zone during Sub-Auroral Polarization Streams (SAPS). However, there is no study that investigates whether ionospheric particles actually escape to the magnetosphere in association with SAPS both in the ionosphere and the magnetosphere. In this study, simultaneous observations of the SAPS electric field were carried out by the SuperDARN radar and the Arase satellite. In 27 simultaneous observation events identified during the analyzed period from June 2017 to Dec. 2019, SAPS were observed by the SuperDARN radar near the calculated footprint of the Arase satellite, and in 20 events almost concurrently the satellite detected electric field enhancements greater than 2 mV/m. In association with the SAPS electric field, the satellite observed an increase of low energy (<1 keV) ions fluxes greater than 1.0x10^5 (s cm^2 sr eV)^-1in 12 events. We performed a statistical analysis of these low energy ion enhancement events.We performed a statistical analysis of these low energy ion enhancement events. The results show that when SAPS occurs, the low-energy ion flux with pitch angles around 0 and 180 degree increases 1.5 times greater than around 90 degree. The Detail of the relationship between these low-energy ion characteristics is discussed.

電離圏プラズマ上昇流は、磁気圏に電離圏粒子を流出させる要素として電離圏-磁気圏結合において非常に重要な役割を担っており、SAPS の発生に伴いサブオーロラ帯で上昇流が発生することが知られている。しかし、SAPS を電離圏/磁気圏の双方で観測し、実際に SAPS に伴い電離圏粒子が磁気圏に流出しているかを調べた研究はない。そこで、本研究では SuperDARN レーダーとあらせ衛星による、SAPS 電場の同時観測及びに、あらせ衛星による粒子観測のデータを解析し、SAPS と電離圏イオン流出との関係について調べた。結果として、2017 年 6 月から 2019 年 12 月までの 27 の同時観測イベントにおいて、20 個のイベントで、あらせ衛星の footprint が SAPS 構造付近を通過した際に、共役関係にある磁気圏側でも 2 mV/m 以上の電場構造を観測することができた。 加えて 12 個のイベントで、SAPS 電場の存在する領域に対応して、あらせ衛星の粒子データで 1.0 × 10^5 (s cm^2 sr eV)^(-1) 以上の低エネルギーイオンフラックスの増大が見られた。 このイオンフラックスの増大についての統計研究を行った結果、SAPS 発生時は、SAPS が発生していない場合にくらべて低エネルギーイオンフラックスがピッチ角 0 °、180 °方向においてピッチ角 90 °方向に比べて 1.5 以上増大していることが見られた 。この特徴的な粒子分布と電場・対流分布との対応関係について講演で報告・議論する。

R006-13
Zoom meeting B ：11/1 PM1 (13:45-15:30)
14:30〜14:45

second harmonic poloidal ULF 波動によるリングカレント陽子の動径輸送：あらせ・RBSP-B 衛星の観測

#山本 和弘 [1)], 関 華奈子 [2)], 能勢 正仁 [3)], 松岡 彩子 [4)], 寺本 万里子 [5)], 野村 麗子 [6)], 笠原 慧 [7)], 横田 勝一郎 [8)], 桂華 邦裕 [9)], 堀 智昭 [10)], 浅村 和史 [11)], 三好 由純 [12)], 笠原 禎也 [13)], 熊本 篤志 [14)], 土屋 史紀 [15)], 小路 真史 [16)], 中村 紗都子 [17)], 北原 理弘 [18)], 篠原 育 [19)], リーブス ジェフ [20)], スペンス ハラン [21)]
([1 東大・理・地惑,([2 東大理・地球惑星科学専攻,([3 名大・宇地研,([4 京都大学,([5 九工大,([6NAOJ,([7 東京大学,([8 大阪大,([9 東大・理,([10 名大 ISEE,([11 宇宙研,([12 名大 ISEE,([13 金沢大,([14 東北大・理・地球物理,([15 東北大・理・惑星プラズマ大気,([16 名大 ISEE,([17 名大 ISEE,([18 名大 ISEE,([19 宇宙研／宇宙機構,([20 ロスアラモス国立研究所,([21 ニューハンプシャー大学

Radial transport of ring current protons by second harmonic poloidal standing Alfven waves: Arase and RBSP-B observations

#Kazuhiro Yamamoto[1)],Kanako Seki[2)],Masahito Nose[3)],Ayako Matsuoka[4)],Mariko Teramoto[5)],Reiko Nomura[6)],
Satoshi Kasahara[7)],
Shoichiro Yokota[8)],Kunihiro Keika{sup
([1UTokyo,([2Dept. Earth & Planetary Sci., Science, Univ. Tokyo,([3ISEE, Nagoya Univ.,([4Kyoto University,([5Kyutech,([6NAOJ,
([7The University of Tokyo,([8Osaka Univ.,([9University of Tokyo,([10ISEE, Nagoya Univ.,([11ISAS/JAXA,([12ISEE, Nagoya Univ.,
([13Kanazawa Univ.,([14Dept. Geophys, Tohoku Univ.,([15Planet. Plasma Atmos. Res. Cent., Tohoku Univ.,([16ISEE, Nagoya Univ.,([17ISEE, Nagoya Univ.,([18ISEE, Nagoya Univ.,([19ISAS/JAXA,([20LANL,([21Univ. New Hampshire

Poloidal standing Alfven waves can obtain their energy from an energy gradient or radial gradient in the phase space density of resonant particles through the drift-bounce resonance. Because the temporal and spatial variations of low energy (1-10 keV) ions are more complicated than high energy (>100 keV) ions, the importance of the low energy ions in the excitation of the poloidal waves has not been fully understood.

In this study, we examine an event with second harmonic poloidal waves observed by the Arase satellite and demonstrate that the poloidal waves were excited by ˜12 keV protons. The azimuthal wave (m) number was estimated to be positive (eastward propagation) and ˜180, based on the finite Larmor radius effect of protons and the theory of the drift-bounce resonance. The steep outward gradient of the proton phase space density well corresponds to the exciting regions of waves (L = 5.7-6.1), suggesting that the outward gradient of protons supplies free energy to the waves.

The time variation of radial distributions of the resonant protons was measured by the Arase and RBSP-B satellites. At L ˜5.7, RBSP-B measured a sudden increase of ˜10 keV protons 1.5 hours after the wave excitation detected by Arase. Evaluating the diffusion coefficient (D{sub}LL{¥sub}) and energy variation of protons with L (dW/dL) given in the analytical formulae, we find that protons can move ˜0.4 Re inward in 1.5 hours and simultaneously lose their energy by ˜2 keV through the drift-bounce resonance. We interpret the sudden flux increase at ˜10 keV as a result of the radial diffusion of ˜12 keV protons.

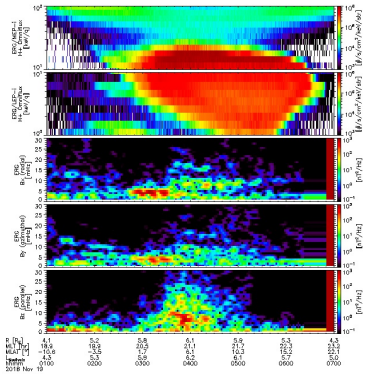

R006-14
Zoom meeting B ：11/1 PM1 (13:45-15:30)
14:45〜15:00

Two types of storm-time Pc5 ULF waves excited in the Magnetosphere-Ionosphere coupled model

#Tomotsugu Yamakawa[3)],Kanako Seki[2)],Takanobu Amano[1)],Naoko Takahashi[5)],Yoshizumi Miyoshi[4)],Aoi Nakamizo[5)]
([1]University of Tokyo,[2]Dept. Earth & Planetary Sci., Science, Univ. Tokyo,[3]The University of Tokyo,[4]ISEE, Nagoya Univ.,[5]NICT

Storm-time Pc5 ULF waves are electromagnetic pulsations (1.67-6.67 mHz), which can be generated by ring current ions associated with the injection from the magnetotail during substorms. The excitation mechanism and global distribution of ULF waves are keys to understand the dynamic variation of the outer radiation belt, since they can drive radial transport of radiation belt electrons [e.g. Elkington et al., 2003]. Theoretically, drift-bounce resonance has been considered to be a candidate excitation mechanism [Southwood, 1976]. Previous spacecraft observations suggest both drift resonance and drift-bounce resonance excitation of ULF waves [e.g. Dai et al., 2013; Oimatsu et al., 2018]. Recently, Yamakawa et al. [2020] could reproduce both the drift resonance and drift-bounce resonance excitation of ULF waves in the global drift-kinetic simulation. However the amplitude of the excited ULF waves is too small compared to spacecraft observations. One possible reason is the damping of field fluctuations at the ionospheric boundary in the model.

In order to improve the ionospheric boundary condition, we have made Magnetosphere-Ionosphere coupling between GEMSIS-RC [Amano et al., 2011] and GEMSIS-POT model [Nakamizo et al., 2012]. We use GEMSIS-RC model in the inner magnetosphere, in which 5D drift-kinetic equation for the PSD of ions and Maxwell equations are solved self-consistently. GEMSIS-POT is a 2-D potential solver in the ionosphere. We use FAC from GEMSIS-RC as an input to GEMSIS-POT for the Region 2 current. The resultant electric field potential is then used as the ionospheric boundary condition of GEMSIS-RC. The coupled model enables us to simulate ion injection from the plasma sheet into the inner magnetosphere.

Simulation results have shown the excitation of two types of Pc5 ULF waves. First, we find the drift resonance excitation of Pc5 waves (P1 waves) in the dayside. They are driven by the positive energy gradient of the PSD of ions with the energy of 50-120 keV. Second, Pc5 waves excited associated with the drift-bounce resonance (P2 waves) are seen in the duskside. They are driven by the inward gradient of the PSD of ions with the energy of 70-90 keV. We find that power spectra and wave frequency of P2 waves are enhanced if we increase the intensity of Region 1 FAC, which is not true for P1 waves. We will also report on what determines the wave frequency and azimuthal wave number of ULF waves and the effects of Region 2 FAC related electric field on the excitation of ULF waves.

R006-15
Zoom meeting B ：11/1 PM1 (13:45-15:30)
15:00〜15:15

A statistical survey of Pc5 waves observed in the dusk and night sectors

#Kento Otani[1,7],Iku Shinohara[2],Mariko Teramoto[3],Kazuhiro Yamamoto[4],Kanako Seki[5],Tomotsugu Yamakawa[6],Naoko Takahashi[13],Kunihiro Keika[6],Satoshi Kasahara[8],Ayako Matsuoka[9],Kenji Mitani[10],Shoichiro Yokota[11],Nana Higashio[12]

[1]Tokyo University,[2]ISAS/JAXA,[3]Kyutech,[4]UTokyo,[5]Dept. Earth & Planetary Sci., Science, Univ. Tokyo,[6]University of Tokyo,[7]The University of Tokyo,[8]The University of Tokyo,[9]Kyoto University,[10]ISEE, Nagoya Univ.,[11]Osaka Univ.,[12]JAXA,[13]NICT

A statistical survey of Pc5 waves observed in the dusk and night sectors

Storm-time Pc5 waves are one of the candidate processes that cause the radial diffusion into the inner magnetosphere. They are thought to be excited by ion-injections from magnetotail to the ring current. Recently, Yamakawa et al. (2019) demonstrate that Pc5 waves can be excited by ion injections through the drift resonance by a numerical simulation. In this paper, we intend to address the Pc5 excitation process based on recent satellite observations.

According to the results of Yamakawa et al. (2019), a pattern of frequency evolution at an observation point is a characteristic feature of Pc5 waves excited by the drift resonance. We have statistically studied Pc5 wave events that show the same frequency evolution pattern observed in the numerical simulation, using the magnetic field observation of Arase (ERG).

We have surveyed data obtained from 24 March 2017 to 31 December 2020. As a result, the number of events observed in the dusk and midnight sectors tends to be larger than in other sectors, compared with the past Pc5 statistics (e.g., Liu et al. 2009). However, since there are still possibilities that our events are contaminated by the other phenomena, such as the wider broadband magnetic field fluctuations like Pi2, we are still checking the detailed properties of selected waves. The present result is obtained by the survey of only the poloidal component of the magnetic fields. We are doing an extend-study of all the three magnetic field components, not only poloidal but also toroidal and compressional components. Moreover, by introducing an additional restriction based on FWHM, we also examine how waveforms of the selected events are far from the sinusoidal wave. We are also investigating the relationship between ion injections and the selected Pc5 events to check the consistency of the drift resonance theory. We will discuss the excitation mechanisms of the observed Pc5 events based on the above analysis results.

R006-16
Zoom meeting B ：11/1 PM2 (15:45-18:15)
15:45〜16:00

磁気赤道周辺での kinetic Alfven wave による電子加速過程に関するテスト粒子計算

#齋藤 幸碩 [1)], 加藤 雄人 [1)], 北原 理弘 [2)], 川面 洋平 [1,4)], 木村 智樹 [3)], 熊本 篤志 [1)]
([1] 東北大・理・地球物理,[2] 名大 ISEE,[3] 東京理科大,[4] 東北大・学際科学フロンティア研究所

Test particle simulation of the electron acceleration process by kinetic Alfven waves around the magnetic equator

#Koseki Saito[1)],Yuto Katoh[1)],Masahiro Kitahara[2)],Yohei Kawazura[1,4)],Tomoki Kimura[3)],Atsushi Kumamoto[1)]
([1]Dept. Geophys., Grad. Sch. Sci., Tohoku Univ.,[2]ISEE, Nagoya Univ.,[3]Tokyo University of Science,[4]Frontier Research Institute for Interdisciplinary Sciences, Tohoku Univ.

Observation from the FAST satellite revealed the downward electrons in the energy range from tens eV to a few keV in the terrestrial high latitude region [Chaston et al., 2002], suggesting that “Alfvenic acceleration” process by dispersive Alfven waves is responsible for the auroral electron precipitation. Alfvenic acceleration has also been studied around the magnetic equator [Artemyev et al., 2015] and in Jupiter [Mauk et al., 2017; Saur et al., 2018]. While these previous studies suggested the critical roles of Alfvenic acceleration in magnetized planets, physical processes controlling the characteristic energy and pitch angle distributions have been still unclear. In this study, to consider the contribution of electron acceleration by kinetic Alfven waves, we develop a test particle code based on the method of Kitahara and Katoh (2019).

First, we perform simulations for ˜500 eV electrons to reproduce the contribution of electron acceleration due to the parallel electric field of kinetic Alfven waves in the terrestrial magnetosphere at L=9, considered by Artemyev et al. (2015). Artemyev et al. (2015) discussed the contribution of the electrostatic component of kinetic Alfvenic waves to electron acceleration and found that electrons of ˜500 eV and equatorial pitch angle α_{eq} ˜80 degrees are accelerated to a few keV. Based on the simulation results obtained in the same initial condition, we discuss the validity of the developed simulation code. Second, we perform simulations incorporating the electromagnetic components of kinetic Alfven waves, neglected in Artemyev et al. (2015). In addition, we carry out simulations under the background condition of the magnetospheric plasma obtained by Plasma Distribution Solver (PDS) [Saito et al., P-EM09-P12, JpGU Meeting, 2021]. The PDS enables us to obtain plasma distribution precisely satisfying boundary conditions of the magnetosphere/ionosphere, which is essentially important in determining the properties of kinetic Alfven waves along a field line. Based on the simulation results, we study the fundamental physics governing Alfvenic acceleration in the magnetosphere.

FAST 衛星の観測により、地球の高緯度領域にて数十 eV から数 keV に至る幅広いエネルギー帯におけるオーロラ電子降下が確認された [Chaston et al., 2002]。このオーロラ電子降下は分散性 Alfven 波による「Alfvenic 加速」によるものと考えられている。Alfvenic 加速は磁気赤道周辺での現象にも適用され [Artemyev et al., 2015]、木星における電子加速機構としても注目されるなど [Mauk et al., 2017; Saur et al., 2018]、磁化惑星における電子加速過程での Alfvenic 加速の重要性は高まっている。一方で、被加速電子の特徴的なエネルギー分布やピッチ角分布を決定づける要因については未解明の問題が残されている。本研究では、kinetic Alfven wave による電子加速過程への寄与を定量的に考察することを目的として、Kitahara and Katoh (2019) の手法を参考としたテスト粒子計算コードを開発して、シミュレーションを実施する。

本研究ではまず、Artemyev et al. (2015) で考えられている地球磁気圏 L=9 での kintetic Alfven wave の磁力線平行方向の電場による電子加速の寄与について、˜500 eV の電子を対象としてテスト粒子計算を行う。Artemyev et al. (2015) では、kinetic Alfven wave の静電成分による電子加速の寄与について考察されており、磁気赤道でのピッチ角が 80 ° 付近で˜500 eV の電子が Kinetic Alfven wave によって数 keV まで加速されることを明らかにしている。次に、Artemyev et al. (2015) では考慮されていない kinetic Alfven wave の磁力線垂直方向の電場と磁場、更に磁力線平行方向の磁場成分を組み込んでテスト粒子計算を行い、波の電磁場各成分による電子加速の寄与について考察する。さらに本研究では、独自に開発した Plasma Distribution Solver [Saito et al., P-EM09-P12, JpGU Meeting, 2021] を用いて、磁気圏・電離圏側の境界条件を厳密に満たすプラズマ分布を求め、初期条件として設定したテスト粒子計算を実施する。電子加速過程の考察においては、背景の磁気圏プラズマの空間分布が、kinetic Alfven wave の性質を決定づけるパラメータとして重要となる。シミュレーション結果に基づいて、Alfvenic 加速の物理素過程について究明する。

R006-17
Zoom meeting B ：11/1 PM2 (15:45-18:15)
16:00〜16:15

地球内部磁気圏における Toroidal mode ULF wave による高エネルギー電子のフラックス増強のシミュレーション研究

#礒野 航 [1)], 加藤 雄人 [1)], 川面 洋平 [3)], 熊本 篤志 [2)]
([1] 東北大・理・地球物理,[2] 東北大・理・地球物理,[3] 東北大学 学際科学フロンティア研究所

Simulation study of the flux enhancement of energetic electrons due to toroidal mode ULF waves in the Earth's inner magnetosphere

#Isono Ko[1)],Yuto Katoh[1)],Yohei Kawazura[3)],Atsushi Kumamoto[2)]
([1]Dept. Geophys., Grad. Sch. Sci., Tohoku Univ.,[2]Dept. Geophys, Tohoku Univ.,[3]Frontier Research Institute for Interdisciplinary Sciences Tohoku University

Previous studies revealed that whistler-mode chorus emissions are generated around the magnetic equatorial plane with a period typically ranging from a few seconds to several minutes [Santolik et al.,2003]. While detailed physics controlling the periodicity has been unsolved, Jaynes et al. (2015) and Zhang et al.(2019) pointed out that the periodic enhancement of chorus emission correlated with toroidal mode ULF waves. Since chorus emissions are generated through an instability driven by keV electrons with temperature anisotropy, the observed correlation suggests that toroidal mode ULF waves are responsible for the temperature anisotropy of energetic electrons. Ono et al. (P-EM19-P08, JpGU-AGU Joint Meeting, 2020) analyzed observation data of the Arase satellite and identified the simultaneous enhancement of chorus emissions and electrons in the energy range of tens of keV, correlated with toroidal mode ULF waves. Ono et al. proposed a mechanism for the modulation of energetic electrons by a toroidal mode ULF wave.

In the present study, we attempted to determine the extent to which high-energy electrons are modulated by toroidal mode ULF waves by using numerical simulations. We used the drift kinetic equation[littlejohn, 1981] to investigate how the spatial distribution of electrons with a pitch angle of 90 degrees changes by toroidal mode ULF wave. The simulation system is assumed to be spatially one-dimensional the longitude direction at L=6 on the magnetic equatorial plane. The system size corresponded to one wavelength of the ULF wave and was divided into 128 grid points, and the time step was set to satisfy the Courant number. We carried out calculations in the time scale corresponding to several periods of the ULF wave cycles.

Simulation results show that the toroidal mode ULF wave causes a change in the density of electrons in the keV energy range. It is suggested that the modulation is greatly affected by the relationship among three characteristic velocities: the phase velocity of the ULF wave, the velocity of the ExB drift of electrons induced by the ULF wave, and the velocity of the grad B drift of electrons. In particular, under a condition where the velocity difference between the grad B drift velocity and the phase velocity of the ULF wave is sufficiently small, electrons are highly concentrated in the same phase of the toroidal mode ULF wave oscillation as reported by Ono et al. Our simulation results clarified that the proposed model is capable of explaining the observed flux variation of energetic electrons.

ホイッスラーモード・コーラス放射は磁気赤道周辺を源として、数秒から数分の周期で周期的に発生することが知られている [Santolik et al., 2003]。コーラス放射の周期性を決定する要因については未解明の問題が多く残されているが、Toroidal mode ULF wave との相関があることが指摘されている [Jaynes et al., 2015; Zhang et al., 2019]。コーラス放射は温度異方性を持った keV 帯の電子によるプラズマ不安定性に起因して発生することから、Toroidal mode ULF wave が高エネルギー電子の温度異方性を引き起こしている可能性が示唆される。Toroidal mode ULF wave による電子の変調については、ドリフト共鳴による MeV 帯の電子のフラックス変動機構 [Elkington et al., 1999] が提案されているが、keV 帯の電子のダイナミクスへの影響は未だ明らかになっていない。Ono et al. (P-EM19-P08, JpGU-AGU Joint Meeting, 2020) では keV 帯の電子のフラックスが Toroidal mode ULF wave の周期と同期して変動する様相が見出され、波動電場成分によるドリフト速度の変調に基づいたモデルが提案されている。しかし定性的な議論にとどまっており、 提案されたメカニズムによってどの程度電子が変調するのかは課題として残されていた。

本研究では、Littlejohn(1981) による drift 運動論の式を用いた数値シミュレーションを実施し、Toroidal mode ULF wave によりもたらされる高エネルギー電子のフラックスの変動を定量的に調べた。ピッチ角 90 度の電子を対象として 1 次元のシミュレーション空間を、磁気赤道平面上の L=6 における経度方向の 1 次元の空間に沿って設定し、ULF wave によって実空間上の分布関数がどのように変化するのかを調べた。系の大きさは ULF wave 1 波長分の長さとして、これを 128 分割し、クーラン数が適切な大きさになるように時間刻み幅を設定して、ULFwave 数周期分の時間について計算を行った。

シミュレーションの結果、Toroidal mode ULF wave が keV 帯の電子の密度に変化をもたらす様相が再現された。その変調の大きさは、3 つの特性速度、すなわち、ULF wave の位相速度、ULF wave によって誘起される電子の E × B drift の速度、ならびに電子の grad B drift の速度の関係によって大きく影響されることが示唆された。特に grad B drift の速度と ULF wave の位相速度の速度差が十分に小さい条件では、Ono et al. で示された観測結果における粒子が集中した位相と同位相に電子が集中し、初期条件で与えた値の 40 倍程度にまで数密度が上昇することが明らかとなった。この結果は Ono et al. により見出された観測結果が、Toroidal mode ULF wave による高エネルギー電子フラックス変

動メカニズムによって説明しうることを示している。

R006-18
Zoom meeting B ：11/1 PM2 (15:45-18:15)
16:15〜16:30

The interaction of sub-relativistic electrons with high-latitude propagating chorus waves observed by the Arase satellite

#Taku Namekawa[1)],Iku Shinohara[2)],Takefumi Mitani[3)],Kazushi Asamura[3)],Tomoaki Hori[4)],Ayako Matsuoka[5)],Shoya Matsuda[6)], Yoshiya Kasahara[7)],Satoshi Kasahara[8)],Shoichiro Yokota[9)],Satoko Nakamura[10)],Masahiro Kitahara[4)],Yoshizumi Miyoshi[4)]
([1]Earth and Planetary Science, Tokyo Univ.,([2]ISAS/JAXA,([3]ISAS/JAXA,([4]ISEE, Nagoya Univ.,([5]Kyoto University,([6]ISAS/JAXA, ([7]Kanazawa Univ.,([8]The University of Tokyo,([9]Osaka Univ.,([10]Dept. Of Geophys., Kyoto Univ.

This study addresses the wave-particle interactions between sub-relativistic electrons and plasma waves at high latitudes by examining the direct measurements made by the Arase satellite. Past studies suggest that whistler-mode chorus waves propagating along the magnetic field lines toward higher latitudes cause precipitation of electrons over a wide energy range from a few keV to several MeV , leading to sub-relativistic/relativistic electron microbursts [e.g., Miyoshi 2020]. However, no direct observational evidence has been obtained so far.

We analyzed data obtained by the HEP [Mitani et al., 2018] and PWE [Kasahara et al., 2018] instruments onboard the Arase satellite [Miyoshi et al., 2018] and found several events in which electrons of several hundreds of keV traveling in the direction of the magnetic field lines show similar fluctuations to those in the wave intensity. In particular, for the event on September 26, 2019, significant sub-relativistic electron flux variations in the direction of the magnetic field lines corresponding to the wave fluctuations were observed at 40 degrees in magnetic latitude. These results may indicate direct observational evidence of the interaction between sub-relativistic electrons and chorus waves at high latitudes, although rigorous verification still needs to be done to prove this with statistical significance.

R006-19
Zoom meeting B ：11/1 PM2 (15:45-18:15)
16:30〜16:45

Effect of quasi-steady scattering on pulsating aurora

#Kazuteru Takahashi[1)],Shinji Saito[2)],Yoshizumi Miyoshi[3)],Kohei Toyama[4)],Kazushi Asamura[5)],Keisuke Hosokawa[6)]
([1]ISEE, Nagoya Univ.,[2]NICT,[3]ISEE, Nagoya Univ.,[4]ISEE, Nagoya Univ.,[5]ISAS/JAXA,[6]UEC

We have studied non-linear wave-particle interactions caused by chorus waves and electrons using the test particle-simulation, GEMSIS-RBW (Saito+, 2012). Using the GEMSIS-RBW, we have studied wave-particle interaction processes contributing atmospheric burst precipitation of energetic electrons such as microbursts and pulsating aurora. In addition to the burst precipitation, quasi-steady precipitation caused by weak-amplitude waves also occurs in the magnetosphere. The quasi-linear approach using the Fokker-Planck equation has been used as a plausible model in previous research. In order to include such quasi-steady precipitations in GEMSIS-RBW, we develop a quasi-linear wave-particle interaction model by adopting stochastic differential equation (SDE) that are equivalent to the Fokker-Planck equation. In this presentation, we present the effect of quasi-steady precipitation on the electron precipitation for pulsating aurora.

R006-20
Zoom meeting B ：11/1 PM2 (15:45-18:15)
16:45〜17:00

Role of nonlinear WPI in energetic electron precipitation by oblique chorus emissions in the outer radiation belt

#Yikai Hsieh[1)],Yoshiharu Omura[2)]
([1]RISH, Kyoto Univ.,([2]RISH, Kyoto Univ.

Energetic electron accelerations and precipitations in the Earth's outer radiation belt are highly associated with wave-particle interactions between whistler mode chorus waves and electrons. We perform test particle simulation to investigate electrons interacting with both parallel and obliquely propagating whistler mode chorus emissions at L=4.5. We build up a database of the Green's functions, which are treated as results of the input electrons interacting with one emission, for a large number of electrons. The loss process of electron fluxes interacting with consecutive chorus emissions is traced by applying the convolution integrals of distribution functions and the Green's functions. By checking the resonance condition and resonant energy, we find that the nonlinear scattering via cyclotron resonance is the main process that pushes energetic electrons into the loss cone in both parallel and oblique cases. Our simulation results show that obliquely propagating chorus causes more energetic electron precipitation than parallel propagating chorus because of the combination of nonlinear trapping via Landau resonance and nonlinear scattering via cyclotron resonance. The precipitation rates at 200keV to MeV of the oblique case agree with observations, while the precipitation rates at MeV of the parallel case is much lower than observations.

We propose a 2-step precipitation process for oblique chorus emissions that contributes to more electron loss: (1) During the first chorus emission, the nonlinear trapping of Landau resonance moves an electron near the loss cone. (2) During the second emission, the nonlinear scattering of cyclotron resonance scatters the electron into the loss cone.

References

[1] Hsieh Y.-K., Kubota, Y., & Omura, Y. (2020). Nonlinear evolution of radiation belt electron fluxes
interacting with oblique whistler mode chorus emissions. Journal of Geophysical Research: Space Physics, 125, e2019JA027465. https://doi.org/10.1029/2019JA027465

[2] Hsieh Y.-K., Kubota, Y., & Omura, Y. Energetic electron precipitation induced by oblique whistler mode chorus emissions, Submitted to Journal of Geophysical Research: Space Physics.

R006-21
Zoom meeting B ：11/1 PM2 (15:45-18:15)
17:00〜17:15

コーラスの伝搬特性と脈動オーロラ-マイクロバースト降り込み電子の関係

#三好 由純 [1)], 齊藤 慎司 [2)], 遠山 航平 [3)], 栗田 怜 [4)], 細川 敬祐 [5)], 浅村 和史 [6)], 高橋 一輝 [3)]
([1] 名大 ISEE,[2] 情報通信研究機構,[3] 名大 ISEE,[4] 京都大学 生存研,[5] 電通大,[6] 宇宙研

Energy spectrum of microburst electron precipitations

#Yoshizumi Miyoshi[1)],Shinji Saito[2)],Kohei Toyama[3)],Satoshi Kurita[4)],Keisuke Hosokawa[5)],
Kazushi Asamura[6)],Kazuki Takahashi[3)]
([1]ISEE, Nagoya Univ.,[2]NICT,[3]ISEE, Nagoya Univ.,[4]RISH, Kyoto Univ.,[5]UEC,[6]ISAS/JAXA

Both pulsating aurora electrons and sub-relativistic/relativistic electron microbursts are burst electron precipitations within 1 second from the magnetosphere to the thermosphere and mesosphere. Recently, we have proposed the theory that relativistic electron microbursts are a high-energy tail of pulsating aurora by chorus waves propagating along the field lines. The theory has been confirmed by several conjunction observations between low-altitude satellites and ground-based observations. The theory predicts that the energy spectrum electron bursts depend on the propagation latitudes of chorus waves. In this study, we conduct the computer simulations to investigate how the propagation latitudes of the chorus waves control the energy spectrum of precipitating electrons, and we discuss the possible conditions to cause relativistic electron microbursts associated with the pulsating aurora.

R006-22
Zoom meeting B ：11/1 PM2 (15:45-18:15)
17:15〜17:30

Statistical study about pitch angle evolutions of sub-relativistic/relativistic electrons of the outer radiation belt

#Inchun Park[1)],Yoshizumi Miyoshi[1)],Satoshi Kurita[2)],Takefumi Mitani[3)],Tomoaki Hori[4)],Takeshi Takashima[5)],Iku Shinohara[6)],Ayako Matsuoka[7)],Nana Higashio[8)],Masahiro Kitahara[4)]
([1]ISEE,Nagoya univ.,[2]RISH, Kyoto Univ.,[3]ISAS/JAXA,[4]ISEE, Nagoya Univ.,[5]ISAS, JAXA,[6]ISAS/JAXA,[7]Kyoto University,
[8]JAXA

The Arase/HEP instrument has observed energetic electrons of the outer radiation belt since March 2017. The Arase satellite has observed more than 20 geomagnetic CIR-driven storms with Dst <-30 nT. We conduct a superposed epoch analysis of the pitch angle and energy spectrum variations of sub-relativistic/relativistic electrons during different storm phases. During the storm main phase, sub-relativistic electron flux increases at L∗=3.5 - 6.0. During the early recovery phase, relativistic electron flux gradually increases in the outer belt. The strong pancake distributions are observed associated with the flux enhancements. Later, the pitch angle distribution becomes isotropic, suggesting that the wave-particle interactions cause the pitch angle scattering. In this presentation, we show the average variations of the pitch angle distribution and discuss possible acceleration mechanisms to cause variations of the pitch angle distribution and energy spectrum.

R006-23
Zoom meeting B ：11/1 PM2 (15:45-18:15)
17:30〜17:45

A statistical study on electron injection events whose peak-energy exceed 100 keV observed in the inner magnetosphere

#Jingxuan Yang[1)],Iku Shinohara[1,2)],Taku Namekawa[1)],Takefumi Mitani[3)],Kazushi Asamura[3)],Satoshi Kasahara[4)],
Nana Higashio[5)],Ayako Matsuoka[6)]
([1]Earth and Planetary Science, Tokyo Univ.,([2]ISAS/JAXA,([3]ISAS/JAXA,([4]The University of Tokyo,([5]JAXA,([6]Kyoto University

The substorm injection plays a crucial role in supplying the free energy to generate relativistic electrons in the radiation belts. However, how injected electrons penetrate the inner magnetosphere and get their energy remains unclear though numbers of studies on substorm injections have been reported. Arase (ERG) often observes electron injections whose maximum energies reach hundreds of keV, while the typical maximum energy of injected electrons is about 100 keV or less.

In this study, we do a statistical survey using high-energy electron experiment (HEP) and extreme high-energy electron experiment (XEP) data. We found 96 electron injection events above 95keV during the period from March 2017 to December 2019. Collecting injection events during the period when the apogee of Arase is located in the nightside, we are examining the statistical properties of the high-energy injection events, e.g., maximum energy at the observation point, the distribution of their estimated source regions, pitch angle anisotropy, and the first adiabatic invariant with relativistic approximation in detail to find whether dependence on the maximum energy is a key to limit the acceleration mechanisms of electron injection or not. We are also checking the electron energy spectra of the dispersionless injection events to find any signatures that indicate the acceleration mechanisms. Further, we also calculate phase space density for comparing with those obtained by other satellites observing magnetotail and previous studies on the profiles of the phase space density depending on L. (e.g., Boyd et al., 2019)

R006-24
Zoom meeting B ：11/1 PM2 (15:45-18:15)
17:45〜18:00

Possible observation plans for high-energy analyzer (PINO) onboard a CubeSat (BIRDS-5)

#Iku Shinohara[1)],Takefumi Mitani[2)],Mariko Teramoto[3)],Kazushi Asamura[1)],Ryota Onogi[1)],Yumie Kawagoe[1)],
Takeshi Takashima[4)]
([1]JAXA/ISAS,([2]JAXA/ISAS,([3]Kyutech,([4]JAXA/ISAS

We are developing a compact high-energy electron analyzer, nicknamed PINO (Particle Instrument for NanO-satellite), thanks to the JSPS KAKENHI support and the collaboration with the Kyushu Institute of Technology. PINO will be installed on a 2-U CubeSat, BIRDS-5J, and the EM (Engineering Model) integration test of BIRDS-5 fleets (two 1U CubeSats and one 2U CubeSat) are going in this summer. After the critical design review based on the results of the EM test, we will soon start to build the FM (Flight Model) of PINO by refurbishing PINO-EM. The BIRD-5 satellites will be ready for launch by next January. They will be released from the international space station (ISS) in Spring 2022.

Since the orbit of the BIRDS-5 fleets is almost the same as ISS, the coverage of the Lm-value is not comprehensive, and the maximum value is less than 7. The satellite attitude is controlled by the magnetic torque of the permanent magnets, and the PINO sensor view is always directed toward almost anti-parallel to the geomagnetic fields. Thus, PINO can observe precipitating high-energy electron fluxes in the northern hemisphere. Due to the electrical power budget limit, we will turn on PINO only for continuous 5 minutes in an orbital revolution. We will focus the PINO observation on conducting simultaneous observations of precipitating high-energy electrons from the outer radiation belt at low and high altitudes. Actually, we found that the conjunction between BIRDS-5 and Arase (ERG) will occur almost once in 3 days at various Lm positions. In this presentation, we will present our present status of the PINO development and current plans of scientific observations.

R006-25
Zoom meeting B ：11/2 AM1 (9:00-10:30)
9:15〜9:30

科学衛星あらせによって観測された低周波波動の統計解析

#天野 駿 [1)], 三宅 壮聡 [2)], 松岡 彩子 [3,4)]
(1 富山県大,(2 富山県大,(3 金沢大,(4 京都大学

Statistical analysis of low frequency waves observed by Arase satellite

#Shun Amano[1)],Taketoshi Miyake[2)],Ayako Matsuoka[3,4)]
(1TPU,(2Toyama Pref. Univ.,(3Kanazawa Univ.,(4Kyoto University

Various types of low frequency waves are observed by Electric Field Detector (EFD) onboard Arase satellite. In this study, we are going to detect these low frequency waves from EFD data, and classify these waves into several types by using machine learning. At first, we use SVM method to detect low frequency waves from 24 hour plots of EFD spectrum data. We tested several parameters of SVM, and detected low frequency waves with more than 96% accuracy ratio. We applied this SVM method to EFD spectrum data from 2017 to 2019, and succeeded in detecting 806 low frequency waves. Next, we try to classify these detected low frequency waves into several types by clustering. We apply K-means method and hierarchical clustering method to the image data of EFD spectrum plot and the numerical data which are the duration time and the center frequency of the low frequency waves, respectively. Therefore, we found 5 types of low frequency waves with different characteristics. In this study, we analyze two types of low frequency waves with narrower frequency range, which named type A and the type B. The type A waves have the frequency range from 0Hz to 50Hz and observed 135 times. The type B waves have the frequency range from 50Hz to 150Hz and observed 145 times. We investigated the observed positions the type A and the type B waves by using the orbit data, and found that the type A and the type B waves are observed on the opposite side of the sun, and the type B waves are observed in the nearer region to the earth. Next, we analyzed the relation between these two type waves with the magnetic field strength and the magnetic disturbances, and found the type A and the type B waves are both observed in the stable magnetic field, and the type B waves are observed in the stronger magnetic field. Future, we are going to analyzing the relation between the low frequency waves with the various ion cyclotron frequencies and the lower hybrid frequency.

本研究では、科学衛星あらせに搭載された電場観測器 (EFD) によって宇宙空間で観測された低周波波動の解析を行う。そのために観測されている低周波波動を分類して、その種類を特定する必要がある。そこで機械学習を利用して低周波波動の分類を行う。まず、EFD の観測データから SVM 法を用いて低周波波動の検出を行った結果、どれも 90%以上の精度で低周波波動を検出できた。その結果、806 個の低周波波動データを検出し、それぞれの発生時間と周波数帯を特定した。次にクラスタリングを用いて低周波波動の分類を行った。スペクトル画像データに K-means 手法、低周波波動検出時に特定した数値データに階層型クラスタリングを用いて分類を行った結果、低周波波動のタイプを 5 種類に分類することができた。本研究では、 5 種類の低周波波動の中で周波数帯が狭い 2 種類に着目して解析を行う。それぞれを typeA,typeB として、typeA は 0 から 50Hz の周波数帯で 135 例観測され、typeB は 50 から 150Hz の周波数帯で 145 例観測された。 2 種類の低周波波動に対して、衛星の軌道データをもとに観測位置を調査した。その結果、typeA,typeB は主に太陽と反対側で観測され、typeB は typeA よりも地球近傍でより観測されていることがわかった。また、2 つの type の低周波波動と磁場強度および磁場擾乱との関係について解析を行った結果、typeA, typeB ともに磁場が安定しているときに観測され、typeB は typeA よりも磁場強度が強い場合に多く観測されることを確認した。今後、観測された低周波波動とイオンサイクロトロン周波数や低域混成周波数との関係について解析を行う。

R006-26
Zoom meeting B ：11/2 AM1 (9:00-10:30)
9:30〜9:45

A statistical study of EMIC wave-particle interactions in the magnetosphere using Arase observations

#ChaeWoo Jun[1)],Yoshizumi Miyoshi[1)],Satoko Nakamura[1)],Masafumi Shoji[1)],Masahiro Kitahara[1)],Tomoaki Hori[1)],Chao Yue[2)],Jacob Bortnik[3)],Larry Lyons[3)],Yoshiya Kasahara[4)],Yasumasa Kasaba[5)],Fuminori Tsuchiya[5)],Atsushi Kumamoto[5)],Shoya Matsuda[6)],Kazushi Asamura[6)],Iku Shinohara[6)],Ayako Matsuoka[7)],Shoichiro Yokota[8)],Satoshi Kasahara[9)],Kunihiro Keika[9)]
([1]ISEE, Nagoya Univ.,[2]Peking University, Beijing, China,[3]AOS, UCLA, Los Angeles, USA,[4]Kanazawa Univ.,[5]Tohoku Univ.,[6]ISAS/JAXA,[7]Kyoto University,[8]Osaka Univ.,[9]The University of Tokyo

We performed a statistical study to demonstrate EMIC wave-particle interaction at different peak wave occurrence regions in the magnetosphere using in-situ observations by Exploration of energization and Radiation in Geospace (Arase) satellite. In our previous study, we found that EMIC waves have four different peak occurrence regions with different geomagnetic environments in the magnetosphere (H-band at 3-8 MLT at L>7; H-band at 11-15 MLT at L=6.5-8; He-band at 9-21 MLT at L=5-7; He-band at 12-19 MLT at L=7-9). This study included the inter-calibrated proton distribution data using LEPi and MEPi instruments in the energy range of 30 eV- 184 keV to investigate proton pitch angle distributions and partial thermal pressures with EMIC wave activities. We found that EMIC waves are observed below the proton instability threshold derived by linear kinetic theory. By using cold plasma approximation, we can compute the minimal resonant energy using the central frequency of EMIC waves and electron number density profile. We found that the minimal resonant energy for most of the EMIC wave events is concentrated between 1-100 keV, except for H-EMIC waves in the morning sector at higher L shells having scattered minimal resonant energy from 1 eV to 10 keV depending on normalized frequency by equatorial proton gyrofrequency, respectively. This result supports possible free energy sources for morning side EMIC waves excited due to suprathermal protons (<100 eV) heated by magnetosonic waves. This presentation shows spatial distributions of EMIC waves in the magnetosphere, energetic proton distributions between with and without EMIC wave activities, and the minimal resonant energy distributions at the different peak occurrence regions. We will discuss possible free energy sources causing EMIC waves at different regions and demonstrate the influence of different generation processes of EMIC waves on energetic proton distributions using in-situ satellite observations and theoretical model calculations.

R006-27
Zoom meeting B ：11/2 AM1 (9:00-10:30)
9:45〜10:00

サブオーロラ帯における７つの PWING 地上観測点を用いた Pc1 地磁気脈動の経度拡がりの統計解析

#劉 杰 [1)], 塩川 和夫 [1,2)], 大山 伸一郎 [1,8)], 大塚 雄一 [1)], 田 采祐 [1,5)], 能勢 正仁 [4)], 長妻 努 [6)], 坂口 歌織 [7)], 門倉 昭 [8)], 尾崎 光紀 [9)],Connors Martin[10)],Baishev Dmitry[11)], 西谷 望 [3)],Oinats Alexey[12)],Kurkin Volodya[12)],Raita Tero[13)]
[1 名古屋大学宇宙地球環境研究所,[2 名大宇地研,[3 名大 ISEE,[4 名大・宇地研,[5 名大 ISEE 研,[6NICT,[7 情報通信研究機構,[8ROIS-DS/極地研,[9 金沢大,[10Centre for Science, Athabasca Univ.,[11 なし,[12 ロシア太陽地球系物理学研究所,[13SGO

Statistical study of longitudinal extent of Pc1 pulsations using seven PWING ground stations at subauroral latitudes

#Jie Liu[1)],Kazuo Shiokawa[1,2)],Shin ichiro Oyama[1,8)],Yuichi Otsuka[1)],ChaeWoo Jun[1,5)],Masahito Nose[4)],Tsutomu Nagatsuma[6)], Kaori Sakaguchi[7)],Akira Kadokura[8)],Mitsunori Ozaki[9)],Martin Connors[10)],Dmitry Baishev[11)],Nozomu Nishitani[3)],Alexey Oinats[12)],Volodya Kurkin[12)],Tero Raita[13)]
[1ISEE,[2ISEE, Nagoya Univ.,[3ISEE, Nagoya Univ.,[4ISEE, Nagoya Univ.,[5ISEE, Nagoya Univ.,[6NICT,[7NICT,[8ROIS-DS/NIPR,[9Kanazawa Univ.,[10Centre for Science, Athabasca Univ.,[11IKFIA, SB, RAS,[12Institute of Solar-Terrestrial Physics, Irkutsk, Russia,[13SGO

Pc1 geomagnetic pulsations correspond to electromagnetic ion cyclotron (EMIC) waves in the magnetosphere and are excited sporadically in the magnetospheric equatorial plane in a frequency range of 0.2-5 Hz. The instantaneous longitudinal extent of the Pc1 waves on the ground has not been estimated yet. In this study, we analyze Pc1 pulsations observed at seven ground stations that distribute longitudinally at subauroral latitudes (˜60 degree magnetic latitudes (GMLAT)), using data for one year from July 2018 to June 2019. The hourly occurrence rates of Pc1 pulsations at all 7 stations have a peak (14-39.6 %) in the post-noon sector and a local minimum (4.1-8.1 %) at midnight. The average frequencies become highest (0.6-1.1 Hz) after midnight and lowest (0.3-0.5 Hz) after noon at all 7 stations. It was observed that Pc1 pulsation frequency tends to increase as the GMLAT of these 7 stations becomes high. Based on these observations, we obtained a peak of probability distribution of the instantaneous Pc1 longitudinal extent as ˜82.5 degree with a half maximum at ˜114 degree. Since this probability distribution can be affected by the spatial distribution of limited number of the stations, we also made model calculations on the observable longitudinal extent using artificial Pc1 waves with a given extent centered at random longitude. The calculation was repeated by changing the extent of the artificial Pc1 waves. Comparison of these model calculation results with the present observations reveals that the typical instantaneous longitudinal extent of the Pc1 waves is 109 degree.

R006-28
Zoom meeting B ：11/2 AM1 (9:00-10:30)
10:00〜10:15

ニュージーランドに設置された誘導磁力計による Pc1, IAR の観測: 初期結果報告

#尾花 由紀[1)], 坂口 歌織[2)], 能勢 正仁[3)], 細川 敬祐[4)], 塩川 和夫[5)],Connors Martin[6)], 門倉 昭[7)], 長妻 努[8)]
([1] 大阪電通大・工・基礎理工,[2] 情報通信研究機構,[3] 名大・宇地研,[4] 電通大,[5] 名大・宇地研,[6]Centre for Science, Athabasca Univ.,[7]ROIS-DS/極地研,[8] 情報通信研究機構

Observations of Pc1 and IAR with an induction magnetometer in New Zealand: initial results

#Yuki Obana[1)],Kaori Sakaguchi[2)],Masahito Nose[3)],Keisuke Hosokawa[4)],Kazuo Shiokawa[5)],Martin Connors[6)],Akira Kadokura[7)], Tsutomu Nagatsuma[8)]
([1]Osaka Electro-Communication Univ.,[2]NICT,[3]ISEE, Nagoya Univ.,[4]UEC,[5]ISEE, Nagoya Univ.,[6]Centre for Science, Athabasca Univ.,[7]ROIS-DS/NIPR,[8]NICT

The plasma populations in the inner magnetosphere have wide energy ranges from ˜eV to ˜MeV. Their interaction with plasma waves in the frequency range of mHz to kHz causes their on-site acceleration and loss into the ionosphere. In order to evaluate the loss of radiation belt particles due to Electromagnetic Ion Cyclotron (EMIC) waves occurring in the deep inner magnetosphere, we installed a new high-sensitivity all-sky camera and induction magnetometer at Middlemarch (L=2.7) in New Zealand where a fluxgate magnetometer has been operated since 2011.

The following results have been obtained so far:

Unique Pc1 pulsations were found in a dynamic power spectrum of the geomagnetic field variations as a band-type structure in the frequency range of ˜0.2-1 Hz before and after a small geomagnetic storm (minimum Dst = -40 nT) in October, 2020. On October 4, before the geomagnetic storm, Pc1 events with different center frequencies were observed intermittently almost throughout the day, regardless of local time. No pulsation was observed in frequency ranges of 0.2 to 30 Hz during the main phase and the early recovery phase after the occurrence of a sudden commencement of the geomagnetic storm, despite expecting to be observed at higher frequencies. On October 6, during the recovery phase, four Pc1 events were observed with a periodic interval of about 3-4 hours following an IPDP (interval of pulsations of diminishing period) type Pc1 occurrence. It was found that these events were also observed at four stations in Canada and Iceland in the opposite hemisphere at the same time.

Ionospheric Alfven Resonator (IAR) is usually found in a dynamic power spectrum of the geomagnetic field variations as spectral resonance structures in the frequency range of 0.1-10 Hz. We found IAR in the data from the induction magnetometer in three consecutive days from October 4 to 6, 2020. A careful inspection reveals that IAR signals extend to the frequency range up to ˜15 Hz at 06-11 UT (17-22 LT) on October 4. To our knowledge, this is the first observation of IAR with such high frequency. After 11 UT, it seems that the high frequency IAR is masked by stronger power of the Schumann resonances; and in the next two days, there is no high frequency IAR. It is a future study to investigate statistical characteristics and excitation mechanisms of the high frequency IAR. It is of another interest to focus on IAR at f ˜1-2 Hz after 08 UT on October 6. This IAR seems to be related to the IPDP-type of Pc1 pulsation that occurs at 07-08 UT. Then the power enhancement shows a seamless transition from Pc1 to IAR. The spectral power density of this IAR is larger than those of IAR on October 4 and 5. These results may indicate a new excitation mechanism of IAR, in which excitation energy is supplied from Pc1 pulsations not from lightning as has been proposed.

ニュージーランドのミドルマーチ観測点（地理緯度 -45.6 °, 地理経度 170.1 °, 磁気緯度 -52.81 °, L 値 2.78）では、2011 年よりフラックスゲート磁力計が稼働して地磁気三成分の 1 秒値観測が行われてきた。ここに、新しく誘導磁力計と高感度全天カメラを設置し、ULF 波、ELF 波、オーロラ発光の同時観測体制を構築した。このプロジェクトでは、放射線帯からの降下粒子による孤立プロトンオーロラの発光と、粒子降下を引き起こすイオンサイクロトロン (Electromagnetic Ion Cyclotron: EMIC) 波動を同時観測することによって、地球にごく近い深内部磁気圏において EMIC 波動に起因する放射線帯の消失が生じていることを立証し、さらに、磁気嵐に伴うプラズマ圏の収縮と放射線帯消失の因果関係を解明することを目指している。

これまでのところ、波動とオーロラ発光の同時出現イベントは確認されていないが、電離圏アルフヴェン共鳴 (Ionospheric Alfven Resonator: IAR) 由来と考えられる高調波構造を持つ波動や Pc1 波動が観測されており、この地域におけるこれらの波動の特性が明らかになりつつある。

2020 年 10 月の小規模な地磁気嵐（最小 Dst = -40 nT）の前後に、誘導磁力計で観測された地磁気変動のパワースペクトル中に、周波数範囲 0.2-1 Hz のバンド型構造として Pc1 脈動が観測された。地磁気嵐開始前の 10 月 4 日には、地方時に関係なく、中心周波数の異なる Pc1 イベントがほぼ一日中断続的に観測された。続く 10 月 5 日、磁気嵐の主相および初期回復相にあたる時間帯においては、0.2-30 Hz の周波数範囲に脈動は観測されなかった。 さらに 10 月 6 日、磁気嵐の回復相においては、IPDP (Interval of Pulsations of Diminishing Period) タイプの Pc1 が発生しており、3-4 時間の周期的な間隔で 4 つの Pc1 イベントが観測された。これらのイベントは、北半球にあるカナダとアイスランドの 4 つの観測点でも同時に観測されていた。

IAR は通常、0.1-10 Hz の周波数範囲のスペクトル共鳴構造として地磁気変動のダイナミックパワースペクトル中に見うけられる。 2020 年 10 月 4-6 日の連続 3 日間の地磁気変動データにおいて IAR が同定された。IAR は 10 月 4 日の 06-11 UT（17-22 LT）には、最大 15 Hz の周波数領域に及んでいた。我々の知る限り、このような高い周波数帯における IAR の観測は世界で初めてである。 10 月 4 日 11 UT の後、この高周波 IAR はシューマン共振の強いパワーによってマスクされているように見える。そして次の 2 日間、高周波 IAR は観測されなかった。高周波 IAR の統計的特性と励起メカニズムを調査することは将来の研究課題である。また、10 月 6 日の IAR は、07-08 UT に発生した IPDP タイプの Pc1 脈動に関連しているように見えて興味深い。この IAR のパワースペクトル密度は 10 月 4 日と 5 日の IAR のそれよりも強く、Pc1 から IAR への波動エネルギーの移行を示しているように見える。これらの結果は、これまでの研究で提案されているように、IAR が雷放電からではなく Pc1 脈動からも励起エネルギーが供給される可能性を示している。

R006-29
Zoom meeting B ：11/2 AM2 (10:45-12:30)
10:45〜11:00

Multipoint Measurement of Fine-Structured EMIC Waves by Arase, Van Allen Probe A and Ground Stations

#Shoya Matsuda[1)],Yoshizumi Miyoshi[2)],Yoshiya Kasahara[3)],Lauren Blum[4)],Chris Colpitts[5)],Kazushi Asamura[1)],Yasumasa Kasaba[6)],Ayako Matsuoka[7)],Fuminori Tsuchiya[6)],Atsushi Kumamoto[6)],Satoko Nakamura[2)],Masahiro Kitahara[2)], Iku Shinohara[1)],Geoff Reeves[8)],Harlan Spence[9)],Kazuo Shiokawa[1)],Tsutomu Nagatsuma[10)],Shin ichiro Oyama[2,11)],Ian R. Mann[12)]
([1]ISAS/JAXA,[2]ISEE, Nagoya Univ.,[3]Kanazawa Univ.,[4]University of Colorado Boulder,[5]Univ. of Minnesota,[6]Tohoku Univ.,[7]Kyoto University,[8]LANL,[9]Univ. New Hampshire,[10]NICT,[11]NIPR,[12]The University of Alberta

Electromagnetic ion cyclotron (EMIC) waves are an important plasma waves that control energetic ion and relativistic electron precipitations in the terrestrial inner magnetosphere. We examined the growth and propagation of fine-structured EMIC waves related to time-varying density irregularities using multipoint measurement data observed by two spacecraft (Japanese Arase and U.S. Van Allen Probe A) and two ground stations (Gakona and Dawson) during a field-line conjunction event on 18 April 2019. We analyzed the wave data obtained by the aforementioned spacecraft and stations, and found that the appearance of fine structures in the observed EMIC waves clearly coincided with the ambient electron density irregularities in the magnetosphere, which can cause periodic wave growth and waveguiding on their propagation. Furthermore, we found that the observed fine-structured EMIC waves were spatially localized in approximately a 185 km range in geomagnetic latitude at an auroral altitude of 100 km. We also found thermal H^+ and He^+ heating ($<$200 eV/q) during the EMIC wave activity.

R006-30
Zoom meeting B ：11/2 AM2 (10:45-12:30)
11:00〜11:15

地上-衛星観測によるIPDPタイプEMIC波動の周波数上昇に関するイベント解析

#平井 あすか [1)], 土屋 史紀 [1)], 小原 隆博 [1)], 笠羽 康正 [1)], 加藤 雄人 [2)], 三澤 浩昭 [1)], 塩川 和夫 [3)], 三好 由純 [3)], 田 采祐 [3)], 栗田 怜 [4)],Connors Martin[5)],Hendry Aaron[6)]
[1 東北大　惑星プラズマ・大気研究センター,[2 東北大・理・地球物理,[3 名大 ISEE,[4 京都大学 生存研,[5Centre for Science, Athabasca Univ.,[6Department of Physics, University of Otago

The mechanism of frequency increase of IPDP type EMIC waves: event analysis of ground and satellite observations

#Asuka Hirai[1)],Fuminori Tsuchiya[1)],Takahiro Obara[1)],Yasumasa Kasaba[1)],Yuto Katoh[2)],Hiroaki Misawa[1)],Kazuo Shiokawa[3)], Yoshizumi Miyoshi[3)],ChaeWoo Jun[3)],Satoshi Kurita[4)],Martin Connors[5)],Aaron Hendry[6)]
[1PPARC, Tohoku Univ.,[2Dept. Geophys., Grad. Sch. Sci., Tohoku Univ.,[3ISEE, Nagoya Univ.,[4RISH, Kyoto Univ.,[5Centre for Science, Athabasca Univ.,[6Department of Physics, University of Otago

Electromagnetic ion cyclotron (EMIC) waves are Pc1-2 waves excited near the magnetic equator by anisotropic ring current ions. EMIC waves have been thought as one of the mechanisms to cause the loss of the electrons in the outer radiation belt. Intervals of pulsations of diminishing periods (IPDP) are one of the EMIC waves observed by ground-based magnetometers. Previous studies suggest that IPDP type EMIC waves are likely to cause electron precipitation more efficiently than other EMIC waves. IPDP events are characterized by an increase in frequency during the event of about half an hour to a few hours. They occur in the dusk sector during substorms. Injected ring current ions are the source of EMIC waves and play a major role in the increase in frequency of IPDP. Two mechanisms for frequency increase relate to drift of ring current ions; one is radial inward drift. Since the magnetic field becomes larger in lower L shell, the local ion gyrofrequency increases as the ring current ions drift inward. This results in generation of waves with rising frequency (Gendrin et al., 1967). The other is energy dispersion of ions in the course of westward drift. High-energy ions drift westward faster and arrive earlier at the meridian of a fixed ground site than low-energy ions. Since wave frequency depends on energy of resonant ions, energy dispersion causes an increase in frequency (Fukunishi, 1969). However, it is still not clear which mechanisms prefer to explain the frequency increase. In this study, we investigate IPDP type EMIC wave event to understand how frequency of IPDP increases. EMIC waves were observed by Van Allen Probe A and ground-based induction magnetometers in 02:30-06:05 UT on 19 April 2017. The event occurred in a substorm during main and early recovery phase of small geomagnetic storm. Van Allen Probe A observed EMIC waves in hot proton populations inside plasmapause in dusk sector. The footprint of Van Allen Probe A was located in North America during the wave activity. Simultaneously, IPDP type EMIC waves were observed at several induction magnetometer stations of the “Study of dynamical variation of Particles and Waves in the Inner magnetosphere using Ground-based network observations (PWING)” project and the Canadian Array for Realtime Investigations of Magnetic Activity (CARISMA). Energetic electron precipitation was detected by subionospheric VLF radio waves received at Athabasca, Canada and POES satellites. The VLF radio wave propagation paths were close to the footprint of Van Allen Probe A and ground-based magnetometers during EMIC wave activity. This suggests that detected electron precipitation was driven by EMIC waves. POES detected 13 electron precipitation events in North America and conjugated region in 0-6 UT. We found that the location of electron precipitation moved to lower L shell. The slope is -0.4 L/hour. Energetic charged particles scattered by EMIC waves precipitate along the magnetic field lines. The location of electron precipitation should reflect the source region of EMIC waves in the magnetic equatorial plane. The result suggests that source region of EMIC waves moved to lower L shell and this motion of the source corresponds to radial inward drift as the mechanism of an increase in frequency of IPDP. The westward drift velocities of the source region were calculated from EMIC waves observed at three stations separated longitudinally. We found that westward drift velocities are independent of the wave frequency. In case of the scenario of energy dispersion, higher-energy ions excite low frequency waves. As the energy of ions that excite EMIC waves decreases, wave frequency increases. If energy dispersion of ions contributes an increase in frequency of IPDP, westward drift velocities indicate different values in each frequency. The result suggests that westward drift of the source region did not cause an increase in frequency.

R006-31
Zoom meeting B ：11/2 AM2 (10:45-12:30)
11:15〜11:30

プラズマ波動の分散関係に基づいた伝搬方向推定手法の検討とあらせ衛星観測データへの適用

#古俣 圭佑[1)], 笠原 禎也[1)], 田中 裕士[1)], 松田 昇也[2)], 太田 守[1)], 土屋 史紀[3)], 熊本 篤志[3)], 松岡 彩子[4)]
([1] 金沢大,[2]ISAS/JAXA,[3] 東北大・理,[4] 京大

Study on direction finding method based on dispersion relation of plasma waves and application to the data observed by Arase

#Keisuke Komata[1)],Yoshiya Kasahara[1)],Yuji Tanaka[1)],Shoya Matsuda[2)],Mamoru Ota[1)],Fuminori Tsuchiya[3)],
Atsushi Kumamoto[3)],Ayako Matsuoka[4)]
([1]Kanazawa Univ.,[2]ISAS/JAXA,[3]Tohoku Univ.,[4]Kyoto Univ.

Various plasma waves observed in the inner magnetosphere are important factors that cause changes in the space plasma environment. The direction of plasma waves is one of the important features, and it is an important clue for the investigation of generation region and propagation path of the waves from in situ observations by scientific satellite. There are various methods for direction finding. In this study, we particularly focus on the method using integration kernel, which are theoretically derived from the dispersion relation of plasma waves. The advantage of the method is that the propagation direction can be estimated from the combination of electric and magnetic wave field data even though the three-dimensional magnetic field data cannot be obtained. Various algorithms have been proposed and evaluated using pseudo data, but there are only several examples applied to the actual observation data.

In this research, we adopted a method named MUSIC (Multiple Signal Classification) method, which is one of the direction finding algorithms using integration kernel. We applied this method to the waveform data measured by the waveform capture (WFC), which is one of receivers of the Plasma Wave Experiment (PWE) on board the Arase satellite. The waveform consists of two components of electric field and three components of magnetic field. First, a correlation matrix, called spectral matrix, was generated from the waveform data. Next, an integration kernel for whistler mode wave was calculated from plasma frequency and cyclotron frequency at the observation point. The plasma frequency and the cyclotron frequency were derived from the data obtained by the high frequency receiver (HFA) and the magnetic field analyzer (MGF) on board the Arase, respectively. Finally, the MUSIC algorithm was applied to the spectral matrix combining with the integration kernel, and propagation direction of the observed plasma wave was derived.

In this presentation, we mainly report the evaluation results of the absolute direction using a spectral matrix combining with electric and magnetic field components, and the precision of the direction finding results under the restricted number of magnetic field components.

内部磁気圏で観測される様々なプラズマ波動は、宇宙プラズマ環境の変動を引き起こす重要な因子である。プラズマ波動の到来方向は、その重要な特徴の一つであり、科学衛星による単地点観測から波動現象の励起源や伝搬経路等を推定するための重要な材料となり得る。到来方向推定には様々な方法が提案されている。本研究では特に、プラズマ波動の分散関係から理論的に導出される積分核を用いる方法に着目する。積分核を用いる方法は、プラズマ波動の磁界から偏波情報が正しく求められない状況下でも、電界データを併用して伝搬方向を推定できるといった利点が挙げられる。過去に様々な解法が提案され、擬似データを用いて評価されているが、実観測データへの応用は一部にとどまっている。

本研究では、あらせ衛星の観測データを用い、積分核を用いた伝搬方向推定手法である MUSIC (Multiple Signal Classification) 法を用いた解析例を紹介する。評価に用いるデータは、プラズマ波動・電場観測器（PWE）の受信器の 1 つである波形捕捉受信器（WFC）で取得された電界 2 成分、磁界 3 成分の波形データである。まず、波形データからスペクトルマトリクスと呼ばれる相関行列を作成する。次に、高周波受信器 (HFA) と磁場観測器 (MGF) で得られたデータから、観測地点のプラズマ周波数と電子サイクロトロン周波数を計算し、ホイスラーモード波の積分核を作成する。最後に、作成したスペクトルマトリクスと積分核に対して MUSIC アルゴリズムを適用し、観測されたプラズマ波動の伝搬方向の導出を行う。

本講演では特に、電界成分を含むスペクトルマトリクスを使用した際の、到来方向の絶対方向推定に対する有効性と、到来方向推定に使用する磁界成分の数が限定的である場合の影響について述べる。

R006-32
Zoom meeting B ：11/2 AM2 (10:45-12:30)
11:30〜11:45

あらせ衛星で観測されるコーラスに関連したラングミュア波動の統計解析

#江田 大輝[1)], 栗田 怜[2,3)], 吉田 永遠[3)], 小嶋 浩嗣[4)], 笠原 禎也[5)], 松田 昇也[6)], 松岡 彩子[7)], 三好 由純[8)], 篠原 育[9)]
([1] 京大院工,[2] 京都大学 生存研,[3] 京大,[4] 京大・生存圏,[5] 金沢大,[6]ISAS/JAXA,[7] 京都大学,[8] 名大 ISEE,[9] 宇宙研／宇宙機構

Statistical investigation of Langmuir waves associated with whistler mode chorus waves observed by the Arase satellite

#Eda Daiki[1)],Satoshi Kurita[2,3)],Towa Yoshida[3)],Hirotsugu Kojima[4)],Yoshiya Kasahara[5)],Shoya Matsuda[6)],Ayako Matsuoka[7)],Yoshizumi Miyoshi[8)],Iku Shinohara[9)]
([1]Engineering, Kyoto U.,[2]RISH, Kyoto Univ.,[3]Engineering, Kyoto U.,[4]RISH, Kyoto Univ.,[5]Kanazawa Univ.,[6]ISAS/JAXA,[7]Kyoto University,[8]ISEE, Nagoya Univ.,[9]ISAS/JAXA

Langmuir waves associated with Chorus have been observed in the magnetosphere. Li et al. (2017) show Van Allen Probes observation of Langmuir waves associated with chorus waves. They point out that the Langmuir waves are excited by electron beams, which are generated by the landau damping of electrons by chorus waves. However, since Li et al. (2017) discusses only two examples of the event, further data analysis is necessary to reveal the mechanism of the event that Chorus causes Langmuir waves. Therefore, in this study, we aimed to examine this chorus-induced Langmuir waves by analyzing the relationship of these waves using the data obtained by the Arase satellite in statistical sense.

We used OFA-MATRIX data to determine the electric field components perpendicular and parallel to the background magnetic field projected onto the satellite spin plane. Then, we extracted the components that are dominant in the parallel direction as Langmuir waves since Langmuir waves have electric field oscillations parallel to the magnetic field. We also extracted the electric field components of Chorus considering the typical wave frequency range. As a result of conducting this analysis on several months data, we were able to identify a large number of narrowband and broadband Langmuir waves. In addition, comparing the electric field components of Chorus and that of Langmuir waves, we were able to confirm the tendency that Langmuir waves arise when Chorus are observed, but there were some cases the tendency was not confirmed. Therefore, we will analyze more data and report the results of statistical analysis of the relationship between Chorus and Langmuir waves in the presentation.

References

Li, J., et al. (2017). Chorus wave modulation of Langmuir waves in the radiation belts. Geophys. Res. Lett., 44, 11,713-11,721. doi: 10.1002/2017GL075877

地球磁気圏では、コーラスに関連したラングミュア波動が観測されている。Li et al. (2017) では、Van Allen Probes の観測データを用いて、コーラスがラングミュア波動を励起する現象について議論されている。この研究によれば、コーラス波動と電子のランダウ共鳴により電子が磁力線平行方向に加速され、この電子によりラングミュア波動が励起されると考えられている。しかし、Li et al. (2017) では議論している現象が 2 例のみであるため、コーラスがラングミュア波動を励起する現象の解明には更なるデータ解析が必要であると考えられる。そこで本研究では、あらせ衛星に搭載されているプラズマ波動観測機 PWE の受信器の一つである OFA で取得されたデータを用いて、コーラスとラングミュア波動の関係を統計的に解析することで、この現象の物理過程を理解することを目的とする。

OFA によって取得されるデータのうち、電界 2 成分から得られたスペクトルマトリックス (OFA-MATRIX) のデータを用いて、スピン面内における背景磁場に垂直および平行な電界成分を求めた。ラングミュア波動は背景地場に対して平行方向に振動するため、背景地場に平行方向の電界が卓越している成分をラングミュア波動として抽出した。また、コーラスの電界成分も、典型的な周波数帯域を考慮して抽出した。この解析を数か月分のデータに対して行った結果、多数の狭帯域および広帯域にわたるラングミュア波動と思われる現象を同定することができた。さらに、コーラスの電界成分とラングミュア波動の電界成分を比較するとコーラス発生時にラングミュア波動が生じる傾向を確認できたが、コーラスが観測されているにも関わらず、ラングミュア波動が観測されない場合も見られた。今後さらに多くのデータを解析し、発表ではコーラスとラングミュア波動の関係性を統計的に解析した結果を示す。

参考文献

Li, J., et al. (2017). Chorus wave modulation of Langmuir waves in the radiation belts. Geophys. Res. Lett., 44, 11,713-11,721. doi: 10.1002/2017GL075877

R006-33
Zoom meeting B ：11/2 AM2 (10:45-12:30)
11:45〜12:00

あらせ衛星のモノポールモードで観測されたコーラス波動の解析

#滝 朋恵 [1)], 栗田 怜 [2)], 松田 昇也 [3)], 小嶋 浩嗣 [4)], 笠原 禎也 [5)], 三好 由純 [6)], 松岡 彩子 [7)], 熊本 篤志 [8)]
([1] 京大・工・電気,[2] 京都大学 生存研,[3]ISAS/JAXA,[4] 京大・生存圏,[5] 金沢大,[6] 名大 ISEE,[7] 京都大学,[8] 東北大・理・惑星プラズマ大気

Analysis of chorus waves observed by the monopole mode of the Arase satellite

#Tomoe Taki[1)],Satoshi Kurita[2)],Shoya Matsuda[3)],Hirotsugu Kojima[4)],Yoshiya Kasahara[5)],Yoshizumi Miyoshi[6)], Ayako Matsuoka[7)],Atsushi Kumamoto[8)]
([1]Engineering, Kyoto Univ.,[2]RISH, Kyoto Univ.,[3]ISAS/JAXA,[4]RISH, Kyoto Univ.,[5]Kanazawa Univ.,[6]ISEE, Nagoya Univ.,[7]Kyoto University,[8]Planet. Plasma Atmos. Res. Cent., Tohoku Univ.

In this study, the chorus waves observed by the monopole mode of the Arase satellite are investigated.

In the monopole observation, it is possible to obtain phase differences or time differences of electric fields by comparing the data between two monopole antennas. The phase differences of the waves or time differences of the structures passing through the antennas are calculated by using correlation analysis and FFT on two observation data. Using these data, the phase velocity of the waves and the relative velocity of the structure to the satellite can be calculated.

In the Arase satellite PWE, a pair of antennas can be regarded as one monopole antenna each, and monopole observation is possible to obtain the differential signal between the antenna and the satellite ground [Kasahara et al., EPS, 2018].

The phase velocity and wavelength of the waves were estimated by monopole observation of the satellite with electrostatic electron cyclotron waves [Shinjo, Master thesis, 2019]. In the observation of electrostatic solitary waves, the relative velocity to the satellite and spatial scale of the corresponding electrostatic potential structures are calculated, and the polarity of the potential is estimated from the analysis of the monopole observation data [Taki, Master Thesis, 2020].

In this presentation, we report on the results of monopole observations of chorus waves. It is expected that the same waveform of the electric field is measured by both antennas for a chorus with fast phase velocity.

On the other hand, the cross-correlation analysis between two antennas for the chorus waves shows that the phase difference between the antennas changes periodically with the spin. The phase difference is larger when the antennas are parallel to the ambient magnetic field, and the phase difference has a minimum value when the antennas are perpendicular.

If we consider the wave normal angle of the chorus waves to be in the same direction as the ambient magnetic field, the electric field oscillates in the vertical plane with respect to the background magnetic field. Due to the directivity of the antenna, it is difficult to observe the electric field when the antenna and the background magnetic field are parallel. When the wave surface is parallel to the antenna, the phase difference is minimal. In order to demonstrate that, we have conducted numerical experiments simulating monopole observation, assuming a plane wave in three-dimensional space. In this way, we are verifying the calculation method of the phase velocity by the monopole observation from the aspect of the observation results and numerical experiments.

We will report the results of the observation and the verification.

本研究では、あらせ衛星モノポール観測時におけるコーラス波動の観測事例を用いて検討する。

モノポール観測では 2 本のモノポールアンテナ間のデータを比較することで電界の位相差や時間差を得ることが可能である。2 つのアンテナから得られた観測データに対して相関解析や FFT を用いて波動や構造がアンテナを通過した位相差・時間差が算出される。これを利用して波動の位相速度や構造の衛星に対する相対速度を計算可能である。

あらせ衛星 PWE では、4 本のアンテナのうち 1 対を、それぞれ 1 本ずつのモノポールアンテナと見なして衛星のグラウンドとの差動を得るモノポール観測が可能である [Kasahara et al., EPS, 2018]。

あらせ衛星では、このモノポール観測を静電電子サイクロトロン波に適用することで、波動の位相速度と、波長を推定する試みが行われている [新城, 修士論文, 2019]。また、静電孤立波の観測では、モノポール観測データの解析から、静電孤立波に対応する静電ポテンシャルの、衛星に対する相対速度、空間スケールに加え、ポテンシャルの極性の推定が行われている [滝, 修士論文, 2020]。

本発表ではまず、モノポール観測モード時における、コーラス波動の観測結果に関して報告する。あらせ衛星のモノポール観測では、アンテナ V1 から衛星のグラウンドを減じた差動を Ev1、衛星のグラウンドからアンテナ V2 を減じた差動を Ev2 として観測している。位相速度が速いコーラス波動の場合、両アンテナで同じ波形の電界が計測されると期待される。一方で、モノポール観測モードで得られたコーラス波動の波形に対して、アンテナ間の相互相関解析を行なった結果、アンテナ間の位相差が、スピンに伴い周期的に変化する結果が得られた。このスピン依存性は背景磁場に対してアンテナが平行の場合に位相差が大きくなり、垂直の場合に極小値を持つことが分かった。

コーラス波動の伝搬方向と背景磁場が同じ方向であると考えると、電界は背景磁場に対して垂直面内で振動する。このとき、アンテナの指向性から、アンテナと背景磁場が平行の場合には電界振動が観測されにくい。また、極小付近では波面がアンテナに平行となり、位相差が極小となる。これらを示すために、3 次元空間で平面波を仮定し、モノポール観測を模擬した数値実験を行なっている。このように、モノポール観測による位相速度の算出方法に関して、

観測結果と数値実験の側面から検証を進めており、観測結果と合わせて、検証の結果についても報告する予定である。

R006-34
Zoom meeting B ：11/2 PM1 (13:45-15:30)
13:45〜14:00

Repetitive EMIC rising tone emissions by anomalous trapping of low pitch angle protons

#Masafumi Shoji[1)],Masahiro Kitahara[1)],Satoko Nakamura[1)],Yoshiharu Omura[2)]
([1]ISEE, Nagoya Univ.,[2]RISH, Kyoto Univ.

Electromagnetic ion cyclotron (EMIC) rising tone emissions which are similar to the whistler mode chorus emissions are generated through the nonlinear interactions with anisotropic protons in the inner magnetosphere. Theoretical studies suggest that whistler waves cause the anomalous trapping of low pitch angle electrons. By test particle simulations, we find that EMIC rising tone emissions also scatter the significant number of low pitch angle protons to the higher pitch angle. Hybrid simulations on the EMIC rising tone emissions, however, have been performed with subtracted Maxwell distribution function for the energetic protons which exclude low pitch angle protons. We perform a self-consistent hybrid simulation with bi-Maxwellian protons to investigate the effect of the anomalous trapping on the generation of the rising tone emissions. We find several EMIC rising tone emissions are generated while only one pair of forward and backward propagating rising tone emissions is generated in the subtracted Maxwellian case. The low pitch angle protons are also scattered to the higher pitch angle obtaining kinetic energy from the EMIC wave in the simulation. The higher pitch angle proton flux formed by the anomalous trapping becomes a part of the energy source of another EMIC emission. The new EMIC wave repeats the process, and then the multiple rising tone emission occurs.

R006-35
Zoom meeting B ：11/2 PM1 (13:45-15:30)
14:00〜14:15

Measurements of nongyrotropic electrons around the cyclotron resonance velocity in whistler-mode waves

#Naritoshi Kitamura[1)],Takanobu Amano[2)],Yoshiharu Omura[3)],Scott Boardsen[4,5)],Daniel J. Gershman[4)],Masahiro Kitahara[7)], Satoko Nakamura[8)],Masafumi Shoji[7)],Yoshizumi Miyoshi[7)],Yuto Katoh[9)],Hirotsugu Kojima[10)],Yoshifumi Saito[11)], Masafumi Hirahara[12)],Shoichiro Yokota[13)],Barbara L. Giles[6)],William R. Paterson[4)],Craig J. Pollock[14)],Olivier Le Contel[15)], Christopher Russell[16)],Robert J. Strangeway[17)],Narges Ahmadi[18)],Per-Arne Lindqvist[19)],Robert E. Ergun[18)]

([1]The University of Tokyo,[2]The University of Tokyo,[3]RISH, Kyoto Univ.,[4]NASA/GSFC,[5]Partnership for Heliophys. and Space Env. Res., Univ. of Maryland in Baltimore County,[6]NASA/GSFC,[7]ISEE, Nagoya Univ.,[8]ISEE, Nagoya Univ.,[9]Dept. Geophys., Grad. Sch. Sci., Tohoku Univ.,[10]RISH, Kyoto Univ.,[11]ISAS,[12]ISEE, Nagoya Univ.,[13]Osaka Univ.,[14]Denali Scientific,[15]LPP, CNRS,[16]Dept. of Earth, Planet. Space Sci., UCLA,[17]Dept. of Earth, Planet. Space Sci., UCLA,[18]LASP, Univ. of Colorado, Boulder,[19]Royal Institute of Technology, Sweden,[20]SWRI

The interaction between the electromagnetic field and charged particles is central for the collisionless plasma dynamics in space. Whistler-mode waves are one of the electromagnetic plasma waves, which play important roles in efficient pitch-angle scattering and acceleration of electrons in solar wind, collisionless shock waves as well as planetary magnetospheres. The nonlinear wave-particle interaction theory for coherent large amplitude waves predicts that electrons around resonance velocities exhibit nongyrotropy due to the trapping motion around them and the nongyrotropic electrons exchange energy and momentum with the waves in the presence of an appropriate inhomogeneity. In this presentation, we show observational results of nongyrotropic electrons around the cyclotron resonance velocity using the data obtained by the Magnetospheric Multiscale (MMS) spacecraft during a whistler-mode wave (about 200 Hz) event around the magnetosheath-side separatrix of the dayside magnetopause reconnection. On the basis of measurements by the Fast Plasma Investigation Dual Electron Spectrometer (FPI-DES) and the search-coil magnetometer (SCM), the relative phase angle of the electron hole to the magnetic field of the whistler-mode wave agrees well with the prediction by the nonlinear theory, and this type of the electrons appeared only around the cyclotron resonance velocity. The electron flux at the hole was about 40% lower than that at the peak in the most pronounced case. This result provides evidence of locally ongoing nonlinear wave-particle interaction between the electrons and whistler-mode waves, and proves that the nonlinear wave growth occurs around the dayside reconnection.

R006-36
Zoom meeting B ：11/2 PM1 (13:45-15:30)
14:15〜14:30

ARTEMIS 衛星観測を用いた月周辺におけるホイッスラーモード波動のスペクトル形状についての解析

#沢口 航 [1)], 原田 裕己 [1)], 栗田 怜 [2)]
[(1] 京大・理・地球物理,[(2] 京都大学 生存研

Spectral properties of whistler-mode waves in the vicinity of the Moon: ARTEMIS observations

#Wataru Sawaguchi[1)],Yuki Harada[1)],Satoshi Kurita[2)]
[(1]Dept. of Geophys., Kyoto Univ.,[(2]RISH, Kyoto Univ.

Whistler-mode waves are naturally occurring electro-magnetic waves with frequency ranges below f_{ce}, where f_{ce} is the electron cyclotron frequency. One of the characteristics of the waves in the terrestrial inner magnetosphere is that there is often a power minimum at 0.5 f_{ce}, as exemplified by the well-known “banded chorus”. Formation mechanisms of the gap remain a subject of discussion. Teng et al. (2019) showed the spatial distribution of the spectral properties of whistler-mode waves in the terrestrial inner magnetosphere. However, that in the vicinity of airless, unmagnetized bodies like the Moon has not been reported.

Although the Moon does not have a dense atmosphere nor a global intrinsic magnetic field, it is known that plasmas of the solar wind and the Earth’s magnetotail interact with the lunar surface and the lunar crustal magnetic field, resulting in various plasma phenomena around the Moon. Whistler-mode waves can be excited by cyclotron resonance between waves traveling toward the Moon and upcoming electrons magnetically reflected from the lunar surface. In the process, a free energy source is provided by effective temperature anisotropy in the electron velocity distribution function caused by absorption of parallel electrons at the lunar surface and magnetic reflection of perpendicular electrons. It should be noted that these lunar whistler-mode waves can have as large amplitudes as those occur in the terrestrial inner magnetosphere and can form complicated spectral shapes that resemble chorus emissions.

Our goal is to understand the formation mechanism of the 0.5 f_{ce} gap by analyzing the spectral properties of whistler-mode waves in the vicinity of the Moon, where the conditions for the wave generation are substantially different from those in the terrestrial inner magnetosphere. Since the Moon orbits the Earth and can be in the solar wind, magnetosheath and magnetotail of the Earth, the background magnetic field and the electron distribution function vary greatly in time around the Moon. Thus, by studying the lunar whistler-mode waves, we will be able to investigate how the difference of the plasma environment has effects on the spectral properties.

We carried out statistical analysis based on Teng et al. (2019) using the magnetic field and plasma data observed by the ARTEMIS. First, We automatically identified whistler-mode wave events. Then, according to the wave power below/above 0.5 f_{ce} and the existence of 0.5 f_{ce} gap, we automatically categorized the events into four groups; lower-band only, upper-band only, banded, and no-gap whistler-mode waves. As a result, the occurrence rate of four types of spectral properties are significantly different from that in the terrestrial inner magnetosphere. In particular, banded events were very rare in the ARTEMIS data. We will also discuss effects of the lunar magnetic anomalies and the location of the Moon on the spectral properties.

ホイッスラーモード波動は電子サイクロトロン周波数 (f_{ce}) 以下の周波数を持つ、自然発生の電磁波動である。地球内部磁気圏におけるホイッスラーモード波動の特徴として、特にホイッスラーモード・コーラス放射に関連して、しばしば 0.5 f_{ce} 付近で強度が極小となるギャップ構造をもつことが知られている。このギャップ構造の生成機構については現在も議論が続いている。また、地球内部磁気圏におけるホイッスラーモード波動の、ギャップ構造を含むスペクトル形状の空間分布については Teng et al. (2019) によって既に報告されているが、月のような非磁化かつ大気の希薄な天体の周辺でのスペクトル形状の分布は明らかになっていない。

月は全球的な固有磁場や濃密な大気を持たないが、太陽風や地球磁気圏尾部のプラズマが月面や地殻磁場と相互作用を起こし、様々なプラズマ現象を引き起こすことが知られており、ホイッスラーモード波動についても、月に向かう波動と月面で磁気的に反射され上昇する電子とのサイクロトロン共鳴により月近くで励起されることが知られている。このホイッスラーモード波動励起においては、月面での平行電子の吸収と垂直電子の磁気的な反射による速度分布関数の実効的な温度異方性が自由エネルギー源となっている。このような月周辺のホイッスラーモード波動の振幅は地球磁気圏で見られるものと同程度に大きく、コーラス放射のような複雑な周波数構造の形成も報告されている。

本研究では地球内部磁気圏とは条件が大きく異なる月周辺におけるホイッスラーモード波動のスペクトル形状を調べることにより、0.5 f_{ce} ギャップなどの周波数構造の生成機構の解明を目指す。月の場合は地球内部磁気圏と異なり、月の位置が太陽風中・マグネトシース・マグネトテールと変化するため、背景磁場の形状や電子の分布関数が時間とともに大きく変化する。これにより、プラズマ環境の違いがスペクトル形状に与える影響も明らかになると期待される。

本研究では ARTEMIS 衛星の磁場と粒子の観測データを用いて地球内部磁気圏における Teng et al. (2019) の手法

を参考に統計解析を行った。ホイッスラーモード波動の自動検出を行い、さらに、0.5f_{ce} の上下でのスペクトル強度と 0.5 f_{ce} 付近での強度極小の有無によって「Lower-band only」、「Upper-band only」、「Banded」、「No-gap」の 4 種類に自動的に分類した。4 種のスペクトル形状の発生頻度は地球内部磁気圏のものとは大きく異なり、特に 0.5 f_{ce} ギャップをもつ Banded の発生数はごく僅かであった。本発表では、月面の磁気異常や、月の位置による効果についても議論する予定である。

R006-37
Zoom meeting B ：11/2 PM1 (13:45-15:30)
14:30〜14:45

Preferential energization of lower-charge-state heavier ions in the near-Earth magnetotail

#Kunihiro Keika[1)],Satoshi Kasahara[2)],Shoichiro Yokota[3)],Masahiro Hoshino[4)],Kanako Seki[4)],Takanobu Amano[4)],Lynn M. Kistler[5)],Masahito Nose[6)],Yoshizumi Miyoshi[7)],Tomoaki Hori[7)],Iku Shinohara[8)]
[(1]The University of Tokyo,[(2]The University of Tokyo,[(3]Osaka Univ.,[(4]The University of Tokyo,[(5]ISEOS, University of New Hampshire,[(6]ISEE, Nagoya Univ.,[(7]ISEE, Nagoya Univ.,[(8]ISAS/JAXA

O+ ions make a significant contribution to plasma pressure in the inner magnetosphere during magnetic storms. The storm-time O+ enhancements are primarily caused by enhanced supply from the ionosphere and effective energization in the magnetotail. In order to characterize the magnetotail process that dominates the effective energization, we examine differences in energy spectra of energetic 10-180 keV/q ions between different ion species: H+, He++, He+. O++, and O+. We use observations made by the MEP-i instrument on the Arase (ERG) spacecraft on the nightside in the radial distance of ˜5 Re to ˜7 Re during the main and early recovery phases of the May 2017 and July 2017 storms. The comparisons of energy spectra show that, for the same charge states, heavier ions are more energized than lighter ions. For the same mass, lower-charge-state ions are more energized than higher-charge-state ions. The spectra exhibited a sharp decrease at high energies for all ion species, while the spectra for more energized ions were shifted toward higher energies, compared to those for less energized ions. The results suggest that the preferential energization results from temperature increase rather than generation of energetic ions at the high-energy tail. Considering temporal and spatial scales of heavy ion kinetic motions, we conclude that the preferential energization of lower-charge-state heavier ions occurs during the course of dipolarization, likely due to non-adiabatic heating in the near-Earth plasma sheet, effective trapping during the transport by localized flow channels, and/or non-adiabatic acceleration around the near-Earth flow-braking region.

R006-38
Zoom meeting B ：11/2 PM1 (13:45-15:30)
14:45〜15:00

磁気圏尾部“乗り換えリコネクション”の磁場トポロジー

#渡辺 正和 [1)], 田中 高史 [2)], 藤田 茂 [3)], 蔡 東生 [4)], 熊 沛坤 [4)]
[(1] 九大・理・地惑,[(2] 九大・国際宇宙天気科学教育センター,[(3] データサイエンスセンター/統数研,[(4] 筑波大・シス情

Magnetic topology of “crossover reconnection” in the magnetotail

#Masakazu Watanabe[1)],Takashi Tanaka[2)],Shigeru Fujita[3)],DongSheng Cai[4)],Peikun Xiong[4)]
[(1]Earth & planetary Sci., Kyushu Univ.,[(2]REPPU code Institute,[(3]ROIS-DS/IMS,[(4]ISIS, U Tsukuba

Recent numerical modeling indicates that the global magnetic topology of the magnetosphere consists of two magnetic nulls and two separators connecting them (the so-called 2-null, 2-separator structure). In particular, this basic structure is seen persistently during periods of northward interplanetary magnetic field (IMF). At the same time, however, it sometimes occurs that even for steady northward IMF conditions, IMF lines intrude into the closed region of the magnetotail, resulting in a peculiar structure with tangled closed geomagnetic lines and unconnected IMF lines. Obviously, this situation implies a (presumably local) breakdown of the 2-null, 2-separator structure. As an explanation of this tangling, we have been advocating “crossover reconnection” in the magnetotail that is normally prohibited in the 2-null, 2-separator structure. In fact, field-aligned electric fields (reconnection electric fields) in the magnetotail strongly support this scenario. However, it is still unclear in what global topology that tangling is formed. In order to answer this question, we have applied to the simulated magnetosphere the geodesic level set method that have been recently developed for the topology analysis of solenoidal vector fields. In the talk, we will report on the analysis results and discuss their interpretations. At a certain time step of a simulation run in which field line tangling was seen, with the spatial resolution of 0.25 Re, we identified four magnetic nulls in the simulated magnetosphere (one in the Northern Hemisphere and three in the Southern Hemisphere). All of them are related to the 2-null, 2-separator structure, while there were no nulls in the magnetotail. The three nulls in the Southern Hemisphere are suggested to be one null originally. We are now examining whether the splitting is due to numerical errors or due to real topology bifurcation.

近年の数値モデリングにより、磁気圏大域磁場トポロジーの基本は、零点 2 個とそれらを結ぶ 2 本のセパレータで構成されるもの（2 零点，2 セパレータ構造）であることがわかっている。特に惑星間空間磁場（IMF）北向き時にはこの構造が普遍的にみられる。しかし一方で、北向き定常 IMF であっても、磁気圏尾部の閉磁力線領域に IMF が侵入し、閉磁力線と IMF が絡み合った構造が現れることがある。この状況では明らかに 2 零点，2 セパレータ構造が（たぶん局所的に）壊れている。この説明として我々のグループは、2 零点，2 セパレータ構造では本来禁止されている磁力線のなぎ換え“乗り換えリコネクション”が起こることを提唱してきた。実際、磁気圏尾部における沿磁力線電場（リコネクション電場）はこの提案を強く支持している。しかし、いかなる大域磁場トポロジーのもとで磁力線の絡みが形成されているかは明らかでない。この問題を解決するため、我々は最近開発された、測地的レベル集合法によるトポロジー解析法をシミュレーションで得られた磁気圏に適用することを試みた。講演ではその解析結果と解釈について報告する。あるシミュレーションの磁力線の絡まりが見られた時刻において、空間解像度 0.25Re の範囲で零点は 4 個（北半球 1 個、南半球 3 個）あった。いずれも 2 零点，2 セパレータ構造に関係するものであり、磁気圏尾部に零点は認められなかった。南半球の 3 個の零点は、本来 1 個の零点であったものと考えられる。この零点の分裂が、数値誤差によるものか、あるいはトポロジー分岐によるものか、現在検討中である。

R006-39
Zoom meeting B ：11/2 PM1 (13:45-15:30)
15:00〜15:15

Effect of whistler waves on electron bounce motion in the Earth's magnetotail

#Fumiko Otsuka[1)],Kaiti Wang[2)],KIROLOSSE MINA GIRGIS[3)],Tohru Hada[4)]
([1]Kyushu Univ.,[2]Tamkang Univ.,[3]Kyushu Univ.,[4]Kyushu Univ.

Whistler waves play an important role in the scattering of energetic electrons in the Earth's magnetosphere. Pitch-angle scattering of trapped electrons caused by the wave-particle interaction via such waves violates the invariant of periodic bounce motion of the electrons in the dipolar magnetic field.We study the effects of whistler waves on the electron bounce motion in the Earth's magnetotail by performing test particle simulations. We use three models for the background magnetic field; a uniform field, a pure dipolar field, and a stretched dipole-like field. Oblique whistler waves, localized around the magnetic equator, are given as a superposition of sinusoidal waves obeying a cold plasma dispersion relation. We solve a relativistic equation of motion of electrons in the given electromagnetic fields. Electron bounce periods are evaluated as functions of the electron energy and the initial pitch-angle and are compared with the adiabatic theory. We demonstrate that the electrons sometimes switch their guiding field lines due to the wave scattering, and their mirror points and bounce periods vary in time. We will discuss these results referring to a THEMIS observation of the dipolarization event detected at ˜10 RE tailside near the magnetic equator.

R006-40
Zoom meeting B ：11/4 AM1 (9:00-10:30)
9:00〜9:15

センサ間のノイズレベルの差異を考慮したプラズマ波の到来波識別手法に関する研究

#田中 裕士 [1)], 太田 守 [1)], 笠原 禎也 [1)]
[(1] 金沢大

A Study of Identification Method of the Arriving Wave Model for Plasma Waves Considering Different Sensor Noise Levels

#Yuji Tanaka[1)],Mamoru Ota[1)],Yoshiya Kasahara[1)]
[(1]Kanazawa Univ.

The analysis of plasma waves measured by scientific satellites is an effective method to investigate the plasma environment in space. Direction finding of plasma waves provides important clues for understanding not only local plasma environment but also the global features along the propagation paths of the waves. Several kinds of direction finding methods are proposed and each method has its own advantages and disadvantages. In order to obtain fast and accurate direction finding results, it is necessary to identify the nature of the arriving waves and apply proper direction finding methods.

In order to identify the nature of the arriving waves, the planarity [Santolik+, 2003] is widely used. The planarity is calculated from the spectral matrix, which includes information on the amplitudes and phase differences of the electromagnetic field. The planarity is used to identify whether the arriving wave is one plane wave or not under the assumption that the noise levels of all electromagnetic field sensors are equal. In general, however, the noise levels of the sensors on board a scientific satellite are not always equal due to the degradation of the sensors during long-term operation period.

In this study, we propose a new identification method for the arriving wave model using the spectral matrix, which can be accurately classified with different noise levels among sensors. Our proposed method realizes robust classifications by introducing the prior information about the sensor noise level and likelihood ratio tests. We verified the effectiveness of the proposed method.

Reference

[Santolik+, 2003] Santolik, O., M. Parrot, and F. Lefeuvre, Singular value decomposition methods for wave propagation analysis, Radio Sci., 38(1), 1010, doi:10.1029/2000RS002523, 2003.

R006-41
Zoom meeting B ：11/4 AM1 (9:00-10:30)
9:15〜9:30

FPGA を用いた帯域分割型スペクトルマトリクス演算モジュールの開発

#川合 真広 [1)], 笠原 禎也 [1)]
(1 金沢大

Development of an FPGA module for spectral matrix generator with a band division function

#Masahiro Kawai[1)],Yoshiya Kasahara[1)]
(1Kanazawa Univ.

Many scientific satellites have been launched to investigate the electromagnetic environment in space, and various types of plasma waves have been observed. However, the data amount measured by plasma wave instruments aboard scientific satellite is much larger than the telemetry data rate to the ground. Onboard CPU has been used for signal processing, but it was impossible to perform real-time processing due to severe restriction of power consumption as well as computation speed. In the present study, we develop a digital receiver which is available for real-time signal processing with a low-power consumption and high-speed computation by using an FPGA (Field Programmable Gate Array).

We have already developed an FPGA module which generates spectral matrix from electric and magnetic field waveforms of three orthogonal components. Spectral matrix is an important key parameter for direction finding of plasma waves. In the generation process of spectral matrix, we perform FFT (Fast Fourier Transform) which causes the frequency resolution fixed for all frequency band. On the other hand, the frequency band to be covered by the plasma wave instruments is wide and we require a frequency resolution appropriate for each frequency range. In this study, we introduce cascaded decimation filters as a pre-processing stage of spectral analysis using FFT to meet the desired frequency and time resolutions for each frequency range. In addition, we are currently developing the modules applicable to the FPGA developed by Intel, which is not a radiation tolerant type. Then we need to transplant the developed modules to a radiation tolerant FPGA, for example, developed by Microsemi.

In the presentation, we introduce the basic design of the FPGA module developed for the spectral matrix generator with a band division function and the evaluation results of the modules after transplant of the modules to the FPGA developed by Microsemi.

宇宙空間の電磁界環境の調査のために多くの科学衛星が打ち上げられており, 様々な種類のプラズマ波動の観測が行われてきた. しかし, 科学衛星に搭載された波動観測器によって観測されるデータ量は地上へ伝送可能な容量に比べて膨大であるため, 信号処理を行いデータ量を削減することで効率的に地上へデータを送信している. 従来は CPU が信号処理を担ってきたが, 処理性能の関係によってリアルタイム処理が困難であったり, 複数の CPU が必要になることで消費電力や回路規模の増大といった問題がある. そこで我々は低消費電力・高速処理が可能な FPGA(Field Programmable Gate Array) に処理の一部を置き換えることで 1 チップでリアルタイム処理可能な波動受信機の開発を進めている.

現在までに, 波動の伝搬方向推定に用いるスペクトルマトリクスを生成するスペクトルマトリクス演算モジュールが開発済である. 波動観測器が対象とする周波数が広帯域なため, それぞれの帯域に合わせた周波数分解能にする必要があるが, 単一の FFT(Fast Fourier Transform) を用いたスペクトル解析では，全帯域で周波数分解能が同一となり, 帯域別に周波数分解能を変更できない. そこで, 本研究ではデシメーションフィルタをカスケード接続した帯域分割モジュールを開発し, FFT モジュールの前段に追加することで，帯域別に所望の周波数および時間分解能が得られるスペクトルマトリクス演算モジュールの実現を目指している. また, 現在の開発環境は民生用の Intel 社の FPGA であるが, 将来的に宇宙環境下で使用可能な Microsemi 社の FPGA でも適用可能とするため, 開発した帯域分割型スペクトルマトリクス演算モジュールの Microsemi 社製 FPGA への移植も検討する.

本発表では FPGA による帯域分割型スペクトルマトリクス演算モジュールの構成と, Microsemi 社製 FPGA へ移植した際の性能評価について報告を行う.

R006-42
Zoom meeting B ：11/4 AM1 (9:00-10:30)
9:30〜9:45

プラズマ波動観測のための波形データ圧縮 FPGA モジュールの開発

#中瀬 一生 [1)], 笠原 禎也 [1)]
(1 金沢大

Development of a data compression module on FPGA for waveform receiver for plasma wave measurements

#Kazuki Nakase[1)],Yoshiya Kasahara[1)]
(1Kanazawa Univ.

Measurement of electromagnetic waveforms in space plasma is important to understand plasma environment, the amount of waveform data, however, is too huge to send to the ground station as it is. The satellites are required to be as small as possible to achieve simultaneous multiple point observation by formation flight satellites and/or to reduce power consumption and development cost.

In order to reduce the size of waveform data, onboard CPU was conventinally used, but it is important to process whole waveform data due to large calculation cost. Furthermore, receivers and processors for plasma wave instruments have to be small to meet the requirements of small satellites. In the present study, we develop a waveform compressor with FPGA (Field Programmable Gate Arrays) that can construct logic circuit by coding in HDL (Hardware Description Language.) We can design a signal processing module that works fast enough to handle all waveform data in real-time.

In the previous research, an FPGA module using sub-band waveform compression has been already developed on an Altera's general-purpose FPGA. This module is developed only for verifying and evaluating the module function, but is not able to apply in the space environment where the FPGA is exposed to severe radiation and temperature conditions. The purpose of this research is to transplant the module onto another FPGA named 'RTG4', which is ensured to work in such a harsh environment.

In the presentation, we introduce an overview of the sub-band waveform compressor module and explain the evaluation of the module with test data.

宇宙プラズマ中における電磁波の波形観測はプラズマ観測を把握する上で重要項目の一つであるが, 観測データの総量が非常に膨大になるため, そのまま地上局に伝送することができない. また近年の科学衛星は, 編隊飛行による同時多点観測や, 消費電力・開発コストの削減の必要性から, 小型化・軽量化が要求される.

波形データの削減のため, 従来は機上搭載の CPU 上で波形データを圧縮していたが, 計算負荷が多大なため, 間欠的にしかデータを取得できなかった. また前述の通り, 観測器の小型・軽量化を行い, 超小型受信機で従来以上の観測性能を満たす必要がある. そこで本研究では, CPU に代わる信号処理デバイスとして HDL（回路記述言語, Hardware Description Language）を記述することで, 電子回路を構成できる FPGA（Field Programmable Gate Arrays）を用いて波形圧縮をリアルタイムに行えるディジタル受信器の開発を行う.

当研究グループではすでに, サブバンド波形圧縮モジュールが Altera 製の民生用 FPGA で開発され, FPGA による信号処理の動作検証や評価を実施済みである. しかし, 実際に科学衛星に搭載するには FPGA が放射線被爆や温度変化などに対応しなくてはならない. そのため, 本研究では宇宙空間での動作実績が保証されている Microsemi 製 FPGA「RTG4」にサブバンド波形圧縮モジュールを移植することを目的とする.

本発表では, 本研究で開発したサブバンド波形圧縮モジュールについて説明した後, テストデータを用いて当モジュールの動作評価を行う.

R006-43
Zoom meeting B ：11/4 AM1 (9:00-10:30)
9:45〜10:00

専用集積回路を用いた超小型プラズマ波動受信器の開発

#石井 響 [1)], 頭師 孝拓 [2)], 小嶋 浩嗣 [3)]
[(1] 奈良高専,[(2] 奈良高専,[(3] 京大・生存圏

Development of the miniaturized plasma wave receiver using application-specific integrated circuits

#Hibiki Ishii[1)],Takahiro Zushi[2)],Hirotsugu Kojima[3)]
[(1]National Institute of Technology, Nara College,[(2]National Institute of Technology , Nara College,[(3]RISH, Kyoto Univ.

Space is filled with dilute plasma, and they exchange their kinetic energy through by radio waves called plasma waves. It is important to observe plasma waves to understand the electromagnetic environment in space. Plasma wave observers have been installed in scientific satellites and have been used for observations. In recent years, it has become important to use multiple instruments for simultaneous observations. In addition, as the number of instruments used in a spacecraft becomes more diversified and the resources allowed per instrument decrease, it is necessary to reduce the size of the instruments. In this study, we will develop a miniaturized plasma wave receiver.

The plasma wave receiver is classified into the waveform type and the spectrum type. The observation result of the waveform type includes phase information, but it cannot be used for continuous observation because of the large amount of data, so it is important to combine it with the spectrum type, which outputs smaller data. The plasma wave receiver to be developed in this study has a configuration that allows the receiver to be operated in either the waveform type or the spectrum type from software by changing the characteristics of the analog circuit.

The plasma wave receiver consists of an analog circuit and a digital circuit. The analog circuit has filters and an amplifier, and the frequency response can be varied by an external signal. In this study, the analog circuit is developed as ASICs (Application Specific Integrated Circuits) to achieve a significant reduction in size compared to conventional receivers. The digital part controls the analog circuits and performs signal processing for the receiver, such as fast Fourier transform and waveform compression. Microcontrollers or FPGAs are expected to be used for the digital part.

In this presentation, we will describe the detailed design and expected performance of the breadboard model of the receiver that we are currently developing.

地球磁気圏は希薄なプラズマで満たされており、プラズマにおけるエネルギーの授受は電波が主体となっている。この電波はプラズマ波動と呼ばれており、この波動を観測することは宇宙の電磁環境を理解するうえで重要である。これまでに理学衛星等にプラズマ波動観測器を搭載した観測が行われてきたが、近年では複数の観測器を用いた多点同時観測が重要とされている。また、探査機に搭載する機器の多様化が進み、観測器一つ当たりに許されるリソースが減少していることから、観測器の小型化が必要とされている。そこで、本研究では超小型プラズマ波動受信器の開発を行う。

プラズマ波動受信器の観測方式は、波形捕捉型とスペクトル型に分類される。波形捕捉型では、位相情報を含むが、データ量が多くなるため連続観測が不可能であり、データ量が小さいスペクトル型と組み合わせて観測することが有効である。本研究で開発するプラズマ波動受信器は、アナログ回路の特性を可変とすることでソフトウェアから受信器を波形捕捉型・スペクトル型のどちらで動作させるか変更可能な構成としている。

開発するプラズマ波動受信器はアナログ回路部とディジタル回路部から構成される。アナログ回路部はノイズ除去のためのフィルタ回路や増幅器を内蔵しており、また外部信号により周波数特性を可変としている。本研究では、アナログ回路部を ASIC（特定用途向け集積回路）として開発することにより、従来の受信器と比較して大幅な小型化を実現する。ディジタル部はアナログ回路の制御、高速フーリエ変換や波形圧縮等の、受信器に必要な制御および信号処理を行う。ディジタル回路部においてはマイクロコントローラや FPGA の利用を想定している。

発表においては現在開発している受信器ブレッドボードモデルの詳細な設計および見込まれる性能について述べる予定である。

R006-44
Zoom meeting B ：11/4 AM1 (9:00-10:30)
10:00〜10:15

Signal and Noise Separation From Satellite Magnetic Field Data Through Independent Component Analysis

#Shun Imajo[1)],Masahito Nose[2)],Mari Aida[3)],Haruhisa Matsumoto[3)],Nana Higashio[3)],Terumasa Tokunaga[4)],Ayako Matsuoka[1)]

([1DACGSM, Kyoto Univ.,([2ISEE, Nagoya Univ.,([3JAXA,([4Kyutech

We propose an application of the independent component analysis (ICA) to separate satellite-induced time-varying stray fields from magnetic field data obtained using onboard multiple magnetometers. The ICA is a method for estimating source signals at multiple sites so that the estimated source signals can become statistically independent of each other. Since stray field variations are statistically independent of external natural field variations, the ICA method is expected to separate the natural variations from stray fields. Thus, we applied the ICA to magnetic field data from the first Quasi- Zenith Satellite, which has two triaxial fluxgate magnetometers, without using an extendable boom. First, we removed the long-period trend from the original data to create detrended data. Then, we applied the FastICA algorithm to the detrended data and obtained six independent components (ICs). The stray fields were successfully separated into three ICs (noise ICs), and the natural signals were represented by the other three ICs (signal ICs). Finally, we restored the observed signals from the signal ICs, and confirmed that the natural phenomena variations were not altered by the processing step. We also proposed a selection method of the noise ICs using the C coefficient, which is the coefficient of the variance of the mixing vectors. There was a large difference in C between the ICs whose C coefficients are the largest third and fourth ones. Overall, these results demonstrate the possibility that the ICA method can support for boom-less magnetic observations in future satellite missions. The result has been published in Imajo et al. [2021, JGR] (doi:10.1029/2020JA028790).

R006-45
Zoom meeting B ：11/4 AM1 (9:00-10:30)
10:15〜10:30

Design of the analog chip utilized in Fundamental Mode Orthogonal Fluxgate Magnetometers

#Masahiko Nakata[1)],Naofumi Murata[2)],Ayako Matsuoka[3)],Satoshi Kurita[4)],Hirotsugu Kojima[4)]
([1]Engineering, Kyoto Univ.,([2]JAXA,([3]Graduate school of science, Kyoto Univ.,([4]RISH, Kyoto Univ.

We are working to design an analog circuit chip dedicated to Fundamental Mode Orthogonal Fluxgate Magnetometers, which will be installed on future scientific satellites. Fluxgate magnetometers are commonly used for measuring DC magnetic fields as well as low frequency magnetic field fluctuations in space missions. Conventional “parallel” fluxgate magnetometers have employed a ring-core sensor, because the sensor shows good noise characteristics and stability of output offset voltages. Parallel fluxgate magnetometers with ring-core sensors have been contributing to a lot of space missions. On the other hand, the sensor is complex in structure, and it requires a sufficiently large core to achieve low-noise detection of magnetic fields. The ring core sensor is hence unsuitable for miniaturization of the instrument. However, progress of micro-/nano-satellites emphasizes a need for miniaturization of onboard instruments. Recently, a new type of fluxgate magnetometers called “Fundamental Mode Orthogonal Fluxgate (FM-OFG)” magnetometer has been introduced. The sensor of the FM-OFG magnetometer consists of a pair of amorphous wire core and a pick-up/feedback coil. There is no need of excitation coils that are necessary for the ring-core sensor. While it is difficult to get below 10 gram per axis with a ring-core sensor, the FM-OFG sensor can be made much lighter at about 1 gram per axis. The FM-OFG sensor causes breakthrough in the miniaturization of fluxgate magnetometers.

To pursue a small and light fluxgate magnetometer, miniaturizing electronic circuits is also crucial. The present paper focuses on miniaturizing the electronic circuits of the FM-OFG magnetometer by developing an analog chip, which is so-called the ASIC (Application Specific Integrated Circuit). We design essential analog components of the FM-OFG electronic circuits and make it a goal to implement them on a small chip with a size of a few tens of millimeter square. The FM-OFG electronic circuits have two main components. They are the part for exciting a wire core and the part for picking up signals from the sensor head and retrieving waveforms of detected magnetic fields based on a feedback configuration. As the first step, we start with designing the latter part of the circuit and evaluating performance of the chip based on circuit simulations.

R006-46
Zoom meeting B ：11/4 AM2 (10:45-12:30)
10:45〜11:00

ASICを用いた粒子センサ用高速プリアンプの小型集積化に関する研究

#菊川 素如 [1)], 浅村 和史 [2)], 栗田 怜 [3)], 小嶋 浩嗣 [1)], 齋藤 義文 [4)]
(1 京大・生存圏,(2 宇宙研,(3 京都大学 生存研,(4 宇宙研

Study on Development and Integration of the High-Speed Current Detection Circuits in Particle Sensors

#Motoyuki Kikukawa[1)],Kazushi Asamura[2)],Satoshi Kurita[3)],Hirotsugu Kojima[1)],Yoshifumi Saito[4)]
(1RISH, Kyoto Univ.,(2ISAS/JAXA,(3RISH, Kyoto Univ.,(4ISAS

Space is filled with extremely low-density plasma, which constantly generates various plasma phenomena. Especially in the vicinity of the planets in the solar system, the solar wind, which is a mass of supersonic plasma blowing from the sun, has a dominant influence. Since each planet has a magnetosphere of completely different size and intensity depending on its nature, in-situ observation will capture plasma phenomena unique to each planet. Therefore real-time observations by satellites are expected to bring very meaningful results in the study of plasma physics.

Plasma observation consists of plasma particle measurements and electromagnetic field measurements, and we are especially focusing on the integration of plasma particle measurement devices. Plasma particle measurement means to obtain the three-dimensional velocity distribution function of electrons and ions flying in space and to measure the mass of each particle. A top-hat type electrostatic energy analyzer (ESA) is used to measure the velocity vector of individual particles, and a TOF type mass analyzer (MA) is used to measure mass of particles. In practice, these are combined and mounted on a satellite to obtain the velocity vector and mass of the particles simultaneously. When particles enter the instrument, weak current pulses are emitted from the Micro-Channel Plate (MCP) inside the ESA or MA. A high-speed preamplifier is required to transmit this current signal to the logic circuit, but the conventional preamplifiers are composed of discrete components, which make the size of the device very large. The purpose of this research is to improve this high-speed preamplifier to be more suitable for use in satellites by making it more integrated using Application Specific Integrated Circuit (ASIC) technology. Similar to the conventional high-speed preamplifiers, we design the system to have a count rate of 10^6/s and to respond to any input at a constant time.

The small, high-speed preamplifier we have developed consists of two blocks. The first block is a current-voltage amplification circuit and the second block is a comparator. The current-voltage amplification circuit converts the weak current pulse coming from the MCP into a voltage signal and amplifies the current signal so that it can be input to the comparator in the next block. In a comparator, we arbitrarily determine the threshold voltage and make a distinction between the noise below the threshold and the signal above the threshold. The small preamplifier we developed in this study has a single channel size of 210 um x 570 um. When installed in a satellite, at least 15 channels will be integrated at the same time, because the same number of small preamplifiers as the number of ESA channels must be connected. Considering the size of each channel, 15 channels can be contained in a single chip of 5mm square, which is much smaller and light-weight than the conventional preamplifiers that are cylindrical shape with 170 mm diameter and 70 mm height.

In this presentation, we introduce the details of the small preamplifier we have developed, including design simulations and measurement results of a prototype chip, and discuss future development.

宇宙空間には非常に密度の低いプラズマが満ちており、それらが絶えず様々なプラズマ現象を生起している。特に太陽系惑星の近傍では、太陽から吹き付ける超音速プラズマの塊である、いわゆる太陽風による影響が支配的となる。各々の惑星はその性質ごとに全く異なる大きさや強度の磁気圏を有するため、そこでの観測はそれぞれに固有なプラズマ現象を捕捉する。すなわち、宇宙空間は一種の巨大なプラズマ実験装置であるともいえ、人工衛星によるリアルタイムな観測はプラズマ物理を研究する上で非常に有意義な成果をもたらすものと考えられている。

プラズマ観測はプラズマ粒子計測と電磁場計測からなるが、我々は特にプラズマ粒子計測機器の小型集積化に取り組んでいる。プラズマ粒子計測とは、宇宙空間を飛翔する電子やイオンの 3 次元速度分布関数を取得し、それぞれの質量を測定することである。粒子一つ一つの速度ベクトルを計測する装置として TOP-HAT 型静電エネルギー分析器 (以下 ESA:Electrostatic Analyzer とする) があり、質量計測の装置としては TOF 型質量分析器 (以下 MA:Mass Analyzer とする) がある。実際には、これらを組み合わせて人工衛星に搭載することで粒子の速度ベクトルと質量を同時に取得する。粒子が機器内に入射すると、ESA や MA に内蔵された MCP:Micro-Channel Plate から微弱な電流パルスが放出される。この電流信号をロジック回路に伝送するには高速プリアンプが必要となるが、既存のものはディスクリート部品によって構成されているため、装置のサイズが非常に大きくなってしまう。本研究は、この高速プリアンプを特定用途向け集積回路 (ASIC: Application Specific Integrated Circuit) 技術を用いて小型集積化し、より人工衛星への搭載に適した形へと改良することが目的である。既存の高速プリアンプと同様、10^6 個/s のカウントレートを有し、あらゆる入力レベルに対して一定の時刻で応答が可能であるように設計を行う。

我々が新たに開発した小型高速プリアンプは、初段の電流電圧変換増幅回路と次段のコンパレータからなる。電流電圧変換増幅回路は、MCP から入力される微弱な電流パルスを電圧信号に変換し、次段のコンパレータに入力可能

なレベルまで増幅する。コンパレータは任意に閾値となる電圧を決定し、閾値以下の雑音とそれ以上の信号とを峻別する役割を担う。

本研究において開発した小型プリアンプは、1 チャンネルの大きさが 210 um x 570 um である。実際の衛星に搭載される際は ESA のチャンネル数と同数の小型プリアンプを接続する必要があるため、少なくとも 15 チャンネルが同時に組み込まれることになる。1 チャンネルの大きさを考慮すると 15 チャンネルを 5mm 角のワンチップに収納することも可能であり、直径 170mm、高さ 70mm の円筒形をしている既存のプリアンプより遥かに小型・軽量である。

本発表では、我々が開発した小型プリアンプの詳細を設計シミュレーションや試作チップの測定結果を交えて紹介し、今後の開発展望について述べる。

R006-47
Zoom meeting B ：11/4 AM2 (10:45-12:30)
11:00〜11:15

将来の惑星探査に向けたASIC技術による10-100 keV電子観測器の小型化

#菅生 真[1)], 笠原 慧[2)], 池田 博一[3)], 小嶋 浩嗣[4)], 頭師 孝拓[5)], 菊川 素如[4)]
(1 東大・理・地惑,(2 東京大学,(3JAXA・宇宙研,(4 京大・生存圏,(5 奈良高専

Miniaturization of 10-100 keV electron sensor for future planetary explorations using ASIC

#Shin Sugo[1)],Satoshi Kasahara[2)],Hirokazu Ikeda[3)],Hirotsugu Kojima[4)],Takahiro Zushi[5)],Motoyuki Kikukawa[4)]
(1Earth and Planetary Science, Univ. Tokyo,(2The University of Tokyo,(3ISAS, JAXA,(4RISH, Kyoto Univ.,(5National Institute of Technology , Nara Col

We developed a front-end ASIC (Application Specific Integrated Circuit) for an APD (Avalanche PhotoDiodes) detector to miniaturize a high energy electron sensor for future planetary explorations. Our sensor's objects are electrons with 10-100 keV energy, which is key energy range for the acceleration of electrons because that is transitional energy range from thermal to non-thermal distributions of energy spectrum. Recently, APDs, which are detectors with high detection efficiency for 10-100 keV electrons, have been applied to an energetic electron sensor onboard the Earth-orbiting satellite and have shown their effectiveness. On the other hand, the energy range of APD is narrow, and combined use with other detectors is indispensable to cover the wide energy range of electrons near the planet and leads to increasing weight. It is not suitable for planetary explorations, which place stringent limitation on payload mass. Therefore, we aim to miniaturize the sensor by applying the ASIC technology to signal processing circuits of the sensor. Our circuit is composed of preamplifiers, shaping amplifiers, peak holders, comparators, and Analog-to-digital converters. We designed an ASIC circuit so that its dynamic range to be 10^6 e^- in consideration of the APD's high gain and confirmed its performance in simulations. Then, we designed the layout of the ASIC and produced a 15 mm-by-15 mm-by-2 mm ASIC chip, which is about 50 times smaller than the previous circuit. In addition, we tested circuit performance, and clarified the linearity of preamplifiers' output voltage up to signal charges equivalent to 100 keV electron irradiation.

本研究では高エネルギー電子検出器 APD (Avalanche PhotoDiodes) 用フロントエンド回路の ASIC (Application Specific Integrated Circuit) 化開発を行い、将来の惑星探査機搭載に向けて電子観測器の小型化を目指している。我々の電子観測器の観測エネルギーレンジは 10-100 keV であり、熱的な分布から非熱的な分布に遷移する、惑星周辺の電子加速機構の研究に重要なエネルギー領域である。近年この 10-100 keV 電子に感度の良い検出器 APD が地球周回衛星に搭載され、その有効性が示されている。しかし検出器 APD はエネルギーレンジが狭く、惑星近傍の電子の広いエネルギーレンジをカバーするためには他の検出器との併用が必要不可欠であるが、重量が増加しペイロード重量制限の厳しい惑星探査機搭載には向かない。そこで本研究では検出器 APD の信号処理部を ASIC 技術によって小型化する。我々の電子観測器の信号処理回路は前置増幅回路、波形整形回路、ピークホールド回路、比較回路、AD 変換回路で構成されている。我々は APD が増幅率を内蔵する特性を考慮して、エネルギーに関するダイナミックレンジ 10^6 e^- となるように最適化した ASIC 回路の設計を行い、シミュレーション上での動作を確認した。次にこの ASIC 回路の素子配置設計を行い、15 mm × 15 mm × 2 mm サイズのチップを製作した。これは ASIC 化前の回路の約 50 分の 1 のサイズである。さらに製作した ASIC チップの性能試験を行い、100 keV 以下の電子入射に相当する信号電荷の入力に対する前置増幅出力の線形性を確認した。

R006-48
Zoom meeting B ：11/4 AM2 (10:45-12:30)
11:15〜11:30

Development by numerical design of double-shell electrostatic energy analyzer with hemispherical field of view

#Atsuya Takasu[1)],Sugimoto Ichiro[1)],Masafumi Hirahara[2)],Shoichiro Yokota[3)]
([1]Nagoya University ISEE,([2]ISEE, Nagoya Univ.,([3]Osaka Univ.

The terrestrial magnetosphere has regions with various structures due to the influence of the solar wind, the terrestrial intrinsic magnetic field and the upper atmosphere of the Earth. In-situ observations with space plasma analyzers are important for understanding the physical phenomena in these areas. While three-dimensional (3-D) velocity distribution functions have been acquired by analyzers with a fully planar field-of-view(FOV) on spin-stabilized satellites, this type of the analyzer is unsuitable for three-axis stabilized satellites to obtain the wide and precise 3-D velocity distributions. As opportunities for applications to three-axis stabilized satellites increase, we are developing a plasma particle analyzer that can sweep over the hemispherical field of view using an electrostatic deflector.

The miniaturization of satellites has been promoted in these decades, and it is necessary to reduce the size and weight of plasma particle analyzers for these small/micro satellites. In the case of observing ions and electrons in the conventional technology, two separate analyzers must be installed, one for ions and another for electrons. However, it could be difficult to mount two analyzers due to the restriction for small/micro satellites. If these two sensor heads of the ion and electron analyzers can be combined into one, it is possible to reduce the total instrument size, weight, and power for the ion and electron observations on small/micro satellites. We have been developing double-shell electrostatic energy analyzer which enables to observe ions and electrons by one sensor head over a hemispherical FOV on a three-axis stabilized satellite.

Similar to the charged-particle analyzers on SELENE(KAGUYA) [Yokota et al., 2005], the hemispherical FOV double-shell electrostatic energy analyzer is cylindrically symmetric and consists of an FOV deflection system, an ion/electron separator, a double-shell electrostatic energy analyzer, and detectors. The design to achieve better performance of the analyzer utilizes the charged particle orbit calculation software SIMION. Particles with energies of 10 keV for ions and 8.3 keV for electrons can be energy-analyzed from 0 to 90 degrees in the deflected angle, and the analyzer constant is about 4.88 for ions and about 4.05 for electrons. Based on the results, a bread board model(BBM) of a hemispherical FOV double-shell electrostatic energy analyzer is under precise design, and we are preparing for calibration experiments of the BBM using the ion and electron beamline in our laboratory. The electron detector is would be a micro channel plate(MCP) assembly or floating-type avalanche photodiode(APD) array, and the ion mass discrimination is based on the Time-Of-Flight (TOF) mass spectroscopy. The design of the TOF mass spectrometer is one of future works.

We report the current status of the hemispherical FOV double-shell analyzer development including the performance evaluation by numerical calculations and the BBM fabrication in a machine shop in Nagoya university.

R006-49
Zoom meeting B ：11/4 AM2 (10:45-12:30)
11:30〜11:45

Floating-mode avalanche photodiode experiments using low-energy electrons

#Seishiro Tanaka[1)],Masafumi Hirahara[1)],Satoshi Kasahara[2)],Shin Kubo[3)]
[(1]Nagoya University ISEE,[(2]The University of Tokyo,[(3]Clear Pulse Co., Ltd.

Avalanche PhotoDiode (APD) is prevailing for high-energy electron detection with rough energy analyses in space observations. For instance, the electron detector system of the Medium-Energy Particle instrument for electrons (MEP-e) for ERG mission consists of an array of APDs [Kasahara et al., EPS 2018]. Kasahara et al. [NIM, 2012] reported that a minimum detectable energy with an APD is 5keV at 20 ℃.

Our purpose is to reduce the lowermost energy of electron energy analyses with APD and to install APDs in low-energy electron analyzers. In order to detect lower-energy electrons below 5keV, we applied the floating voltage to APD so that the incident electrons could be accelerated up to energies enough large for the APD detection, depending on the difference of voltage. We could detect low-energy electrons even below 5keV by applying up to +5kV as a low-pass filtered floating voltage to the incident surface of APD.

While we could analyze 5keV electrons by about 4keV energy-resolution without the floating voltage at 20 ℃ in our beam line facility, we also confirmed the effect on the total incident energies of the floating voltages by an equivalent energy-resolution. We found that secondary electrons generated by direct impacts of beam line electrons in the vicinity of APD were also accelerated to 5keV by the floating voltage and detected. We also identified another type of secondary electrons generated by beam line electrons back-scattered from APD. These 5keV-electron detections showed that a few-eV electrons were substantially accelerated and successfully energy-analyzed by the floating-mode APD. Our experiments actually indicate that the floating-mode APDs could be applied as low-energy electron detectors with a high-sensitivity and a rough energy analysis capability.

R006-50
Zoom meeting B ：11/4 AM2 (10:45-12:30)
11:45〜12:00

A new calibration method for LEPe low-energy electron data of the ERG satellite

#Yoichi Kazama[1)],Kazushi Asamura[2)],Satoshi Kasahara[3)],Shoichiro Yokota[4)],Tomoaki Hori[5)],ChaeWoo Jun[6)],Yoshizumi Miyoshi[5)],B.-J. Wang[7)],S.-Y. Wang[8)],Sunny W. Y. Tam[9)],Yoshiya Kasahara[10)],Shoya Matsuda[11)],Atsushi Kumamoto[12)], Fuminori Tsuchiya[12)],Yasumasa Kasaba[13)],Masafumi Shoji[5)],Ayako Matsuoka[14)],Mariko Teramoto[15)],Takeshi Takashima[16)], Iku Shinohara[17)]
([1]ASIAA,[2]ISAS/JAXA,[3]The University of Tokyo,[4]Osaka Univ.,[5]ISEE, Nagoya Univ.,[6]ISEE, Nagoya Univ.,[7]ASIAA, Taiwan,[8]ASIAA, Taiwan,[9]Institute of Space and Plasma Sciences, National Cheng Kung University, Taiwan,[10]Kanazawa Univ.,[11]ISAS/JAXA,[12]Planet. Plasma Atmos. Res. Cent., Tohoku Univ.,[13]Tohoku Univ.,[14]Kyoto University,[15]Kyutech, [16]ISAS, JAXA,[17]ISAS/JAXA

The ERG (Arase) satellite carries the LEPe instrument that measures three-dimensional electron distributions with energies from ˜20 eV to 20,000 eV to investigate plasma environments in the inner magnetosphere. A calibration method and its parameters are obviously crucial to obtain accurate physical quantities of electrons such as differential flux. In this presentation, we present a newly developed calibration method for low-energy electron measurement of the LEPe instrument. The new calibration method is based on a four-year-long electron dataset made by the instrument since the launch, considering voltage settings of the MCP (micro-channel plate) device. In the new method, we have three steps of data processing for more accurate electron energy flux from raw count rates: 1) correction of response to background counts, 2) normalization of sensitivity differences between anode channels and 3) estimation of MCP efficiency profiles. We are now preparing a new dataset of electron measurement by using the new calibration method, which will be soon available from the ERG Science Center.

R006-51
Zoom meeting B ：11/4 AM2 (10:45-12:30)
12:00〜12:15

Performance of Medium-Energy Particle experiments (MEPs) onboard ERG: a long-term view

#Satoshi Kasahara[1)],Shoichiro Yokota[2)],Kunihiro Keika[1)],Tomoaki Hori[3)],Kazuhiro Yamamoto[1)]
([1]The University of Tokyo,[2]Osaka University,[3]Nagoya University

ERG (Exploration of energization and Radiation in Geospace, also called “Arase”) is the geospace exploration spacecraft, which was launched on 20 December 2016. One of the key observations is the measurement of ions and electrons in the medium-energy range (10-200 keV), since these particles excite EMIC, magnetosonic, and whistler waves, which are theoretically suggested to play significant roles in the relativistic electron acceleration and loss. Medium-Energy Particle experiments - electron analyser (MEP-e) measures the energy and the direction of each incoming electron in the range of 7 to 87 keV. The sensor covers 2-π radian disk-like field-of-view with 16 detectors, and the solid angle coverage is achieved using spacecraft spin motion. Medium-Energy Particle experiments - ion mass analyser (MEP-i) measures the energy, mass, charge state, and direction of each incoming ion in the medium-energy range ($<$10 to $>$180 keV/q). MEP-i thus provides the velocity distribution functions of medium-energy ions (e.g., protons and oxygen ions). MEPs have carried out continuous observations fore more than 4 years without any significant malfunction or degradation. Here we report the long-term trend of the sensor characteristics such as efficiency, in comparison with other instruments onboard ERG for higher and lower energy ranges.

R006-52
Zoom meeting B ：11/4 AM2 (10:45-12:30)
12:15〜12:30

Evaluation of the errors in analyzing energetic electron flux data obtained by Arase/HEP

#Tomoaki Hori[1)],Takefumi Mitani[2)],Takeshi Takashima[3)],Yoshizumi Miyoshi[1)],Iku Shinohara[4)]
([1]ISEE, Nagoya Univ.,([2]ISAS/JAXA,([3]ISAS, JAXA,([4]ISAS/JAXA

The evaluation of measured flux errors is important for detailed quantitative analysis of energetic electron fluxes in the inner magnetosphere. The previous study developed an error estimation method for the energetic electron flux measured by the high-energy electron experiments (HEP) onboard the Arase satellite. The developed method is based on counting statistics of the raw electron count measurement, considering the error propagation due to the count-spectrum deconvolution matrices used for the count-to-flux conversion. In this study we extend the previous work to assess the full range of errors accompanying the actual analysis of directional electron fluxes, such as time-averaged pitch-angle-sorted flux. Our preliminary analysis shows that the flux error due to counting statistics is often comparable to the flux value in the differential flux range less than 10^4/s/sr/keV/cm^2, indicating that a flux value at an individual directional channel sampled in a single data accumulation time (˜0.5 s) is well within its uncertainty level. Averaging them over a 15-deg pitch angle bin for a spin period (˜8 s) improves the flux-to-error ratio typically by a factor of 2-4, allowing for a quantitative analysis of a flux difference of such a factor level. Accordingly a further time integration over several spin periods is needed to lower the uncertainty level to an order smaller than its flux value. The flux-to-error ratio becomes worse (smaller) when the satellite is exposed to fairly high fluxes of MeV electrons, for instance, in the radiation belt proper; a much longer integration time is necessary for achieving the same level of flux uncertainty.

R006-53
Zoom meeting B ：11/4 PM1 (13:45-15:30)
13:45〜14:00

第 24 太陽周期中のオーロラ活動：南極昭和基地における観測（２）

#門倉 昭 [1)]
([1]ROIS-DS/極地研

Auroral activity during the solar cycle 24: Observations at Syowa Station, Antarctica (2)

#Akira Kadokura[1)]
([1]ROIS-DS/NIPR

Auroral activities observed at Antarctic Syowa Station during the solar cycle 24, from 2009 to 2020, are analyzed. In this presentation, characteristics of auroral activity observed with the Scanning Photometer (SPM) will be focused.

Specifications of the SPM are as follows:

- Wave length: CH1: 482.5, 2: 483.5, 3: 484.5, 4: 485.5, 5: 486.5, 6: 487.5, 7: 670.5, 8: 844.6 nm
- FWHM: CH.1-6, 8：0.6 nm、CH.8：5.0 nm
- FOV: 3.0 deg
- Scan speed: 180 deg/10 sec
- Sampling rate: 20 Hz

SPM observation at Syowa Station is carried out during February to October in nighttime hours without moon, and its operation is stopped in the case of bad weather condition of blizzard.

We analyzed annual mean value of SPM data in each bin of 10 minute interval and 18 deg elevation angle in 14:00UT to 05:00UT time axis and 0 deg to 180 deg elevation axis, and following results were obtained:

- In 2013, auroral activity was most quiet, and characteristic energies of precipitation electrons and protons were lowest.
- In 2015, auroral activity was most active.
- Comparing the auroral activities around the solar minimum both in 2009 to 2010 and in 2019 to 2020, precipitation electron and proton characteristic energies are higher and lower in the former period than in the latter period, respectively.

第 24 太陽周期中（2009 年〜2020 年）に南極昭和基地で観測されたオーロラ活動について、特に掃天フォトメータの観測データを主とした解析結果について紹介する。下記に掃天フォトメータの仕様を示す：

・観測波長： 8 波長：CH1: 482.5, 2: 483.5, 3: 484.5, 4: 485.5, 5: 486.5, 6: 487.5, 7: 670.5, 8: 844.6 nm
・波長半値幅：CH1-6, 8：0.6 nm、CH8：5.0 nm
・全視野角：3.0 deg
・掃天速度：180 deg/10 sec
・データ取得速度：20 Hz

CH1-6 は、プロトンオーロラの H β 発光輝線（486.1nm）のドップラーシフト特性の観測を目的とし、CH7, 8 はそれぞれ、窒素分子（N2IP）と酸素原子（OI）からの発光輝線で、電子オーロラのエネルギー特性の観測を目的とする。

昭和基地のオーロラ光学観測期間は 2 月下旬から 10 月中旬までの間で、掃天フォトメータはその間、あらかじめ組み込まれたスケジュールファイルに従って自動運用され、定量的なデータを取得することを目的に、月が出ていない暗夜のみに運用するようにしていて、ブリザードなどの悪天時には観測を中止している。年毎のオーロラ活動の特徴を調べるため、年毎に全観測データの平均値を求め比較する。時間軸方向には、世界時で 14 時から翌朝の 5 時までを 10 分毎に、仰角方向には、0 度（低緯度側）から 180 度（高緯度側）までを 18 度毎に区分し、その 18 度、10 分間に観測された全データの平均値を求める。

このようにして求めた年平均ケオグラムより、下記のような特徴が見られた：

・2013 年のオーロラ活動が最も静かで、降下電子、降下プロトンともにエネルギーが最も低かった。
・2015 年が最も活発だった。
・Solar minimum に近い 2009 年〜2010 年と 2019 年〜2020 年を比較すると、前者は後者に比べ、降下電子エネルギーが高く、降下プロトンエネルギーは低かった。

講演では、これらの解析結果を紹介する。

R006-54
Zoom meeting B ：11/4 PM1 (13:45-15:30)
14:00〜14:15

Tromso AI：ノルウェー・トロムソにおけるオーロラのリアルタイム検出システム

#南條 壮汰 [1)], 野澤 悟徳 [2)], 細川 敬祐 [1)], 山本 雅毅 [3)], 川端 哲也 [2,4)], 津田 卓雄 [1)]
([1] 電通大,[2] 名大・宇地研,[3] キヤノン株式会社,[4] ノルウェー北極大学

Tromsoe AI: automated auroral detection system in Tromsoe, Norway

#Sota Nanjo[1)],Satonori Nozawa[2)],Keisuke Hosokawa[1)],Masaki Yamamoto[3)],Tetsuya Kawabata[2,4)],Magnar G. Johnsen[4)], Takuo Tsuda[1)]
([1]UEC,[2]ISEE, Nagoya Univ.,[3]Canon Inc.,[4]UiT The Arctic University of Norway

As an activity of citizen science, images taken by amateur photographers using commercial digital cameras have been used for scientific research. Such digital images contain a lot of background noise in various wavelengths, unlike professional optical data captured with a narrow-band optical filter. However, digital cameras have three RGB channels and are able to capture what we see in full color. This capability often enables to us identify characteristic features that are difficult to be noticed in professional monochromatic data (MacDonald et al., 2018; Shiokawa et al., 2018). Furthermore, it has been suggested that colors in a digital image can be used to estimate the average energy of pulsating auroral electrons (Nanjo et al., 2021, in revision); thus, digital cameras have a potential to play an essential role for professional scientific research of auroras. However, unlike professional researchers, who automatically observe auroras overnight, photographers have to wait for an auroral appearance to take pictures, which is often a heavy burden on their observations. To reduce this constraint, it is important to provide a system that notifies us of the auroral appearance in real-time. One of the reasons why such a system has not been developed so far is that the aurora's complex and diverse morphology has prevented highly accurate automatic detection. However, with the improvement of deep learning techniques, that problem has almost been solved (Clausen and Nickisch, 2018; Kvammen et al., 2020). In this study, we developed an AI classifier that automatically detects auroras instead of the human eye using a deep neural network model and then combined it with real-time observation using a digital camera in Tromsoe, Norway (Nozawa et al., 2018) in order to build a website "Tromsoe AI" that notifies users of auroral occurrences in real-time. In the presentation, we will explain how to use the website and discuss the solar activity, seasonal and local time dependence of auroral occurrence rates obtained by classifying images from the past 10-year observations in Tromsoe.

市民サイエンスの取り組みとして，アマチュアの写真家が市販のデジタルカメラを用いて撮影した画像を，科学研究に用いる事例が増えている。デジタルカメラによって撮影された画像は，狭帯域の光学フィルタを用いて撮影された本格的な光学データと異なり，様々な波長の光をノイズとして含む。しかしながら，デジタルカメラは RGB の 3 つのチャネルを持ち，人間が知覚するままを捉えるため，プロ向けの観測機材では気づきにくい特徴を同定することがある (MacDonald et al., 2018; Shiokawa et al., 2018)。更に，デジタル画像上の色から，脈動オーロラを発光させる降下電子の平均エネルギーを見積もれることが示唆されており (Nanjo et al., 2021, in revision)，デジタルカメラはオーロラの光学観測機器として，今後も重要な役割を担うことが期待される。しかしながら，パソコンの制御によって一晩中自動で観測を行う研究用途の計測と異なり，アマチュアの写真家は，オーロラの発生を待ってから撮影を行うため，観測にかかる負担が大きい。この制約を減らすためには，オーロラの発生をリアルタイムに通知するシステムを提供することが重要である。これまでにそのようなシステムが開発されなかった原因の一つは，オーロラの形態が複雑かつ多岐にわたるため，高精度な自動検出が行えなかったことにある。しかしながら，人工知能 (Artificial Intelligence: AI) 技術の中でも画像分類のタスクで高い精度を示す深層学習の発展に伴い，その問題が解決しつつある (Clausen and Nickisch, 2018; Kvammen et al., 2020)。そこで，本研究は，深層学習を用いて人の目 (eye) の代わりにオーロラを自動検出する分類器を開発し，ノルウェー・トロムソにおけるデジタルカメラを用いた定常観測 (Nozawa et al., 2018) と組み合わせることによって，オーロラの発生をリアルタイムに通知するウェブサイト " Tromsø AI" を構築した。発表では，ウェブサイトの使い方の解説と，分類器を使い過去 10 年分の観測画像を分類することで得たオーロラの発生率の太陽活動・季節・地方時依存性についての議論を行う予定である。

R006-55
Zoom meeting B ：11/4 PM1 (13:45-15:30)
14:15〜14:30

Aurora image segmentation with deep PNU learning

#Ryoya Katafuchi[1)],Yoshizumi Miyoshi[2)],Terumasa Tokunaga[1)]
([1]Kyutech,[(2]ISEE, Nagoya Univ.

All-sky imaging of aurora has been a powerful tool for studying the generation mechanism of aurora and the coupling system of the magnetosphere and the ionosphere. Long-term ground-based optical observations of aurora with ASI (all-sky imaging) systems have generated vast amount of imaging data for several decades. This has led to growing interest in an establishment of computational methods that can automatically quantify the dynamic behavior of the aurora from ASI data.

Image segmentation is the process of separating a digital image into meaningful segments. This process play an important role to quantify the shapes and sizes of aurora arc from ASI data. Recently, several studies have succeeded in developing high-performance aurora classifiers based on deep learnings for ASI data [Clausen and Nickisch, 2018; Kvammen et al., 2020]. Although these data-driven aurora detectors and classifiers will be powerful tools for polar studies, the segmentation task is more challenging: there is no publicly available datasets containing pixel-level annotations that can be used for aurora segmentations.

The present study proposes a novel image segmentation technique designed for smaller training data. Our idea relies on PNU (positive, negative and unlabeled) learning for binary classification of patch images. Sakai et al. [2018] proposed a fundamental framework and demonstrated superior performances of PNU learning for semi-supervised binary classification problems using simple classifiers. In this study, we extend the loss function of PNU learning that makes it possible to apply the backpropagation algorithm for training CNN (convolution neural networks).

Using the THEMIS ground-based All-Sky Imager data (https://data.phys.ucalgary.ca/sort_by_project/THEMIS/asi/stream0/), we performed experiments for automatic segmentation of discrete arcs. Our method consists of two phases: the training phase and the test phase. In the training phase, we prepare 100 positive (discrete arcs) and negative (others) patches. These positive and negative patches are manually extracted from the THEMIS ASI data. In addition, 3,000 unlabeled patches are randomly extracted from throughout the dataset. The three types of data are used to train the CNN model called ResNet18 for binary classification (PNU learning). In the test phase, patch images are extracted by a raster scanning from input ASI data. The extracted patches are classified into “discrete arcs” and “others” using the trained ResNet18. Finally, boundaries of segmented discrete arcs are corrected based on an unsupervised learning using the fully-connected CRF (conditional random field). In the presentation, we will report initial results of our segmentation technique for THEMIS ASI data. Then, we will discuss the further developments of the proposed method towards the integrated analysis tool for ASI data.

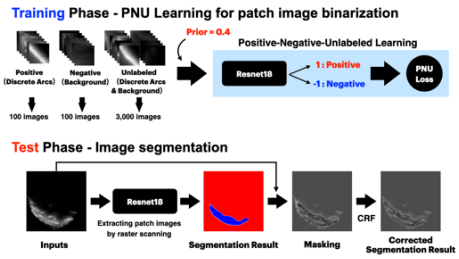

R006-56
Zoom meeting B ：11/4 PM1 (13:45-15:30)
14:30〜14:45

昼側 PsA に寄与する降下電子に関する研究

#安倍 峻平 [1)], 細川 敬祐 [1)], 小川 泰信 [2)]
(1 電通大,(2 極地研

Characteristics of Precipitating Electrons Contributing to Dayside PsA

#Shumpei Abe[1)],Keisuke Hosokawa[1)],Yasunobu Ogawa[2)]
(1UEC,(2NIPR

Pulsating aurora (PsA) is a type of diffuse aurora which shows quasi-periodic modulation of luminosity. It has been known that PsA is usually observed during the late recovery phase of substorms in a magnetic local time (MLT) sector extending from the post-midnight to dawn. Previous studies indicated that PsA originates from quasi-periodic precipitation of electrons, which are scattered by whistler-mode chorus waves near the equatorial plane of the magnetosphere.

Most of the previous studies of PsA are focused on observations on the nightside and dawnside since direct optical observations from the ground cannot be made during daylight hours. However, it has been known that PsA can occur at the dayside, especially from the morning to the noon sector). Recent studies, for example, Han et al. (2015), showed that occurrence of the dayside PsA is not limited to the recovery phase of substorms. As for the generation mechanism, previous studies have indicated that it is caused by electron precipitation due to chorus waves, similar to the night side cases. However, despite the same generation mechanism, the dayside PsA has different characteristics from the nightside PsA, such as the pulsating period. The factors that determine such differences are not yet known. In addition, the spatial distribution of electron precipitation causing the dayside PsA has not been clarified due to the lack of simulataneous observations between dayside PsA and low-latitude satellite particle measurement.

In this study, we investigated the energy distributions of precipitating electrons observed by the DMSP satellite (Defense Meteorological Satellite Program) during several dayside PsA events, observed by the ground-based all-sky WATEC imagers in Longyearbyen, Norway. We also examined the chorus wave observed by the THEMIS satellite the magnetosphere on the same magnetic field line. A series of investigations showed that the precipitating electrons contributing to the dayside PsA have a similar energy distribution to that of the nightside PsA. In addition, it was found that the electron precipitation contributing to the dayside PsA also exists at lower latitudes than the dayside PsA observed in previous studies. These results suggest that the chorus wave that contributes to the dayside PsA has different characteristics from those of the nightside PsA.

ディフューズオーロラのうち，準周期的な発光を伴うものを脈動オーロラ (Pulsating Aurora : PsA) と呼ぶ． PsA は主にサブストームの回復期に発生することが知られており，磁気的地方時 (Magnetic Local Time : MLT) の真夜中から朝方にかけて多く観測される．先行研究では， PsA の発生は準周期的な電子降下に起因し，その電子降下は磁気圏赤道面付近でのホイッスラーモードコーラス波動によるピッチ角散乱によって引き起こされることが示されている．

日照のある時間帯では観測が行えない為、PsA に関する先行研究は真夜中から朝にかけての観測に関するものが大半である．しかし、PsA 自体は昼側でも発生することが知られている。Han et al(2015) では、サブストームの回復期に限らない定常的な昼側 PsA の発生が示された。その発生機構については、夜側と同様に磁気圏のコーラス波動に起因する電子降下によって発生することが先行研究で示唆されている。しかしながら、同じ機構を持つにも関わらず、昼側 PsA は明滅周期などに夜側とは異なった特徴を持つ。そのような差異を決定づける要素が何であるかはまだ知られていない。また、観測時間の制限が存在するため、昼側 PsA を作り出す電子降下の空間的な分布についても明らかにされていない。

本研究では、複数のイベントについて、DMSP 衛星 (Defence Meteorogical Satellite Program) によって観測された降下電子のエネルギー分布と、同一磁力線上で対応する地上全天撮像装置によって観測された PsA、及び磁気圏において THEMIS 衛星で観測された電磁波動を比較した。これにより、昼夜の差異、コーラスとの対応、降下電子の空間的分布等を調査した。一連の調査により、昼側 PsA に寄与する降下電子は夜側と同等のエネルギー分布を持つものの、いくつかの点において異なる特徴を持つことが示された。また、従来の研究で観測されてきた昼側 PsA より低緯度の領域においても、昼側 PsA に寄与する電子降下が存在していることが分かった。これらの結果より、昼側 PsA に寄与するコーラス波動本体が、夜側と異なる特徴を持つことが示唆された。

R006-57
Zoom meeting B ：11/4 PM1 (13:45-15:30)
14:45〜15:00

多波長から推定する脈動オーロラの降下電子エネルギー

#遠山 航平 [1)], 栗田 怜 [2)], 三好 由純 [3)], 細川 敬祐 [4)], 小川 泰信 [6)], 大山 伸一郎 [1)], 齊藤 慎司 [5)], 野澤 悟徳 [7)], 川端 哲也 [7)], 浅村 和史 [8)]
([1] 名大 ISEE,[2] 京都大学 生存研,[3] 名大 ISEE,[4] 電通大,[5] 情報通信研究機構,[6] 極地研,[7] 名大・宇地研,[8] 宇宙研

Precipitating electron energy of pulsating aurora estimated from multi-wavelength optical observations

#Kohei Toyama[1)],Satoshi Kurita[2)],Yoshizumi Miyoshi[3)],Keisuke Hosokawa[4)],Yasunobu Ogawa[6)],Shin ichiro Oyama[1)],Shinji Saito[5)],Satonori Nozawa[7)],Tetsuya Kawabata[7)],Kazushi Asamura[8)]
([1]ISEE, Nagoya Univ.,[2]RISH, Kyoto Univ.,[3]ISEE, Nagoya Univ.,[4]UEC,[5]NICT,[6]NIPR,[7]ISEE, Nagoya Univ.,[8]ISAS/JAXA

Pulsating aurora (PsA) is characterized by quasi-periodic intensity modulations with a period of a few to tens of seconds which is known as the main modulation. Electrostatic Cyclotron Harmonic waves and whistler-mode waves are known to cause the pitch angle scattering of energetic electrons in the magnetosphere. In particular, whistler-mode chorus waves play a crucial role in the pitch angle scattering of electrons. The lower-band chorus causes precipitation of electrons whose energy is greater than several keV [Miyoshi et al., 2015]. The energy of precipitating electrons causing PsA may be estimated from ground-based optical observations. Ono [1993] observed the emission intensities of PsAs at wavelengths of 427.8 and 844.6 nm using a photometer in Antarctica, and estimated the energy of precipitating electrons by combining the ratio of the emission intensities at the two wavelengths and the model calculation. However, Ono [1993] conducted observations using the instrument with a narrow field-of-view, and the energy estimation using all-sky imagers has not yet been performed. In Tromsoe, Norway, several highly-sensitive EMCCD cameras have been operated, which have simultaneously observed all-sky images of the emission intensity at the two wavelengths (427.8 and 844.6 nm) with a sampling frequency of 10 Hz. In this study, we investigate the spatio-temporal variations of precipitating electron energy using these EMCCD camera data. We estimated the precipitating electron energy of PsA by comparing the emission intensity ratio of the two emission lines using the all-sky image and the emission intensity calculation results obtained by the GLobal airglOW (GLOW) model [Solomon, 2017]. We have also developed a code coupling simulation using both the test particle simulation GEMSIS-RBW that calculates wave-particle interactions and the GLOW model, and we compared the ratios at different wavelength between the model and the observations. The analysis showed that the spatial distribution of precipitating electron energies are not uniform, and a few keV differences are found inside the patch.

脈動オーロラは、主脈動と呼ばれる数秒から数十秒の準周期的な明滅が特徴である。静電サイクロトロン波動やホイッスラー波動は、磁気圏における高エネルギー電子のピッチ角散乱の原因となることが知られている。特に、ホイッスラーモードのコーラス波動は、電子のピッチ角散乱に重要な役割を果たしていて、Lower band のコーラス波動は、数 keV 以上のエネルギーを持つ電子の大気への降り込みを引き起こすと考えられている [Miyoshi et al., 2015] 。脈動オーロラを引き起こす降下電子のエネルギーは、地上の光学観測から推定することができる。Ono[1993] は，南極でフォトメータを用いて脈動オーロラを 427.8nm と 844.6nm の二つの波長で観測し，発光強度の比とモデル計算を組み合わせることで，降水電子のエネルギーを推定した。しかし、Ono[1993] は視野の狭い観測装置を用いた観測であり、全天カメラを用いたエネルギー推定はまだ行われていない。ノルウェーのトロムソーでは、複数の高感度 EMCCD カメラが稼働しており、2 つの波長（427.8nm と 844.6nm）における発光強度の全天画像を 10Hz のサンプリング周波数で同時に観測している。本研究では，これらの EMCCD カメラを用いて，降下電子エネルギーの時空間的な変化を調べた。全天画像を用いた 2 つの輝線の発光強度比と、GLobal airglOW（GLOW）モデル［Solomon, 2017］で得られた結果を比較することで，脈動オーロラの降水電子エネルギーを推定した。また、テスト粒子シミュレーションと GLOW モデルで得られた発光強度比を、観測で得られた発光強度比と比較した。本報告では、脈動オーロラの降下電子エネルギーの時間変化および空間分布について報告する。このうち、空間分布については、脈動オーロラのパッチ内部における降下電子のエネルギー分布は一様ではなく、パッチの各領域において数 keV 程度の非一様性があるという結果が得られた。

R006-58
Zoom meeting B ：11/4 PM1 (13:45-15:30)
15:00〜15:15

Spectroscopic and imaging observations of SWIR aurora (1.1-1.3 microns) at Longyearbyen: Current status of the developments

#Takanori Nishiyama[1,6],Masato Kagitani[2],Yasunobu Ogawa[1,6,7],Fuminori Tsuchiya[3],Takuo Tsuda[4],Takeshi Sakanoi[5]
([1]NIPR,[2]PPARC, Tohoku Univ,[3]Planet. Plasma Atmos. Res. Cent., Tohoku Univ.,[4]UEC,[5]PPARC, Grad. School of Science, Tohoku Univ.,[6]The Graduate University for Advanced Studies, SOKENDAI,[7]Joint Support-Center for Data Science Research, ROIS

We are currently developing and testing a 2-D imaging spectrograph with a fast optical system and high spectral resolutions to challenge twilight/daytime aurora measurements from the ground. It is designed for short-wavelength infrared (SWIR) wavelength, in which sky background intensity is weaker than in visible, ranging from 1.1 to 1.3 microns and covering strong auroral emissions in N_2^+ Meinel band (0-0) and N_2 1st Positive bands (1-2, and 0-1). Its field-of-view (FOV) and angular resolution are 55 degrees and 0.11 degrees per pixel, respectively. If a 30-microns slit is used, spectral bandpass around 1.1 microns are 0.52 nm and 0.22 nm with two different gratings (950 lpmm and 1500 lpmm). A signal-to-noise ratio for 1 kR emissions is estimated to be larger than 1.0 in a few seconds exposure time. Therefore, we expect that temporal variability of particle precipitations such as those associated with dayside reconnection and pulsating auroras can be investigated with sufficient sampling rates of about 10-15 seconds. In a test observation, we successfully measured airglow emissions of OH (5-2), (6-3), and (7-4) bands in 1.07-1.23 microns (shown in an attached figure).

In addition to the spectrograph, we start to design and develop a brand-new SWIR imager focusing on aurora emissions in N_2^+ Meinel band (0-0). The imager consists of a few commercial SWIR lenses for security/defense purposes, plano-convex lenses, a custom optical filter and an InGaAs FPA (640 x 512 pixels). Total optical system is fast (F-number 1.4) and we examined that the point spread function is less than 5 pixels in full width at half maximum even near the end of the FPA. The FOV is 92 degrees and slightly wider than that of the spectrograph. The more detailed specification of the imager will be shown in this presentation.

The both instruments are going to be installed at The Kjell Henriksen Observatory/The University Centre in Svalbard (KHO/UNIS), Longyearbyen (78.2^{o}N, 15.6^{o}E) by the end of 2022. Taking geographical advantage of the observatory, 24-hours continuous observations can be expected near the winter solstice. Coordinated studies with active/passive radio remote sensing, such as EISCAT Svalbard radar and VLF/LF radio wave receivers, are also planned to estimate precisely energy flux of precipitating particles associated with aurora and sub-sequent changes in electron density and neutral/ion temperatures. Possible scientific targets are as follows: dayside reconnections and wave-particle interactions monitored by aurora emissions, ion upflow from resonant scattering of N_2^+ ions, and atmospheric waves seen as neutral temperature modulations. We will also discuss about the observational strategies and future collaborations.

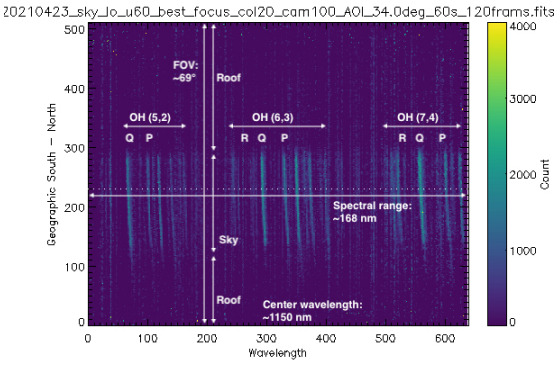

R006-59
Zoom meeting B ：11/4 PM2 (15:45-18:15)
15:45〜16:00

地球電離圏の電荷交換衝突におけるカーブ軌道効果

#家田 章正 [1)]
(1 名大宇宙地球研

Curved Trajectory Effect on Charge-Exchange Collision at Ionospheric Temperatures

#Akimasa Ieda[1)]
(1ISEE, Nagoya Univ.

Collision between ions and neutral particles is an essential characteristic of Earth's ionosphere. This ion-neutral collision is usually caused by the polarization of neutral particles. This collision can also be caused by charge exchange, if the particle pair is parental, such as atomic oxygen and its ion. The total collision frequency is not the sum of the polarization and charge-exchange components, but is essentially equal to the dominant component. The total is enhanced only around the classic transition temperature, which is near the ionospheric temperature range (typically 200-2000 K). However, the magnitude of this enhancement has differed among previous studies; the maximum enhancement has been reported as 41% and 11% without physical explanation.

In the present study, the contribution of the polarization force to the charge-exchange collision is expressed as a simple curved particle trajectory effect. As a result, the maximum enhancement is found to be 22%. It is discussed that the enhancement has been neglected in classic models partly due to confusion with the glancing particle contribution, which adds 10.5% to the polarization component. The enhancement has been neglected presumably also because there has been no functional form to express it. Such an expression is derived in this study.

電離圏と磁気圏の結合を理解するためには、電離圏電気伝導度を定量的に把握することが必要である。電気伝導度の主体は、イオンと中性粒子の衝突断面積である。この断面積は、２つの成分を持つが両成分の和ではなく、高温では電荷交換成分に、低温では中性粒子の分極による成分に漸近する。両成分が等しくなる遷移温度は、電離圏温度（200-2000 K）付近である。これまで電離圏分野の古典的研究では、遷移温度において、トータルの衝突断面積は、分極成分や電荷交換成分に等しいと近似されてきた。すなわち、両成分は結合しないと仮定されてきた。一方、原子衝突分野の研究では、トータルの断面積は、電離圏の古典的研究よりも 1.4 倍大きいと近似されている。この電離圏分野と原子衝突分野の違いの根拠は不明瞭であった。

本研究では、電荷交換衝突と分極衝突の結合を、カーブ粒子軌道効果により表現した。すなわち、粒子軌道が曲がることにより電荷交換衝突断面積が実効的に増大する効果を取り入れた。その結果、遷移温度において、トータルの断面積は、電荷交換成分から 22%増大することを見いだした。原子衝突分野では、この結合を物理的意味のない二乗平均により表現したために過大評価している。電離圏分野の古典的研究がこの結合を無視した原因は、カーブ粒子軌道効果と、外部境界付近をかすめる軌道の小さい効果とを、混同したことであると思われる。もうひとつの原因は、結合を表現する理論式がなかったためであると思われる。その様な理論式は本研究で初めて導いたので、今後は電荷交換衝突と分極衝突の結合を無視せずに含めて、イオン-中性衝突断面積を計算すれば良い。

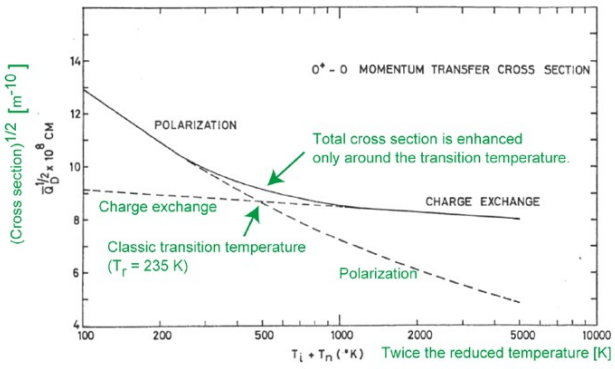

Figure 1. Figure 2 of Banks (1966) explains the classic model. Reused with permission from Elsevier (license number 5005811313501). Our clarifications are shown in green. The square root of the O^+–O momentum-transfer cross sections are shown against twice the ion–neutral reduced temperature. The solid line shows the total cross section, which consists of two components, shown by the dashed lines. The total is not the sum of the two components, but is essentially equal to the polarization component at low temperatures and to the charge-exchange component at high temperatures. The total cross section is larger than that of either component only around the transition temperature, where the two components intersect. The corresponding maximum enhancement was stated to be 11% in Banks (1966), although it was not explained how the total cross section was calculated.

R006-60
Zoom meeting B ：11/4 PM2 (15:45-18:15)
16:00〜16:15

Temporal variations of enhanced low-energy electron fluxes associated with the auroral arc near the nightside polar cap boundary

#Kazuki Yashima[1)],Satoshi Taguchi[1)],Keisuke Hosokawa[2)]
([1]Grad school of Science, Kyoto Univ.,([2]UEC

Near the nightside polar cap boundary there often occur broadband precipitating electrons, in which the fluxes of the low-energy electrons are strongly enhanced. These electrons can produce a tall red aurora. Previous satellite observations have clarified the energy profiles and spatial characteristics of the broadband electron precipitation, but we still do not understand how the broadband electron precipitation grows or decays near the nightside polar cap boundary. In this study, to understand the temporal variations of the broadband electron precipitation, we have developed an automated method for estimating the temporal variations of the distribution of the 630-nm auroral volume emission rate, and of the energy flux of the precipitating electrons by analyzing auroral image data obtained by an all-sky imager (located at Longyearbyen, Svalbard), and comparing the auroral distribution with predicted 630-nm emissions calculated by the Global Airglow model. The results show that the energy fluxes of the low-energy electron precipitation are enhanced intermittently, and that the horizontal width of the electron precipitation region tends to become narrow when the enhanced low-energy electron precipitation occurs. We discuss these relationships in terms of the motion of the aurora.

R006-61
Zoom meeting B ：11/4 PM2 (15:45-18:15)
16:15〜16:30

2018年12月28日の地上EMCCDカメラとあらせ衛星の共役観測に基づくPi2波とイオン振動とオーロラ光振動との対応関係

#陳 リウェイ [1)], 塩川 和夫 [2)], 三好 由純 [3)], 大山 伸一郎 [3)], 田 采祐 [4)], 小川 泰信 [5)], 細川 敬祐 [6)], 風間 洋一 [7)],Wang Shiang-Yu[8)],Tam S. W. Y.[9)],Chang T. F.[9)],Wang B.-J.[10)], 浅村 和史 [11)], 笠原 慧 [12)], 横田 勝一郎 [13)], 堀 智昭 [3)], 桂華 邦裕 [14)], 笠羽 康正 [15)], 熊本 篤志 [16)], 土屋 史紀 [16)], 小路 真史 [3)], 笠原 禎也 [17)], 松岡 彩子 [18)], 篠原 育 [19)], 今城 峻 [20)]
([1] 宇地研,[2] 名大宇地研,[3] 名大 ISEE,[4] 名大 ISEE 研,[5] 極地研,[6] 電通大,[7]ASIAA,[8] 中央研究院天文及天文物理研究所,[9] 台湾・國立成功大学,[10]ASIAA, Taiwan,[11] 宇宙研,[12] 東京大学,[13] 大阪大,[14] 東大・理,[15] 東北大・理,[16] 東北大・理・惑星プラズマ大気,[17] 金沢大,[18] 京都大学,[19] 宇宙研／宇宙機構,[20] 名大・ISEE

Correspondence of Pi2 pulsations, ion pressure fluctuations, and aurora luminosity measured by a conjugate observation

#Liwei Chen[1)],Kazuo Shiokawa[2)],Yoshizumi Miyoshi[3)],Shin ichiro Oyama[3)],ChaeWoo Jun[4)],Yasunobu Ogawa[5)],Keisuke Hosokawa[6)],Yoichi Kazama[7)],Shiang-Yu Wang[8)],S. W. Y. Tam[9)],T. F. Chang[9)],B.-J. Wang[10)],Kazushi Asamura[11)],Satoshi Kasahara[12)],Shoichiro Yokota[13)],Tomoaki Hori[3)],Kunihiro Keika[14)],Yasumasa Kasaba[15)],Atsushi Kumamoto[16)],Fuminori Tsuchiya[16)],Masafumi Shoji[3)],Yoshiya Kasahara[17)],Ayako Matsuoka[18)]
([1]ISEE,[2]ISEE, Nagoya Univ.,[3]ISEE, Nagoya Univ.,[4]ISEE, Nagoya Univ.,[5]NIPR,[6]UEC,[7]ASIAA,[8]Institute of Astronomy and Astrophysics, Academia Sinica, Taiwan,[9]PSSC, NCKU, Taiwan,[10]ASIAA, Taiwan,[11]ISAS/JAXA,[12]The University of Tokyo,[13]Osaka Univ.,[14]University of Tokyo,[15]Tohoku Univ.,[16]Planet. Plasma Atmos. Res. Cent., Tohoku Univ.,[17]Kanazawa Univ.,[18]Kyoto University,[19]ISAS/JAXA,[20]ISEE, Nagoya Univ.

While many substrom-related observations were made, few conjugate observations of substorm auroral arcs have been reported particularly on such arcs connecting to in the inner magnetosphere at L˜5. In this presentation, we show a substorm event where the footprint of the Arase satellite was located equatorward (earthward in the equatorial magnetosphere) of the a brightening arc at L˜5. The event was observed on December 28, 2018. The ground-based electron-multiplying charge-coupled device (EMCCD) camera at Gakona (62.39oN, 214.78oE), Alaska observed the substorm auroral break-up at ˜0743 UT, while the Arase satellite just equatorward of the brightening arc observed a series of quasi-periodic variations in the electric and magnetic field and medium-energy ion spectra with periods of ˜100-300 s when the auroral break-up happened. Ground-based magnetometers over North American continent and Hawaii observed Pi2 pulsations with periods of ˜110 s. The Pi2 pulsations at high latitudes present approximately one-to-one correspondence with the oscillation of the substorm aurora brightness, suggesting that high-latitude Pi2 oscillations are caused by field-aligned current oscillations. Another correlation between the variation in plasma sheet ion pressure and the luminosity of the substorm brightening arc was also identified. This may indicate that the field-aligned current oscillation is caused by the pressure oscillation of the plasma sheet ions. The amplitude of the filtered ion pressure variation is several times larger than that of the filtered magnetic pressure, suggesting a pressure-driven instability plays a role in the formation of these oscillations and substorm brightening arc in this event. Through this event we will present the relationship between the auroral arc evolution on the ionosphere and the source wave and particle features in the magnetosphere on the basis of these measurements at just earthward of the brightening arc.

R006-62
Zoom meeting B ：11/4 PM2 (15:45-18:15)
16:30〜16:45

Automatic FLR identification in ionospheric and ground/sea back-scatters from multiple SuperDARN radars, and density estimation

#Hideaki Kawano[1)],Akira Sessai Yukimatu[2)],Nozomu Nishitani[3)],Yoshimasa Tanaka[4)],Satoko Saita[5)],Tomoaki Hori[3)]
([1]Dept. Earth Planet. Sci., and ICSWSE, Kyushu Univ.,([2]NIPR/SOKENDAI,([3]ISEE, Nagoya Univ.,
([4]NIPR/ROIS-DS/SOKENDAI,
([5]NITkit

There are several kinds of waves in the solar wind, including those associated with Sudden Impulses. They can propagate into the magnetosphere, and where the wave frequency matches the eigen-frequency of a geomagnetic field line, which runs through the ground, the ionosphere, and the magnetosphere, the FLR (field-line resonance) can excite eigen-oscillations of the field line and the plasma frozen-in to the field line. The FLR can be identified by the combination of the maximum in the power and the steepest change in the phase at the eigen-frequency. From thus identified FLR frequency one can estimate the density along the magnetic field line, because, in a simplified expression, ‘ heavier’ field line oscillates more slowly.

SuperDARN radars, which observe VLOS (Velocity along the Line of Sight), are expected to monitor the two-dimensional (2D) distribution of the FLR frequency, from which we can estimate 2D plasma-density distribution on the magnetospheric equatorial plane, including the location of the plasmapause. However, visual identification of the FLR in the lots of VLOS data is time-consuming, and the visual identification could miss FLR events superposed by non-FLR oscillations of VLOS. Thus, we started developing computer codes to automatically identify the FLR.

We have so far developed a set of computer codes to automatically identify the FLR for a beam of a radar by using the amplitude-ratio method and the cross-phase methods; these methods cancel out the superposed perturbations by dividing the data from a Range Gate (RG) by the data from a nearby RG along the same beam, because the FLR frequency tends to depend on the latitude more strongly than the superposed perturbations. Another advantage of applying these methods to the SuperDARN VLOS data is that we can choose any pair of RGs (along the same beam) with different distances, and thus can identify what distance is the best to identify the FLR. This distance reflects the resonance width, which is an important quantity reflecting the diffusion and dissipation of the FLR energy. This set of codes succeeded in identifying FLR events causing oscillations in the beam signals backscattered from the ionosphere, and those backscattered from the ground or the sea.

We are now developing an all-in-one IDL code which unifies the above-stated set of codes and is applied to VLOS data of all the beams of a radar at once. The automatically identified FLR events would include events simultaneously observed at several locations by several radars, increasing the possibility of monitoring the 2D distributions of plasma density distribution on the magnetospheric equatorial plane and identify magnetospheric regions. We intend to show such events at the meeting.

R006-63
Zoom meeting B ：11/4 PM2 (15:45-18:15)
16:45〜17:00

Lomb-Scargle periodogram analysis of Pc5 waves observed by the SuperDARN Hokkaido East Radar and ground-based magnetometers

#Koki Morita[1)],Nozomu Nishitani[1)],Tomoaki Hori[1)]
([1]ISEE, Nagoya Univ.

Ultralow frequency (ULF) waves in the Pc5 frequency range (˜1.7-6.7 mHz) observed in geospace are considered to be magnetohydrodynamic (MHD) waves mainly excited in the magnetosphere. They propagate along the earth's magnetic field lines and reach the ionosphere, causing perturbation of the ionospheric plasma motion and the magnetic field. ULF waves observed by the Super Dual Auroral Radar Network (SuperDARN) can be categorized into toroidal and poloidal modes with respect to their polarization. We analyzed Pc5 oscillation modes in ULF waves using the SuperDARN Hokkaido East high-frequency (HF) radar data. We applied the Lomb-Scargle periodogram method to the Doppler shifts of ionospheric irregularities obtained by the radar. First, we automatically identified Pc5 waves with normalized peak powers larger than the significance level of 99 % considering the false alarm probability based on white Gaussian noise. Next, we compared the eigenfrequency, amplitude and phase of Doppler velocity oscillations in the Pc5 range among different beams at a fixed MLAT. The results were that the eigenfrequency, amplitude and phase were clearly correlated with the beam number, i.e., magnetic longitude. The eigenfrequency result was interpreted from the MLT dependence of the length of the magnetic field line. We identify the modes from the amplitude result and the longitude propagation direction from the phase result. Furthermore, the time-series data of Pc5 Doppler velocities obtained from the radar showed a high correlation with ground-based magnetic field data at Moshiri (Japan). We will discuss the details of this relation from the viewpoint of field-aligned currents.

R006-64
Zoom meeting B ：11/4 PM2 (15:45-18:15)
17:00〜17:15

ULF modulation of the D-region ionosphere observed by VLF/LF transmitter signals

#Kentaro Tanaka[1)],Hiroyo Ohya[2)],Fuminori Tsuchiya[3)],Kazuo Shiokawa[4)],Yoshizumi Miyoshi[5)],Mariko Teramoto[6)],Martin Connors[7)],Hiroyuki Nakata[8)]
([1]Eng, Chiba Univ.,([2]Engineering, Chiba Univ.,([3]Planet. Plasma Atmos. Res. Cent., Tohoku Univ.,([4]ISEE, Nagoya Univ.,([5]ISEE, Nagoya Univ.,([6]Kyutech,([7]Centre for Science, Athabasca Univ.,([8]Grad. School of Eng., Chiba Univ.

The Very low-frequency (VLF; 3-30 kHz)/low-frequency (LF;30-300 kHz) technique is most sensitive to the ionization of the D-region ionosphere, which is caused by energetic electron precipitation (EEP) with energies typically $>$100 keV (Rodger et al., 2012). Several studies have reported ionospheric modulations due to ultra low-frequency (ULF) Pc5 and Pi2 modulations (Asnes et al., 2004). Modulation of D-region due to ULF waves during a substorm was reported (Miyashita et al., 2020). However, it is still now clear how the ULF waves cause the modulation in VLF/LF transmitter signals. In this study, we investigate another EEP event which is associated with the ULF modulation that occurred in North America at 11:20-11:35 UT on October 9, 2017, using the VLF/LF transmitter signals. The four transmitters were NLK, WWVB, NDK, and NAA in USA. One receiver at Athabasca (ATH, 54.7 N,246.7 E,L=4.3), Canada was used. The time at 11:20-11:35 UT on October 9, 2017, was quiet time because the SYM-H, AE indices, the solar wind speed and dynamic pressure were stable up to 6 hours before this event. During magnetically quiet time, oscillations in amplitude of VLF/LF waves with a period of 200-300 s were observed on the NLK-ATHA and NDK-ATHA paths. Furthermore, the H-component of ground-based magnetic field variations around ATH and the low-latitudes showed periodic variations of 200-300 s. In this presentation, we will discuss the cause of these VLF/LF oscillations.

R006-65
Zoom meeting B ：11/4 PM2 (15:45-18:15)
17:15〜17:30

VLF 帯送信電波伝搬の数値計算を用いた電磁イオンサイクトロン (EMIC) 波動に伴う下部電離層擾乱のモデリング

#野本 博樹 [1)], 芳原 容英 [1)], 土屋 史紀 [2)], 平井 あすか [3)]
([1] 電通大,[2] 東北大・理・惑星プラズマ大気,[3] 東北大　惑星プラズマ・大気研究センター

Modeling of Perturbation in the Lower Ionosphere caused by EMIC waves using Numerical Simulation of subionospheric VLF signals

#Hiroki Nomoto[1)],Yasuhide Hobara[1)],Fuminori Tsuchiya[2)],Asuka Hirai[3)]
([1]UEC,[2]Planet. Plasma Atmos. Res. Cent., Tohoku Univ.,[3]PPARC, Tohoku Univ.

It is known that electromagnetic ion cyclotron (EMIC) waves generated at the magnetic equator scatter ring-current protons and radiation-belt electrons due to wave-particle interactions. The scattered protons are precipitated into the ionosphere and produce the isolated proton aurora (IPA). At the same time, the precipitated radiation-belt electrons cause perturbations in the lower ionosphere, and anomalies in the propagation of VLF transmitter signals are observed. Observation of the VLF transmitter signal is an effective to monitor disturbances in the lower ionosphere, but the energy of the precipitating electrons cannot be determined directly from the VLF observations. In this study, we develop the disturbance model for the lower ionosphere based on the ground-based IPA and EMIC wave data, and evaluate them by comparing observed anomalies in the VLF transmitter signals. We analyzed the single IPA event observed in Athabasca, Canada on March 27, 2017. A two-dimensional FDTD (Finite-Domain Time Difference) method is used to calculate the temporal variations of the magnetic amplitude of the VLF transmitter signals (24.8 kHz) passing through the IPA region based on the IPA and EMIC data and compared with the measured VLF data. Specifically, the location and width of the disturbances were determined with IPA intensity data, and the temporal variation of the disturbance altitude was determined with EMIC wave data. When the altitude of the disturbances in the lower ionosphere is ranged from 57 km to 86 km, the mean value of the magnetic field amplitude attenuation due to the radio propagation anomaly is 11.4 dB in the observation and 11.0 dB in the numerical computation. The duration of the anomaly is 13 minutes in the observation and 11 minutes in the numerical computation. Furthermore, it has been confirmed that the electron energy required to reach this disturbance altitude range is in the MeV band, suggesting that EMIC waves have a strong influence on the lower ionospheric disturbances.

磁気赤道面で発生した電磁イオンサイクトロン (EMIC) 波動は、波動粒子相互作用によりリングカレントプロトンと放射線帯電子を散乱することが知られている。散乱されたプロトンは電離層に降下し孤立プロトンオーロラ（IPA）が発生する。この時に同時に降下する放射線帯電子は、下部電離層の擾乱 (電離) を引き起こし、VLF 帯送信電波の伝搬異常が観測される。VLF 帯送信電波は、下部電離層の擾乱を観測する有効な観測手段であるが、観測から降下する電子のエネルギーを直接決定できないという問題がある。本研究では、地上で観測された IPA と EMIC 波動データに基づく下部電離層の擾乱モデルを開発し、IPA と同期して発生した VLF 帯送信電波の伝搬異常の観測と比較することにより、その評価を行う。解析対象 IPA イベントは 2017 年 3 月 27 日にカナダのアサバスカで観測された 1 事例である。数値解析には 2 次元 FDTD 法（時間差分つき有限要素法）を用い、IPA 発生領域を通過する VLF 帯送信電波（24.8kHz）の磁界振幅の時間変化について、IPA と EMIC データをもとに計算し、実測データと比較した。具体的には、擾乱発生位置と擾乱領域幅を IPA の発光強度データにより設定し、擾乱高度の時間変動を EMIC 波動データにより設定した。下部電離層の擾乱高度が 57˜86km である時に、電波伝搬異常による磁界振幅減衰量の平均値は、観測値で 11.4dB となり数値解析結果では 11.0dB となり両者の間に比較的良い一致が見られた。また、送信電波伝搬異常の継続時間についても、観測値は 13 分、数値解析結果は 11 分となり良い一致が見られた。さらに、この擾乱高度範囲に到達するために必要な電子のエネルギーは MeV 帯であることが確認されたことから、EMIC 波動が下部電離層擾乱に強い影響を持っていることが示唆される。

R006-66
Zoom meeting B ：11/4 PM2 (15:45-18:15)
17:30〜17:45

高感度全天カメラと Van Allen Probes 衛星によるサブオーロラ帯孤立プロトンオーロラの複数例同時観測

#中村 幸暉[1)], 塩川 和夫[1)], 能勢 正仁[1)], 長妻 努[2)], 坂口 歌織[2)], スペンス ハラン[3)], リーブス ジェフ[4)], フンステン ハーバート[4)],Macdowall Robert J.[5)],Smith Charles W.[3)],Wygant John[6)],Bonnell John[7)]
([1] 名大宇地研,[2] 情報通信研究機構,[3] ニューハンプシャー大学,[4] ロスアラモス国立研究所,[5]NASA/GSFC,[6] ミネソタ大,[7]UCB

Multi-event analysis of simultaneous observation of isolated proton auroras using all-sky cameras and the Van Allen Probes

#Kohki Nakamura[1)],Kazuo Shiokawa[1)],Masahito Nose[1)],Tsutomu Nagatsuma[2)],Kaori Sakaguchi[2)],Harlan Spence[3)],Geoff Reeves[4)],Funsten Herbert[4)],Robert J. Macdowall[5)],Charles W. Smith[3)],John Wygant[6)],John Bonnell[7)]
([1]ISEE,[2]NICT,[3]Univ. New Hampshire,[4]LANL,[5]NASA/GSFC,[6]Univ. of Minnesota,[7]UCB

Proton auroras are generated by energetic protons precipitating from the magnetosphere through charge exchange collisions with atmospheric particles in the ionosphere. In particular, isolated proton aurora (IPA), which has a thinly east-west stretched structure, appears at subauroral latitudes associated with Pc1 geomagnetic pulsations. Previous studies suggested that the IPA is caused by electromagnetic ion cyclotron (EMIC) waves which scatter pitch angle of energetic protons into the loss cone in the magnetosphere and making their precipitation into the ionosphere. EMIC waves are considered to make rapid loss of the radiation belt electrons into the atmosphere through wave-particle interaction. The IPA is the projection of the wave-particle interaction region on the ionosphere. Thus, simultaneous observation of magnetospheric EMIC waves and IPAs is important to understand the scale sizes and the mechanisms of the wave-particle interaction region. Nakamura et al. [JGR, 2020; doi: 10.1029/2020JA029078] reported the correspondence between two IPAs observed at Athabasca and two localized EMIC waves in the magnetosphere. In this study, we detected three events of simultaneous observation of IPAs and plasma and electromagnetic variations in the magnetospheric source region of IPAs by using all-sky cameras deployed by the PWING project (Athabasca, Gakona, Husafell, Magadan, Nyrola, Kapuskasing, Tromsoe, and Istok), ISEE Magnetometer Network, and the Van Allen Probes satellites. As a result, we could find out three events during which the footprints of the Van Allen Probes satellites passed near or over IPAs at Kapuskasing and isolated EMIC waves were observed by the satellites. The events are on March 22 (~08:30 UT), April 22 (~06:40 UT), and September 7 (~04:00 UT), 2018. All events were observed during geomagnetically quiet times. The equatorward boundaries of the EMIC waves correspond to the increase of the energetic proton flux. The poleward boundaries of the EMIC waves correspond to the cliff-like plasma density decrease. These characteristics were common to all three events. Large electromagnetic DC field variations, which are usually observed during ordinary auroral arc crossings, were not observed during these IPA crossings. Based on these results, we will discuss possible cause of localization of IPAs and EMIC waves in the magnetosphere.

プロトンオーロラは、磁気圏から高エネルギープロトンが降り込み、電離圏で大気中の粒子と電荷交換衝突して発生する。その中でも、サブオーロラ帯に現れ、東西方向に薄く伸びた構造を持つ孤立プロトンオーロラ（IPA）は、Pc1 地磁気脈動と同期して出現する。先行研究より、IPA は、磁気赤道面付近で発生する電磁イオンサイクロトロン（EMIC）波動が、高エネルギープロトンをロスコーン内にピッチ角散乱させ、電離圏に降り込ませることで発生すると示唆されてきた。EMIC 波動は、波動粒子相互作用を経て放射線帯粒子を大気中へ急速に損失させると考えられている。これらのことから、磁気圏の EMIC 波動と、波動粒子相互作用領域の電離圏投影である IPA の同時観測は、波動粒子相互作用の空間規模や仕組みを理解する上で重要となる。Nakamura et al. [JGR, 2020; doi: 10.1029/2020JA029078] では、カナダの Athabasca で観測された二つの IPA と、二つの局在化した磁気圏 EMIC 波動の対応を示すことに成功した。本研究では、PWING プロジェクトで展開された 8 つの観測点（Athabasca, Gakona, Husafell, Magadan, Nyrola, Kapuskasing, Tromsoe, Istok）の全天カメラ、ISEE Magetometer Network の誘導磁力計、および Van Allen Probes 衛星を用いて、Pc1 地磁気脈動に伴って発生した IPA とその磁気圏発生源領域のプラズマ・電磁場変動の同時観測イベントを捜索・解析した。その結果、Kapuskasing において同時観測イベントを 3 例見つけ出すことに成功した。それらの日時は 2018 年 3 月 22 日 ~08:30 UT、2018 年 4 月 22 日 ~06:40 UT、2018 年 9 月 7 日 ~04:00 UT であり、いずれも磁気静穏時であった。これらの例では、衛星のフットプリントが IPA 上もしくはその付近を通過した時間に、衛星で孤立した EMIC 波動が観測されており、Nakamura et al. [2020] の結果と一致した。また、観測されたすべての EMIC 波動の強度の強まり・弱まりは、それぞれプロトンフラックスが急激に上昇する領域・電子密度が急激に減少し始める領域と強い相関があることが分かった。また、衛星のフットプリントが IPA 上もしくはその付近を通過した際に、通常のオーロラアーク通過時に期待されるような直流電磁場変動は観測されなかった。講演では、IPA や EMIC 波動の先行研究とこれらの観測事実を照らし合わせて、IPA とその発生源である磁気圏 EMIC 波動の関連、およびそれらの局在化の原因を議論する。

R006-67
Zoom meeting B ：11/4 PM2 (15:45-18:15)
17:45〜18:00

地上多点リオメータ観測に基づく 2018 年 8 月 25-28 日の磁気嵐中のサブストームにおける宇宙電波雑音吸収の経度広がりの研究

#加藤 悠斗 [1)], 塩川 和夫 [1)], 田中 良昌 [2)], 尾崎 光紀 [3)], 門倉 昭 [4)], 大山 伸一郎 [1)], 西谷 望 [1)],Oinats Alexey[5)],Kurkin Volodya[5)],Connors Martin[6)],Baishev Dmitry[7)]
([1] 名大 ISEE,[2] 国立極地研究所/ROIS-DS/総研大,[3] 金沢大,[4]ROIS-DS/極地研,[5] ロシア太陽地球系物理学研究所,[6] アサバサカ大,[7]SHICRA SB RAS, YaSC SB RAS

Longitudinal extent of CNA observed by multipoint ground-based riometers during storm-time substorms on August 25-28, 2018

#Yuto Kato[1)],Kazuo Shiokawa[1)],Yoshimasa Tanaka[2)],Mitsunori Ozaki[3)],Akira Kadokura[4)],Shin ichiro Oyama[1)],Nozomu Nishitani[1)],Alexey Oinats[5)],Volodya Kurkin[5)],Martin Connors[6)],Dmitry Baishev[7)]
([1]ISEE, Nagoya Univ.,[2]NIPR/ROIS-DS/SOKENDAI,[3]Kanazawa Univ.,[4]ROIS-DS/NIPR,[5]Institute of Solar-Terrestrial Physics, Irkutsk, Russia,[6]Athabasca Univ.,[7]SHICRA SB RAS, YaSC SB RAS

Cosmic Noise Absorption (CNA) is a phenomenon caused by absorption of ˜30-MHz radio waves in the D-region ionosphere at altitudes of ˜90 km associated with high-energy (˜30 keV) electron precipitation. Thus, the CNA enhancement in the post-midnight to noon local times is consistent with the eastward drift and energization of electrons in the inner magnetosphere. However, there are few examples of CNA observations at multi-point stations distributed in longitude. The longitudinal extent of CNA with its time evolution has also not been well understood. In this study, we investigated the longitudinal extent of CNA by using simultaneous riometer observations at six stations at subauroral latitudes at Athabasca (ATH; 54.6N, 246.4E, MLAT: 61.5N) and Kapuskasing (KAP; 49.4N, 277.8E, MLAT: 59.0N) in Canada, Husafell (HUS; 64.7N, 339.0E, MLAT: 64.9N) in Iceland, Istok (IST; 70.0N, 88.0E, MLAT: 65.9N) and Zhigansk (ZGN; 66.8N, 123.4E, MLAT: 61.9N) in Russia, and Gakona (GAK; 62.4N, 214.8E, MLAT: 63.2N) in Alaska. These stations are located encircling the earth at ˜60 MLAT by the PWING project. We have conducted simultaneous observation of CNA at these stations since October 2017 and focused on a geomagnetic storm of August 25-28, 2018. We identified 8 isolated storm-time substorms, and studied the relationship between the substorm onset and the CNA. For all the 8 substorms, some stations observed CNA enhancements. In 5 out of 8 substorms, we found the CNA enhancements started around midnight and propagated eastward around the Earth. This result indicates the eastward drift of high-energy electrons, which is the source of the CNA, due to gradient and curvature drift in the geomagnetic field. In 2 out of the 5 cases, we found CNA propagated not only eastward but also westward. We also studied correlation between CNA and ELF/VLF wave intensity at ˜1 kHz, and found a tendency of positive and negative correlations for CNA below and above 0.2 dB, respectively. In the presentation, we will discuss the longitudinal extent, local time dependence, and source mechanisms of CNA based on these observations.

宇宙電波雑音吸収 (CNA) は、高エネルギー (˜30keV) 電子の降り込みに関連して、高度 90km 付近で 30MHz 帯の電波が吸収されることによって生じる現象である。そのため、内部磁気圏で高エネルギー化し経度方向に東向きにドリフトする電子によって、CNA は地方時で夜中過ぎから昼にかけて増大すると考えられている。しかし、これまでに経度方向に複数の観測点で CNA を観測した例が少なく、CNA の時間発展に伴う経度広がりについては未だ明らかになっていない。そこで本研究では、カナダの Athabasca (ATH; 54.6N, 246.4E, MLAT: 61.5N)、Kapuskasing (KAP; 49.4N, 277.8E, MLAT: 59.0N)、アイスランドの Husafell (HUS; 64.7N, 339.0E, MLAT: 64.9N)、ロシアの Istok (IST; 70.0N, 88.0E, MLAT: 65.9N)、Zhigansk (ZGN; 66.8N, 123.4E, MLAT: 61.9N)、アラスカの Gakona (GAK; 62.4N, 214.8E, MLAT: 63.2N) のサブオーロラ帯の 6 観測点で同時観測を行うことで、CNA の経度広がりを調べた。これらの観測点は、PWING プロジェクトで整備され、地球を取り囲むように磁気緯度 60 ° 付近に設置されている。私たちは 2017 年 10 月から 6 観測点での CNA の同時観測を行い、2018 年 8 月 25-28 日の磁気嵐に着目した。この期間中に孤立したサブストームは 8 例観測され、各サブストームの開始と CNA について解析を行った。その結果、8 例すべてのサブストームの開始に伴って、CNA が増大している観測点が存在することがわかった。8 例中 5 例では、CNA は真夜中付近の観測点で最も早く増大し、地球近傍を東向きに伝搬していく特徴が見られた。この結果は、CNA の発生原因となる高エネルギー電子が地球近傍で磁場勾配ドリフトと曲率ドリフトの影響を受け、東向きに移動することにより説明できる。また、5 例のうち 2 例では、東向きのみならず西向きに伝搬する CNA も観測された。そして、高エネルギー電子と相互作用すると考えられる 1kHz の電波強度と CNA の相関解析を行ったところ、CNA が 0.2dB 未満では正の相関が、0.2dB 以上では負の相関が見られる傾向があった。講演では、これらの CNA について経度広がりや地方時依存性、発生原因を議論する。